
Exploring the impact of the energy transition on electricity distribution systems: The beginning of a journey in search of equilibrium in the game between the network operator and its users

Auteur : Cornet, Manon

Promoteur(s) : Cornélusse, Bertrand

Faculté : Faculté des Sciences appliquées

Diplôme : Master : ingénieur civil électricien, à finalité spécialisée "Smart grids"

Année académique : 2022-2023

URI/URL : <http://hdl.handle.net/2268.2/18230>

Avertissement à l'attention des usagers :

Tous les documents placés en accès ouvert sur le site le site MatheO sont protégés par le droit d'auteur. Conformément aux principes énoncés par la "Budapest Open Access Initiative"(BOAI, 2002), l'utilisateur du site peut lire, télécharger, copier, transmettre, imprimer, chercher ou faire un lien vers le texte intégral de ces documents, les disséquer pour les indexer, s'en servir de données pour un logiciel, ou s'en servir à toute autre fin légale (ou prévue par la réglementation relative au droit d'auteur). Toute utilisation du document à des fins commerciales est strictement interdite.

Par ailleurs, l'utilisateur s'engage à respecter les droits moraux de l'auteur, principalement le droit à l'intégrité de l'oeuvre et le droit de paternité et ce dans toute utilisation que l'utilisateur entreprend. Ainsi, à titre d'exemple, lorsqu'il reproduira un document par extrait ou dans son intégralité, l'utilisateur citera de manière complète les sources telles que mentionnées ci-dessus. Toute utilisation non explicitement autorisée ci-avant (telle que par exemple, la modification du document ou son résumé) nécessite l'autorisation préalable et expresse des auteurs ou de leurs ayants droit.



Exploring the impact of the energy transition on electricity distribution systems

The beginning of a journey in search of equilibrium in
the game between the network operator and its users

MASTER THESIS COMPLETED BY

Manon Cornet

IN ORDER TO OBTAIN THE DEGREE OF

**Master of Science in Electrical Engineering,
Professional Focus: Smart Grids**

SUPERVISOR

Pr. Bertrand Cornélusse

UNIVERSITY OF LIÈGE

School of Engineering and Computer Science

ACADEMIC YEAR

2022-2023

ABSTRACT

In the contemporary landscape, power systems are undergoing significant transformations driven by the imperative need for an energy transition towards a completely decarbonized energy system. This master thesis, in particular, focuses on how distribution network operators should plan this transformation considering they have to face both a massive integration of renewable energy sources (RES) and an increased electrification of mobility, heating and industrial processes, through the use of low-carbon technologies (LCTs). This is the so-called *distribution network development planning problem (DNDP)*.

This master thesis lays the foundation for a broader research project whose purpose is to develop a new framework to solve the DNDP problem based on a co-optimization approach. This approach distinguishes from previous works as it models the interactions between the distribution network operator and its users, whose standpoints were previously neglected. We translated our co-optimization framework into a bilevel mathematical optimization program where the upper-level represents the DNO's optimization program, while the lower-level models the aggregation of the optimization programs of all its grid users.

In conclusion, this research not only provides a first bilevel formulation for the DNDP problem but also establishes a tool for exploring various setups of the bilevel problem. This tool facilitated the execution of a preliminary sensitivity analysis, the outcomes of which shed light on the equilibrium dynamics between the strategies of the distribution network operator and its users.

ACKNOWLEDGEMENTS

I want to express my sincere gratitude to the University of Liège for giving me the opportunity to embark on this academic adventure. A huge thank you goes to my advisor, Prof. Bertrand Cornélusse, whose guidance and encouragement have been priceless.

I also want to acknowledge the incredible efforts of the faculty and staff. Your dedication to education has made a significant impact on my growth.

Finally, and most importantly of all, I would like to thank my family, friends, and boyfriend for their constant love. Your belief in me has been my driving force.

To everyone who has played a part in shaping my academic path, I am truly thankful.

TABLE OF CONTENTS

List of Tables	v
List of Acronyms	vi
1 Description of the research problem	1
1.1 Introduction	1
1.2 State of Art	3
1.3 Problem Statement.	6
1.4 Work Environment	8
2 Mathematical Optimization Background	9
2.1 Definition of Mathematical Optimization.	9
2.2 Duality	10
2.3 Karush-Kuhn Tucker Conditions	12
2.4 Classes of Single-Level Optimization Programs.	12
2.4.1 Linear Programming	14
2.4.2 Convex Programming	15
2.4.3 Mixed-Integer Linear Programming	16
2.4.4 Mixed-Integer Nonlinear Programming	17
2.5 Bilevel Programming.	18
2.5.1 Definition of a Bilevel Program	19
2.5.2 Solving Bilevel Programming Problems	21
2.5.3 Comparison Between Multi-Objective Optimization and Bilevel Optimization	21
3 A Story of Data	25
3.1 Load Profiles	25
3.2 Low Carbon Technologies Profiles	27
3.3 PV Profiles	29
3.4 Profiles Summary	29
3.5 Test Network.	30
4 Microgrid Optimization	32
4.1 Description of the problem	32

4.2	The Lower-Level Optimization Program	33
4.3	Adding Storage	36
5	Distribution Network Expansion Planning	37
5.1	Description of the Problem.	37
5.2	The AC Power Flow Equations	38
5.2.1	Power Flow Convex Relaxations	39
5.3	The Radiality Constraints	40
5.4	Examples of DNEP Models from the Literature	42
5.5	The Upper-Level Optimization Program	45
6	The Leader-Follower Problem	50
6.1	Description of the Problem.	50
6.2	The Optimization Program	51
6.3	Sensitivity Analysis Performed for the ISGT Conference Paper	51
6.4	Implementation of the Model	54
6.5	Sensitivity Analysis performed with the <code>Bilevel.jl</code> module	57
7	Conclusion and Perspectives	65
7.1	Summary of Results	65
7.2	Discussion and Future Work	67
Appendix		70
Bibliography		71

List of Tables

3.1	Characteristics of the load profiles, LCTs profiles and PV profiles datasets	30
3.2	All Aluminum Conductors (data from [51])	31
5.1	Results of the implementation of the MISCOP programs proposed in [12] and [23]	42
6.1	Description of test cases used for the ISGT sensitivity analysis.	52
6.2	Results obtained with the bilevel model for the ISGT sensitivity analysis.	53
6.3	Description of test cases used in the sensitivity analysis. In this table, the row colored in grey highlights the base case scenario	57
6.4	Solve Time and MIP Gap of the BP program for every radiality constraint formulation across all 23 simulation configurations. A dash in the table denotes simulations that were unable to find a feasible solution within the allocated time.	59
6.5	Characteristics of the resulting network in the 23 test cases. A dash in the table denotes simulations that were unable to find a feasible solution within the allocated time.	60

LIST OF ACRONYMS

ANM active network management

BFM Branch-Flow Model

BIM bus-injection model

BP bilevel programming

DNDP distribution network development planning

DNEP distribution network expansion planning

DNO distribution network operator

EC energy community

EHP electric heat pump

ESS energy storage system

EV electric vehicle

KKT Karush-Kuhn Tucker Conditions

LCT low carbon technology

LP linear programming

MICP mixed-integer convex programming

MILP mixed-integer linear programming

MINLP mixed-integer nonlinear programming

MIP mixed-integer programming

MO multi-objective

MPEC mathematical problem with equilibrium
constraints

PV photovoltaic

RES renewable energy sources

SOCOP second-order conic programming

Chapter 1

DESCRIPTION OF THE RESEARCH PROBLEM

1.1 Introduction

In the relentless battle against the ever escalating climate and energy crisis, the urgency to take decisive actions has reached unprecedented levels. Policies enacted at the European level have laid the foundation for a transformative vision, pushing nations to adopt rigorous measures aimed at achieving an ambitious objective: zero net carbon emissions in Europe by 2050 [1]. To attain carbon neutrality, a myriad of pathways unfold before us. One such pathway is illustrated in FIGURE 1.4, which underscores the urgent and substantial reductions in CO_2 emissions that are required in sectors, such as power generation, transportation, industrial processes, and residential heating and cooling.

In the face of this profound challenge, a momentous shift lies ahead. As we strive to revolutionize these key polluting sectors, the widespread adoption of renewable energy sources (RES) and an increased electrification of mobility, heating and industrial processes, through the use of low carbon technologies (LCTs), are emerging as central strategies. For instance, Belgium's Fitfor55-MIX scenario, as illustrated in FIGURE 1.2a, necessitates a remarkable transition in electric passenger vehicle adoption, with the penetration rate soaring from 1.7% in 2020 to 27% by 2030. Similarly, FIGURE 1.2b displays a parallel trend, revealing the Fitfor55-MIX's projection of an 8.6% share for electric heat pumps (EHPs) in the country's heating demand by 2030.

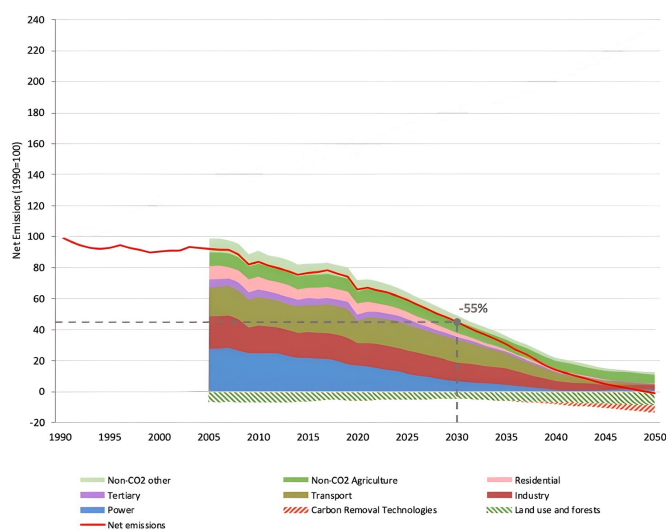


Figure 1.1. Illustration of a possible trajectory leading to climate neutrality in Europe, showcasing the net carbon emissions expressed as a percentage relative to the 1990 carbon emissions level (taken from [2]).

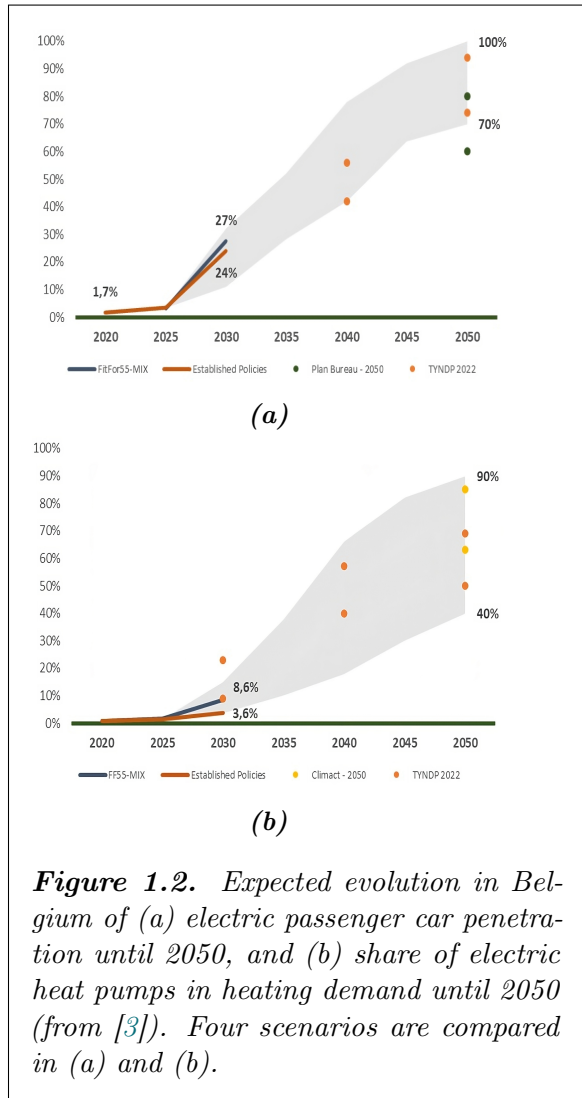


Figure 1.2. Expected evolution in Belgium of (a) electric passenger car penetration until 2050, and (b) share of electric heat pumps in heating demand until 2050 (from [3]). Four scenarios are compared in (a) and (b).

Moreover, FIGURE 1.3 provides a glimpse into the anticipated integration of renewable energy sources, notably showcasing the Fitfor55-MIX scenario's expectation of approximately 11GW of PV capacity. These figures highlights the critical role that RES and LCTs will play in reshaping the energy landscape.

This transition will significantly impact electricity networks, as they will have to cope with both an increase in production volatility and an increase in power consumption. The scale of the transition towards a fully decarbonized global energy system necessitates substantial investments in electricity networks. Estimates indicate that between \$92 trillion and \$173 trillion of investment will be required between 2020 and 2050. Moreover, every 1% of additional efficiency in demand during this period could yield a staggering \$1.3 trillion in value [4], underscoring the importance of well-planned and optimized electricity networks in achieving a sustainable energy future.

This master thesis proposes a method to build a distribution network development planning (DNDP) [5] tool, which aims at planning how distribution networks must evolve in order to achieve an efficient transition towards a decarbonized energy sector. This thesis adopts a co-optimization approach that considers jointly the interactions between grid operators and grid users.

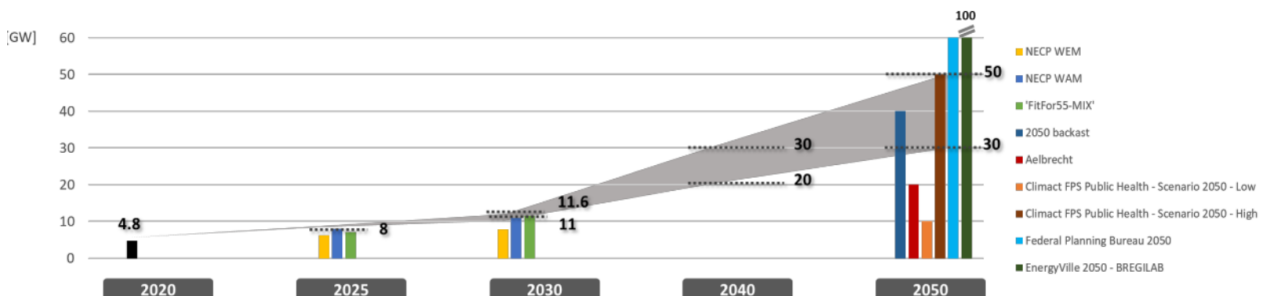


Figure 1.3. Range for solar capacity in Belgium (from [3]).

1.2 State of Art

The swift integration of RES and LCTs into distribution networks can give rise to diverse technical obstacles, such as line congestions and potential under or over-voltages [6], [7]. In [7], a Monte Carlo analysis was conducted to examine the thermal and voltage effects resulting from different penetration levels of RES and LCTs into low-voltage distribution systems. The study revealed that a high penetration of PVs and LCTs (i.e. above 50% of the households connected to a feeder) can indeed lead to significant issues in the majority of the examined feeders. An explicit example of this outcome is available in a document authored by the same researchers [8]. In that document, FIGURE 1.4a depicts the impacts of various LCTs within a residential network feeder in Great Britain, including the consequences of shifting households' heating systems to electric EHPs. In this particular scenario, the figure reveals a threefold rise in peak current entering the distribution network during the winter season. Additionally, it can be seen that EVs further increase this peak, although their impact will likely be seen during nighttime in residential networks. FIGURE 1.4b, from the same document, illustrates that PV panels, on the other hand, create issues during summer.

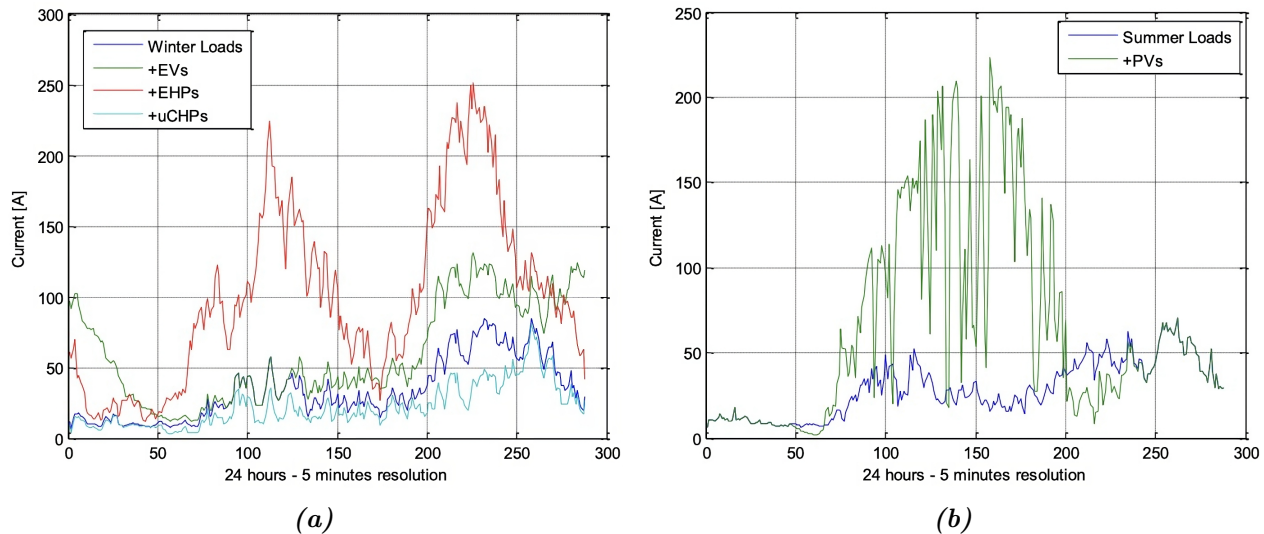


Figure 1.4. Current entering a feeder from a British low-voltage distribution network. This feeder supplies 55 loads through 1431 m of cables. (a) **Comparison for all the winter cases**, i.e. without LCT, with EVs, with EHPs and with μ CHPs. (b) **Comparison for all the summer cases**, i.e. with and without PVs. Both figures are parts of figures 34 and 35 from [8].

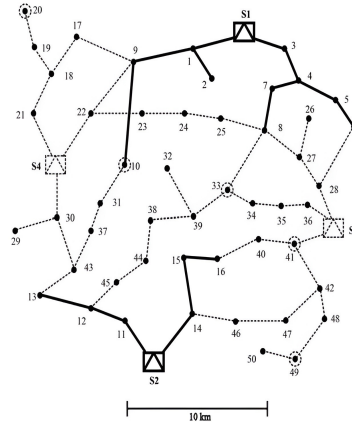
It is important to acknowledge that different use cases (e.g., a business park) or a similar setup in a different part of the world, would yield alternative conclusions. This underscores the necessity for decision-making tools to guide the design and operation of distribution networks.

A renowned tool in the literature for identifying strategies to reinforce distribution networks is the distribution network expansion planning (DNEP) problem. It aims to establish an optimal and cost-effective plan that includes the enhancement of existing distribution feeders and substations, as well as the installation of new ones. This plan must cater to the projected demand over the defined time horizon while adhering to the technical constraints of the network [9], [10].

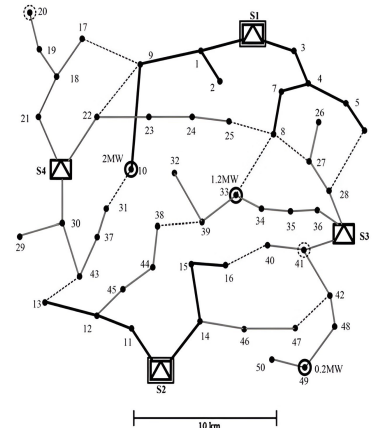
The main methods for solving DNEP problems are analytical, exact optimization, and heuristic methods [9]. Analytical methods are limited to simple cases. Among exact optimization methods, reference [12] presents two exact convex relaxations of DNEP as mixed-integer conic programming problems. It also proposes methods to strengthen their continuous relaxations through the introduction of auxiliary variables and loop elimination constraints. Furthermore, the author claims that, besides providing an optimality guarantee, such mixed-integer conic programming formulations solve faster than a mixed-integer nonlinear programming (MINLP) formulation. However, the DNEP model presented in [12] has limitations. First, it computes reinforcement decisions based on a single power injection profile for the network, e.g., the worst-case moment of the year. This moment is not necessarily easy to determine, especially with the massive integration of RES and LCTs. Then, it considers a passive distribution network, meaning that the power profile of grid users is considered inflexible.

Another way of mitigating issues caused by RES and LCTs is to use active network management (ANM) [13], i.e. short-term policies that control the power injected by generators or withdrawn by loads. Recent research has shown that implementing ANM strategies can increase the share of RES and reduce significantly reinforcement costs [14].

Note: Dotted lines represent possible sites for the expansion of the system. S1-S4 are the substations. Node 10, 20, 33, 41 and 49 with the dotted circles are the possible sites for the DG installation.



(a)



(b)

Figure 1.5. Example of DNEP model simulation results (from [11]). (a) **Initial test network.** (b) **Expanded network** obtained by the DNEP model in the paper.

In recent years, new DNEP models have emerged to address the limitations of the method presented in [12]. These models incorporate active network management (ANM), renewable energy sources (RES), energy storage system (ESS), and low carbon technologies (LCTs). In [15] and [16], the DNEP is modeled as a MINLP that includes RES and uncertainties in the planning. In [17], the DNEP problem is enriched by considering distributed ESSs. Reference [11] goes further by modeling a DNEP problem that considers ANM schemes, including demand response management, RES curtailment, and dispersed ESSs. Hence, the DNEP problem is well-established and has already received much attention.

However, a gap has been identified in all these research works as they solely focus on the distribution network operator (DNO)'s perspective, overlooking the behavior of grid users resulting from their interactions with the DNO. From the grid users' standpoint, there is already a large body of research which aimed at optimizing the sizing and operation of a microgrid or an energy community (EC), as seen in [18], [19]. Nevertheless, few articles consider the problems of the grid users and the grid operator as being coupled. For instance, while it is technically feasible to reinforce the grid to accommodate the demand growth due to EHPs and EVs, it comes at a significant cost. Knowing this cost, grid users may change their plan, for instance, reduce their energy needs by shifting to lighter, less energy-demanding vehicles or installing stationary battery storage to increase their self-consumption.

In this master thesis, we are interested in bilevel programming (BP) as the tool we use to clear the gap mentioned in the previous paragraph. BP describes a type of optimization programs well-suited to model co-optimization scenarios, where it involves an upper-level (leader) optimization problem and one or more lower-level (follower) optimization problems [20]. This mathematical tool has already been used in previous research works focused on the DNDP problem [21], [22]. In [21], the study approaches generation and distribution network development as an upper-level problem, while the lower-level problem concentrates on demand response. In contrast, [22] sets the upper-level problem to optimize distribution network development, with the lower-level problems involving RES and demand aggregators.

To conclude, BP is already a recognized tool in the power system research community for tackling the DNDP problem. Nevertheless, to the best of our knowledge, the DNDP problem has not been previously modeled using a BP program that incorporates a lower-level representing the behavior of users as a microgrid optimization problem, where their investment decisions are directly coupled to the DNO's policy.

1.3 Problem Statement

The main objective of this master thesis is to lay the foundations for an innovative framework dedicated to formulating network development plans within low and medium voltage distribution networks. Given the extensive scope of this problem, which can fluctuate based on the geographical location of the network, the local policies in place at this location, and technological considerations, the framework will be designed with the intent to cope with as many as possible variants of this problem. For instance, these variations could range from developing plans for a new distribution network in an underserved region to strategizing for already established networks. As this master thesis is part of the initial steps aimed at constructing this new framework, it will narrow the scope of this problem by focusing on a specific version described in detail within this section.

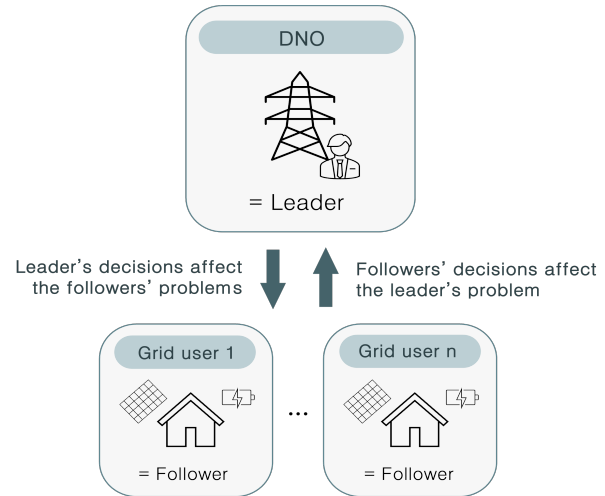


Figure 1.6. Illustration of the considered bilevel optimization problem.

Unlike existing literature tackling this problem, which predominantly focuses on the distribution network operator (DNO)'s perspective, this work approach considers both the DNO and the grid users' viewpoints. In fact, the distribution network development planning (DNDP) issue is treated as a strategic game involving these two parties, where the decisions of one actor influence the other's decisions and vice versa. This results in a two-level problem, where grid users and the DNO engage in decision-making processes at their respective levels. In such problem, the upper-level, also called the leader, makes the initial decision, and the lower-level, or follower, observes and responds accordingly. The solution to this problem lies therefore in finding an equilibrium between the strategies of both actors. This is proposed to be modelled by a bilevel optimization program, that can be illustrated in FIGURE 1.6.

The upper-level problem of this program models the decision-making process of the DNO, aiming to reinforce its network when the number of LCTs and RES increases. The problem considers a long time horizon, e.g. 30 years, corresponding to the investment's lifetime and imposes a *budget balance* constraint, which aims to ensure that the DNO gets back its investments, plus a certain margin, from network tariffs billed to users. To build the upper-level problem, this work considers the DNEP models proposed in references [12], [23]. However, they are modified to include multiple time steps and this budget balance constraint.

The lower-level represents the grid users of the network. They have the option to purchase grid connection capacity from the DNO, defining the maximum power they can inject or withdraw from the grid. They can also choose to invest in PV panel installations. Grid users' demand is assumed to be known and inflexible, but the analysis considers various scenarios for the penetration of EVs and EHPs. To remunerate the electricity injected into the grid when self-consumption is not possible, a feed-in tariff is implemented. The objective of grid users is therefore to minimize all their investments, e.g. PV panel installations, and operational costs, e.g. electricity purchased from the grid. Furthermore, grid users are presumed to be entirely rational and thus, consistently make optimal decisions.

The DNO aims to minimize total reinforcement costs and Joule losses in its network. They typically recover costs, along with a defined margin, through capacity and energy tariffs paid by grid users. Tariffs are treated as exogenous parameters, enabling sensitivity analysis. For instance, high distribution tariffs may lead users to invest in renewable generation, while the grid operator may improve the network's hosting capacity with increased budget. Conversely, low tariffs may encourage users to consume more from the grid, resulting in potentially higher revenues for the DNO. This close interdependence between tariffs, users, and operators' behavior is a crucial aspect this work seeks to capture.

The primary objective of this master thesis was to establish the initial model of the problem outlined in detail above. This model serves as the foundation for a more comprehensive DNDP problem, which will be the subject of my future Ph.D. thesis. To achieve this, the problem was incrementally constructed, adding complexity as the work progressed. The approach that was used can be summarized by the following key stages:

1. A first step was to develop a microgrid optimization program representing the base case for the lower-level problem. In this model, investment in PV systems is allowed, and restrictions are imposed on the power users can draw from or inject into the grid.
2. Then, the model for the upper-level problem had to be derived. This stage was done in two iterations. First, we implemented and evaluated the DNEP models proposed in [12] and [23]. Then, we took inspiration from these two formulations to create our own version of the DNEP problem, which introduces multiple time steps, lower-level variables and include a *budget balance* constraint. This constraint ensures that the investments made by the DNO, along with an appropriate margin, are recovered through network tariffs charged to grid users.
3. Subsequently, a formulation for the bilevel problem was created, combining the previously mentioned models.

4. An initial set of tests was conducted on our bilevel optimization program. These tests were performed with a formulation of the problem that remains unchanged throughout the tests, only input parameters were modified. These results are submitted to the IEEE PES ISGT EUROPE 2023 conference [24] in a paper that highlights the initial outcomes of the research.
5. Lastly, we implemented the bilevel model using a modular code that allows to test alternative formulations of the model. Some experiments were conducted to gain valuable insights into the equilibrium reached in diverse configurations of the problem.

1.4 Work Environment

My master thesis took place in the Smart Microgrids team of the Montefiore Institute, the Electrical Engineering and Computer Science research unit at ULiège. The team's expertise lies in developing algorithmic solutions based on mathematical programming and machine learning to solve problems of planning, operation, and control in power systems.

The master thesis was supervised by Pr. Bertrand Cornélusse, who leads the microgrid team. Throughout the research, I collaborated closely with my supervisor and Geoffrey Bailly, a PhD student from the same team. Geoffrey and I divided the objectives outlined in SECTION 1.3, but a significant part of the work was carried out collaboratively. My main focus was on formulating the upper-level problem and on implementing a modular code for the bilevel simulations, whereas Geoffrey mainly focused on the lower-level part. We worked together on the rest of the research, including the bilevel experiments for the ISGT paper. Additionally, the ISGT paper results were based on the bilevel model and simulations that we both implemented. Throughout the process, we received valuable support and guidance from Pr. Bertrand Cornélusse and Dr. Mevludin Glavic, an experienced researcher in the field of power systems, who also contributed to the paper's writing.

Chapter 2

MATHEMATICAL OPTIMIZATION BACKGROUND

This chapter provides an overview of fundamental mathematical optimization concepts that are essential for a thorough understanding of the master thesis's subject matter. The first sections of the chapter cover fundamental aspects of mathematical optimization, including the general form of a constrained optimization program, the concept of duality and the Karush-Kuhn-Tucker conditions. Subsequently, a section is dedicated to the different classes of optimization programs and their properties. Emphasis is placed on classes of optimization programs that are relevant to the context of this thesis, i.e. linear, convex and mixed-integer programs. These sections provide concise summaries of the material present in references [25]–[27] for continuous optimization, and [28]–[30] for discrete optimization. Lastly, the chapter introduces readers to the field of bilevel programming, which serves as the framework for formulating our approach to the distribution network development planning problem (DNDP). This last part is mainly inspired from S. Dempe's books [31], [32], M. Cerulli's Ph.D. thesis [33], and C. Fricke's slides [34].

2.1 Definition of Mathematical Optimization

Mathematical optimization is a discipline that involves formulating a problem in the form of an *optimization program*, then determining its *optimal solution* from a set of feasible options. Formally, an optimization program is a mathematical model that seeks to find the vector of *variables* $\mathbf{x} \in X$ that minimizes (or maximizes) the value of an *objective function* $f : X \rightarrow \mathbb{R}$ under a set of *inequality constraints* $g_i : X \rightarrow \mathbb{R}$ and *equality constraints* $h_i : X \rightarrow \mathbb{R}$. All values of the vector \mathbf{x} that respect the constraints of the problem define the *feasible set*. The *solution*, denoted \mathbf{x}^* , is a point of the feasible set at which the objective function reaches its smallest or highest value, depending on the direction of optimization. It is obtained using an algorithm, called a *solution method*. In this thesis, the focus is on constrained optimization programs. The general form of such programs can be written as in PROBLEM 2.1.

General Form of Constrained Optimization Programs

$$\begin{aligned}
 & \underset{\text{w.r.t. } \boldsymbol{x}}{\text{minimize}} && f(\boldsymbol{x}) \\
 & \text{subject to} && g_i(\boldsymbol{x}) \leq 0 \quad i = 1, 2, \dots, k \\
 & && h_j(\boldsymbol{x}) = 0 \quad j = 1, 2, \dots, m \\
 & && \boldsymbol{x} \in X
 \end{aligned} \tag{2.1}$$

where $X \subseteq \mathbb{R}^n$ represents the set of feasible solutions, k is the number of inequality constraints and m is the number of equality constraints.

2.2 Duality

Duality considers that optimization programs can be approached from two different perspectives: the *primal problem* and the *dual problem*. The original problem is referred to as the primal problem, while the dual problem is derived from the primal by following the steps outlined below:

1. From PROBLEM 2.1, the *Lagrangian* $\mathcal{L} : \mathbb{R}^n \times \mathbb{R}^k \times \mathbb{R}^m \rightarrow \mathbb{R}$ can be built by combining the objective function f and the constraints g_i and h_j into a weighted sum. The weights λ_i and ν_j that are introduced in this sum are called the *Lagrange multipliers*.

$$\mathcal{L}(\boldsymbol{x}, \boldsymbol{\lambda}, \boldsymbol{\nu}) := f(\boldsymbol{x}) + \sum_{i=1}^k \lambda_i g_i(\boldsymbol{x}) + \sum_{j=1}^m \nu_j h_j(\boldsymbol{x}) \tag{2.2}$$

where $\boldsymbol{\lambda} = [\lambda_1, \lambda_2, \dots, \lambda_k]^T$ and $\boldsymbol{\nu} = [\nu_1, \nu_2, \dots, \nu_m]^T$.

2. Then, the *Lagrange dual function* $\mathcal{W} : \mathbb{R}^k \times \mathbb{R}^m \rightarrow \mathbb{R}$ can be derived by finding the minimum value of the Lagrangian.

$$\mathcal{W}(\boldsymbol{\lambda}, \boldsymbol{\nu}) := \min_{\boldsymbol{x}} \mathcal{L}(\boldsymbol{x}, \boldsymbol{\lambda}, \boldsymbol{\nu}) \tag{2.3}$$

3. Finally, the *dual problem* consists in the maximization of the Lagrange dual function $\mathcal{W}(\boldsymbol{\lambda}, \boldsymbol{\nu})$ subject to dual feasibility constraints.

$$\max_{\text{w.r.t. } \boldsymbol{\lambda}, \boldsymbol{\nu}} \mathcal{W}(\boldsymbol{\lambda}, \boldsymbol{\nu}) \quad \text{subject to} \quad \lambda_i \geq 0 \quad i = 1, \dots, k \tag{2.4}$$

Consider \mathbf{x}^* and $(\boldsymbol{\lambda}^*, \boldsymbol{\nu}^*)$ as optimal solutions to the primal and dual problems, respectively. Let $f^* = f(\mathbf{x}^*)$ and $\mathcal{W}^* = \mathcal{W}(\boldsymbol{\lambda}^*, \boldsymbol{\nu}^*)$. Assuming that the primal is a minimization problem, the value of the dual function can be interpreted as a lower bound to the value f^* of the optimal primal objective function. Hence, solving the dual problem amounts to finding the highest lower bound on f^* . This comes from the concept of *weak duality*.

If $\tilde{\mathbf{x}}$ and $(\tilde{\boldsymbol{\lambda}}, \tilde{\boldsymbol{\nu}})$ are respectively feasible solutions of the primal and dual problems, weak duality states that the value of the dual objective function is always lower or equal than the value of the primal objective function when evaluated at those feasible solutions, i.e. $\mathcal{W}(\tilde{\boldsymbol{\lambda}}, \tilde{\boldsymbol{\nu}}) \leq f(\tilde{\mathbf{x}})$. The minimum deviation $f(\tilde{\mathbf{x}}) - \mathcal{W}(\tilde{\boldsymbol{\lambda}}, \tilde{\boldsymbol{\nu}})$ between the primal and the dual functions is called the *duality gap*. *Strong duality*, on the other hand, occurs when the duality gap is null at optimality, i.e. $f^* = \mathcal{W}^*$. While weak duality is valid for any optimization programs, strong duality only holds in specific cases. Schematically, weak and strong duality can be illustrated as in FIGURE 2.1.

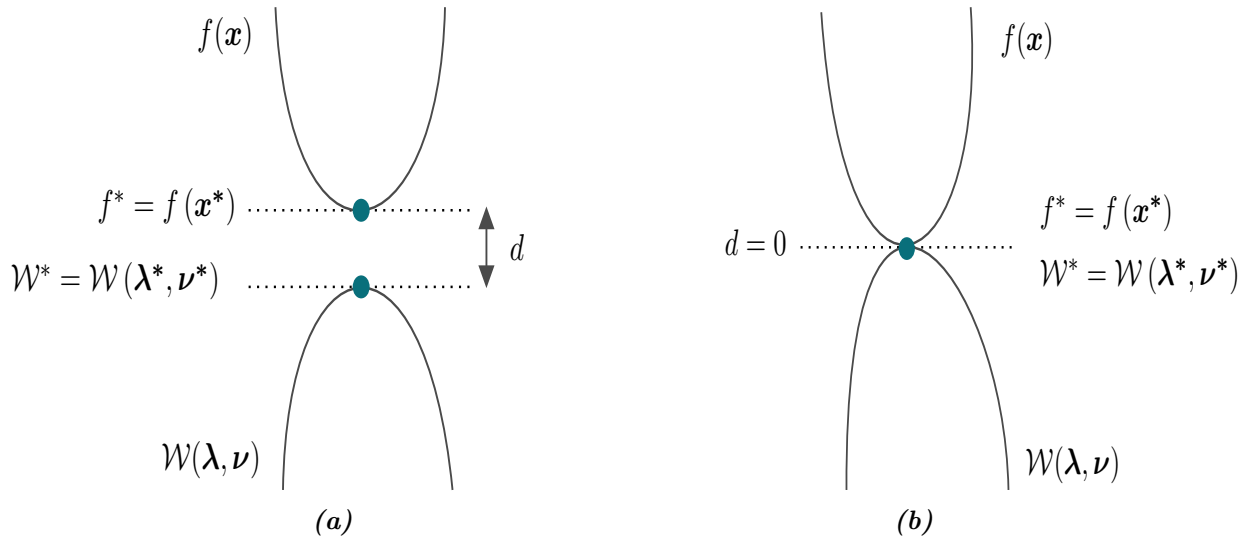


Figure 2.1. Illustration of duality in PROBLEM 2.1. (a) **Weak duality.** In this situation, the duality gap d is always greater than zero, including at optimality. The optimal objective function value of the dual \mathcal{W}^* therefore provides a lower bound on the optimal objective function value of the dual f^* , i.e. $\mathcal{W}^* \leq f^*$. (b) **Strong duality.** This alternative situation shows a null duality gap d at optimality, i.e. $f^* = \mathcal{W}^*$.

2.3 Karush-Kuhn Tucker Conditions

Karush-Kuhn Tucker (KKT) conditions are necessary conditions for optimality in constrained optimization problems. In simple words, this means that if $\tilde{\mathbf{x}}$ is a local optimum for PROBLEM 2.1, then the KKT conditions must be satisfied at this point. In some specific cases, the KKT conditions are also sufficient, which guarantees the local optimality of a point satisfying these conditions. This holds true, for instance, for convex optimization problems. The KKT conditions are written in EQUATIONS 2.5a to 2.5d :

KKT Conditions

Assuming that f , g_i and h_j are differentiable, a necessary condition for $\tilde{\mathbf{x}} \in \mathbb{R}^n$ to be a local minimum for PROBLEM 2.1 is

$$\nabla_{\tilde{\mathbf{x}}} \mathcal{L} = 0 : \quad -\nabla_{\tilde{\mathbf{x}}} f(\tilde{\mathbf{x}}) = \sum_i \lambda_i \nabla_{\tilde{\mathbf{x}}} g_i(\tilde{\mathbf{x}}) + \sum_j \mu_j \nabla_{\tilde{\mathbf{x}}} h_j(\tilde{\mathbf{x}}) \quad (2.5a)$$

$$\nabla_{\lambda} \mathcal{L} = 0 : \quad g_i(\tilde{\mathbf{x}}) \leq 0 \quad i = 1, 2, \dots, k \quad (2.5b)$$

$$\nabla_{\mu} \mathcal{L} = 0 : \quad h_j(\tilde{\mathbf{x}}) = 0 \quad j = 1, 2, \dots, m \quad (2.5c)$$

$$\lambda_i g_i(\tilde{\mathbf{x}}) = 0 \quad i = 1, 2, \dots, k \quad (2.5d)$$

$$\mu_i \geq 0 \quad i = 1, 2, \dots, k \quad (2.5e)$$

where EQUATION 2.5a imposes the gradient of the Lagrangian with respect to $\tilde{\mathbf{x}}$ to be zero, EQUATION 2.5b and EQUATION 2.5c are constraints imposing *primal feasibility*, EQUATION 2.5d represents the *complementary slackness* conditions and EQUATION 2.5b represents the *dual feasibility* constraints.

2.4 Classes of Single-Level Optimization Programs

Based on the properties of the functions f , g_i , h_j , and the set X , PROBLEM 2.1 can fall into different classes of optimization programs, each with its own methods, properties and algorithms for finding a solution to the problem. When building an optimization problem, it is therefore crucial to identify its type to ensure a proper and accurate analysis.

A first approach to categorize a problem is by examining the characteristics of its set X . When the set X is continuous (e.g. $X = \mathbb{R}^n$), the variables contained in the vector \mathbf{x} can take on an infinite number of values. The field of mathematical optimization that studies such programs is called *continuous optimization*. By contrast, *discrete optimization* refers to a class of optimization programs wherein the set of feasible points X contains discrete points. More specifically, an *Integer Programming (IP)* problem is a type of discrete

programming problem that arises when the components of \boldsymbol{x} can take on pure integer values (e.g. $X = \mathbb{Z}_+^n$) or binary values (e.g. $X = \{0, 1\}^n$).

In more general cases, some components of \boldsymbol{x} are not restricted to be integer or binary values. This implies that the set X contains a combination of continuous and discrete variables (e.g. $X = \mathbb{Z}^p \times \mathbb{R}^{n-p}$). The class of optimization programs that involves a set X with these characteristics is known as *Mixed-Integer Programming (MIP)*.

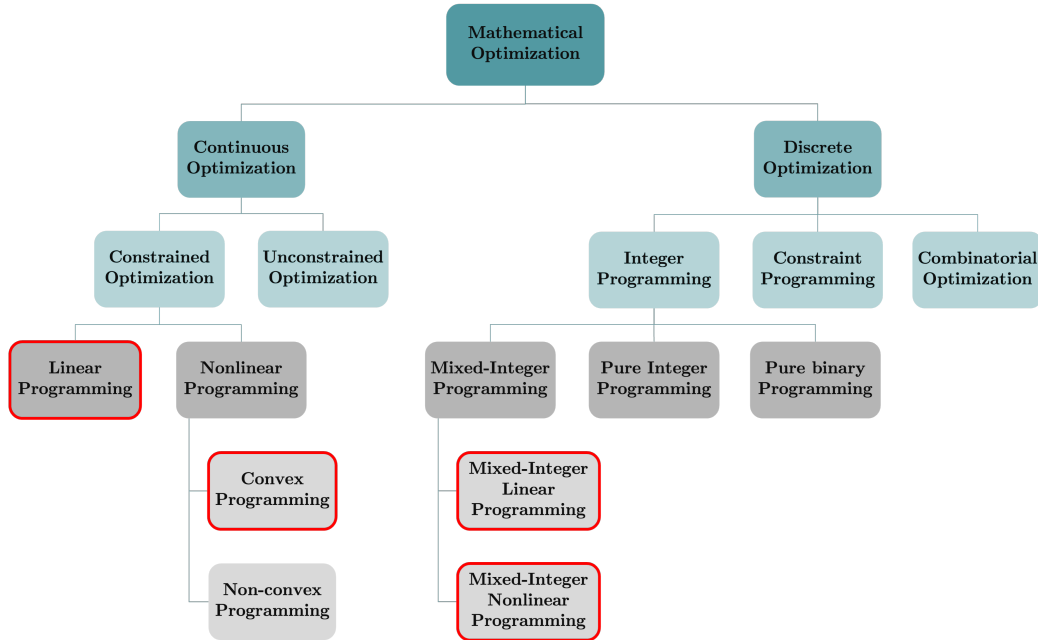


Figure 2.2. Hierarchical diagram showing the main classes of optimization programs. This thesis focuses on the classes of programs that are highlighted in red.

In contemporary power system infrastructure planning, MIP assumes a crucial role as one of the main tools supporting power system operators in making decisions about infrastructure investments. Indeed, various decisions faced by the network operator, such as building new power lines, replacing existing ones, expanding substations capacity, or investing in power production units, can be naturally modelled by integer or binary variables. In such models, continuous variables typically represent the flows and the generation of power within the system. In this thesis, we are highly interested by this family of optimization programs as a program of this type is used to formulate the upper-level of our adapted version of the DNDP. To effectively delve into MIP programs, gaining knowledge about continuous programming concepts is essential. This section will therefore concentrate on two categories of continuous optimization programs: linear and convex programming, followed by an introduction to MIP programs, including both their linear and non-linear formulations. These classes of programs are highlighted in red in FIGURE 2.2, which illustrates the main categories of continuous and discrete optimization problems.

2.4.1 Linear Programming

The simplest form of optimization programs is linear programming. An optimization program belongs to the *linear programming (LP)* class when both the objective function f and the constraints g_i and h_j are linear. In standard form, LP programs can be written as

Standard Form of LP Programs

$$\begin{aligned} \underset{\text{w.r.t. } \boldsymbol{x}}{\text{minimize}} \quad & f(\boldsymbol{x}) = \boldsymbol{c}^T \boldsymbol{x} \\ \text{subject to} \quad & \boldsymbol{a}_i^T \boldsymbol{x} = b_i \quad i = 1, \dots, m \\ & \boldsymbol{x} \in \mathbb{R}_+^n \end{aligned} \tag{2.6}$$

where n is the number of variables, m is the number of constraints, $\boldsymbol{a}_i \in \mathbb{R}^n$ is a vector of coefficients, $b_i \in \mathbb{R}$ is the right-hand-side of constraint i and $\boldsymbol{c} \in \mathbb{R}^n$ is the objective function vector.

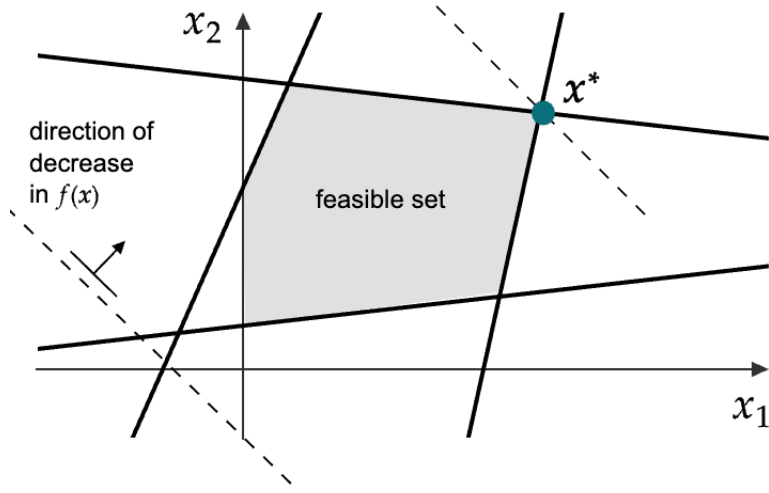


Figure 2.3. Feasible set of a two-dimensional LP problem (adapted from [27])

In LP programs, the *feasible set* is a polyhedron. An example of feasible set in the case of a two-dimensional LP program is illustrated in Figure 2.3. There exist several methods for solving LP problems, the two best known being the simplex method [35] and the interior point methods [36]. Although the simplex method has an exponential worst-case complexity, it demonstrates excellent performance in practice [37]. By contrast, interior point methods offer a way to solve linear programs with polynomial worst-case complexity. Another major feature of LP programs is their strong duality property, from which the *complementary slackness* conditions are directly derived. Detailed explanations about duality in LP programs can be found in the lecture on duality given in COURSE [26]. As a consequence, LP programs have very nice properties, making them easy to solve in practice, even when involving millions of variables.

2.4.2 Convex Programming

Convex programming refers to a more general class of optimization programs. An optimization program, whose general form is written in PROBLEM 2.1, is convex if the objective function f is convex, the equality constraint functions h_j are affine and the inequality constraint functions g_i are convex. LP programs are special cases of convex programs.

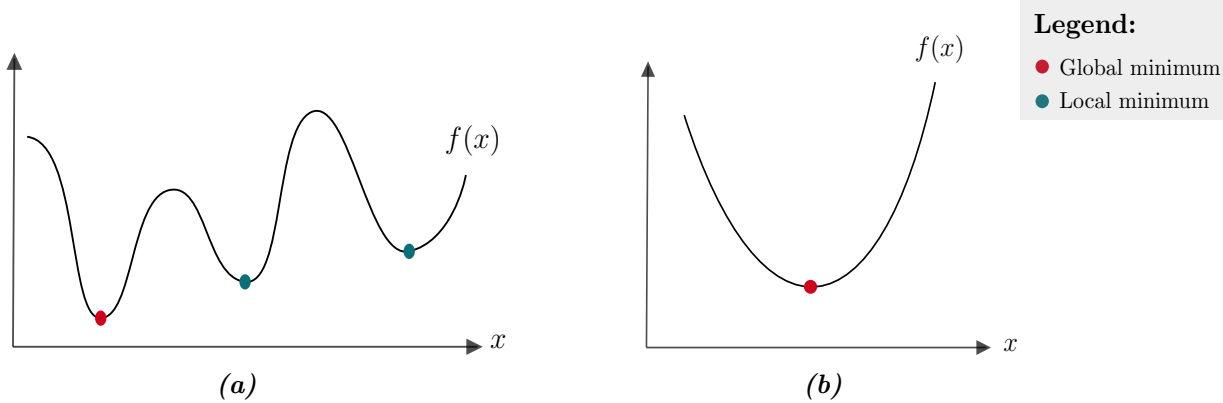


Figure 2.4. Illustration of local and global minima in convex and non-convex functions. (a) **Non-convex function.** When the function $f(x)$ is non-convex, it contains several local minima and only one global minimum. (b) **Convex function.** When $f(x)$ is convex, there is only one minimum that is global.

FIGURE 2.4 depicts global and local minimina in convex and non-convex functions. SUBFIGURE 2.4b illustrates a major property of convex functions: any local minimum of the function is a global minimum. By contrast, SUBFIGURE 2.4a demonstrates that non-convex functions can have several local minima that are not global. As a result, convex programs possess a crucial property stating that each of their local minimum \tilde{x} is, in fact, a global optimal solution x^* . This is not the case for non-convex programs.

Regarding duality, convex programs are generally weak dual. However, there exists a subcategory of the convex programming class, known as *conic programming*, that ensures the strong duality property. Such programs features a linear objective function and constraints that define a cone. Notable families of conic programs include *Second-Order Cone Programming (SOCP)* and *Semi-Definite Programming (SDP)*.¹

In addition, the KKT conditions are necessary and sufficient conditions for optimality in convex programs. This implies that it is sometimes possible to solve the system of equations defined by the KKT conditions in order to find the optimal solution of a convex problem.

Due to their nice characteristics, convex programs can be efficiently optimized. In particular, interior point methods allow the polynomial time resolution of conic programs. Thus, formulating problems as convex optimization programs is often a desirable objective.

¹Refer to [38] for more information about conic programming.

2.4.3 Mixed-Integer Linear Programming

Mixed-integer linear programming (MILP) refers to a specific case of MIP programs where both the objective function and the constraints are linear. Applying this definition to PROBLEM 2.1 requires f , g_i and h_j to be linear, whereas X must be a set that contains continuous and discrete values. We consider a general form MILP program in PROBLEM 2.7:

General Form of MILP Programs

$$\begin{aligned}
 & \underset{\text{w.r.t. } \mathbf{x}, \mathbf{y}}{\text{minimize}} && \mathbf{c}^T \mathbf{x} + \mathbf{d}^T \mathbf{y} \\
 & \text{subject to} && A\mathbf{x} + G\mathbf{y} \leq \mathbf{b} \\
 & && \mathbf{x} \in \mathbb{Z}_+^n \text{ (or } \mathbf{x} \in \{0, 1\}^n\text{)} \\
 & && \mathbf{y} \in \mathbb{R}_+^m
 \end{aligned} \tag{2.7}$$

where \mathbf{c} and \mathbf{d} denote the coefficients of the objective for variables \mathbf{x} and \mathbf{y} , A and G are matrices containing the linear coefficients corresponding to the inequality constraints, \mathbf{x} is the vector of integer (or binary) variables and, finally, \mathbf{y} is the vector of continuous variables.

MILPs are more challenging to solve than LPs because there is no polynomial-time algorithm capable of solving them. This is a result of the fact that MILPs fall into the category of NP-hard problems. The main idea underlying MILP solution methods is to generate and refine bounds on the optimal value of the solution. This is indeed the principle behind the well-known *Branch-and-Bound* algorithm.

The latter employs an iterative process aiming to reduce, at each iteration, the gap between a primal and a dual bound. These bounds represent, respectively, an upper bound and a lower bound to the minimization problem. When the two bounds meet, optimality is reached. In general, the primal bound is derived by discovering a feasible solution to the problem, while the lower bound is obtained by solving its *LP relaxation*. For PROBLEM 2.7, the LP relaxation replaces the constraint $\mathbf{x} \in \mathbb{Z}_+^n$ by $\mathbf{x} \in \mathbb{R}_+^n$. In case of binary constraints, it replaces binary constraints $\mathbf{x} \in \{0, 1\}^n$ by $\mathbf{x} \in [0, 1]^n$. A comparison between the feasible set of the MILP program and the feasible set of its LP relaxation is illustrated in FIGURE 2.5.

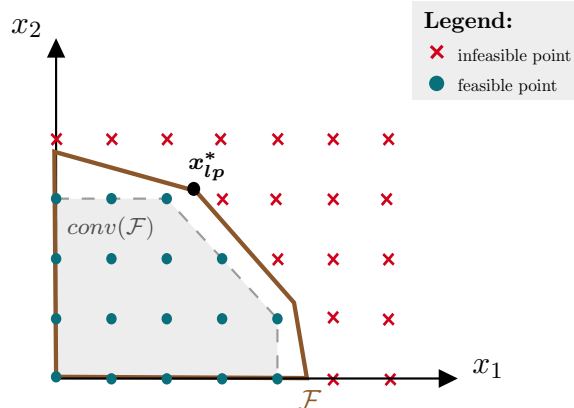


Figure 2.5. Illustration of the feasible points of a two-dimensional MILP program along with the feasible set \mathcal{F} of its LP relaxation and its convex hull $conv(\mathcal{F})$.

Additionally, this figure also depicts the *convex hull*, which is the smallest LP polyhedron that include all the feasible discrete points. A MILP formulation is ideal when the set of its LP relaxation \mathcal{F} is the convex hull $\text{conv}(\mathcal{F})$. In this case, solving the associated LP relaxation allows to find an optimal integer solution.

The branch-and-bound method can be further improved by combining it with a cutting plane algorithm. This results in the *branch-and-cut* algorithm. Its objective is to discover valid inequalities that "cut" the feasible set of the LP relaxation. Notably, widely used MILP solvers like Gurobi [39] and CPLEX [40] implement this approach and other sophisticated techniques, such as heuristics, to further enhance the solving process by finding high-quality solutions in a time-efficient manner.

2.4.4 Mixed-Integer Nonlinear Programming

Based on the information presented in [30] and [28], the following section serves as a brief and informative summary, presenting an overview of the class of optimization programs known as *mixed-integer nonlinear programming (MINLP)*.

Mixed-integer nonlinear programming (MINLP) is a subfield of MIP dedicated to study optimization problems featuring nonlinear objective functions and constraints. Going back to the general form of an optimization program written in PROBLEM 2.1, a MINLP requires a nonlinear objective function f or the functions g_i and h_j to define a nonlinear feasible set. MINLP is probably one of the broadest field in mathematical optimization as it couples the complex worlds of Nonlinear Programming (NLP) and Mixed-Integer Programming (MIP). In fact, many real-life applications can be modeled as MILNP. Indeed, modeling real-world problems often necessitates the representation of both decision-making processes and physical phenomena, which are rarely linear.

From SUBSECTION 2.4.3, we know that solving a MILP, being the simplest form of MIP, is already an NP-hard problem to solve. Therefore, adding non-linearity to the problem can only further increase its complexity. Besides being NP-hard, MINLP programs are also *incomputable*, which means that there exists no algorithm that is able to solve any problem belonging to the MINLP family. This makes this family of programs excessively challenging to solve. Nevertheless, certain specific categories of MINLP programs do have available solution methods. This applies to convex MINLP, which is also known as mixed-integer convex programming (MICP).

To say that a MIP program is convex is an abuse of language since the introduction of discrete variables make them nonconvex by nature. MICP programs therefore describe a subclass of MINLP programs for which a relaxation of the integrality constraints results in a convex feasible set. In PROBLEM 2.1, this arises when the function f is convex, the inequality constraint function g_i is convex for all i and the equality constraint function h_j is affine for all j . As for convex optimization programs, it is also possible to define a subclass of MICP that focuses on programs having SOCP constraints. They are called Mixed-Integer Second-Order Conic Programming (MISOCP).

The approach to solving MINLP problems follows the same principle as for MILP problems: the objective is to bound the optimal solution. However, the primary distinction lies in how dual bounds are generated. In MINLP, dual bounds are obtained by solving relaxations of the problem, which are non-linear and require NLP solving methods. For MICPs, efficient algorithms can successfully solve the convex relaxations, resulting in some cases in global optimal solutions. The assurance of finding global optima ensures the convergence of methods like Branch-And-Bound to a global solution. Among the algorithms used to solve MICPs, notable examples include the NLP-based Branch-And-Bound, the Outer Approximation, the Generalized Benders Decomposition, and the Extended Cutting Plane.

To conclude, MINLP continues to be a highly active area of research because there exists a considerable number of MINLPs that remain challenging to solve efficiently. Thanks to their nice properties, it is common to attempt approximating a MINLP by expressing it in the form of MILP or MICP approximations. This precise approach will be pursued in this master thesis, focusing on problem formulations centered around MICP or MILP.

2.5 Bilevel Programming

Bilevel programming (BP) describes a branch of mathematical optimization that studies mathematical programs containing an optimization problem in their constraints [41]. The roots of Bilevel Programming theory date back to 1934, when the German economist von Stackelberg introduced a game theory framework, now known as the Stackelberg game, where two players interact with each other in turns [42]. In this game, the player that makes the first move is called the *leader*, whereas the *follower* denotes the player who responds to the leader's actions. Therefore, a hierarchy exists among the players, and exchanging the roles of the two players can lead to a substantially different game solution. An illustration of a *leader-follower* game is provided in FIGURE 2.6. This result in game theory was therefore naturally extended to the mathematical programming world.

In this work, BP is used to model our “one-leader multi-follower” approach to the distribution network development planning (DNDP) problem. Thus, this section aims to introduce the fundamental concepts of the BP theory.

It begins by defining a bilevel optimization program in SUBSECTION 2.5.1. In SUBSECTION 2.5.2, we then explore how such programs can be reformulated as single-level programs and present various solution methods. Furthermore, SUBSECTION 2.5.3 provides a comparison between the fields of multi-objective optimization and bilevel optimization. This comparison is illustrated using a simple toy example, justifying the interest in using bilevel programming to model the interaction between the distribution network operator

and its users. The content of this section is primarily derived from the books of S. Dempe [31], [32], M. Cerulli’s Ph.D. thesis [33], and C. Fricke’s slides [34].

2.5.1 Definition of a Bilevel Program

According to Dempe [31], a bilevel program refers to an optimization problem where the set of variables is divided into two vectors, namely, \mathbf{x} and \mathbf{y} . The specificity of this type of program lies in \mathbf{x} , which is determined as an optimal solution of a secondary mathematical programming problem that depends on the variable \mathbf{y} . In simpler terms, a bilevel program is an optimization program that includes another optimization program within its constraints. The latter enforces some of the variables of the bilevel to be determined by its optimal solution. The outer optimization program is called the *upper-level* problem and the optimization program that belongs to the constraints is called the *lower-level* problem. The general form of a bilevel program can be expressed as follows:

General Form of a Bilevel Program

$$\begin{aligned}
 & \underset{\text{minimize}_{w.r.t. \mathbf{x}}}{\quad} && F(\mathbf{x}, \mathbf{y}) \\
 & \text{subject to} && G_i(\mathbf{x}, \mathbf{y}) \leq 0 \quad i = 1, 2, \dots, k \\
 & && \mathbf{y} \in \underset{\mathbf{y} \in Y}{\text{argmin}} \{f(\mathbf{x}, \mathbf{y}) \mid g_j(\mathbf{x}, \mathbf{y}) \leq 0, \quad j = 1, 2, \dots, m\} \\
 & && \mathbf{x} \in X
 \end{aligned} \tag{2.8}$$

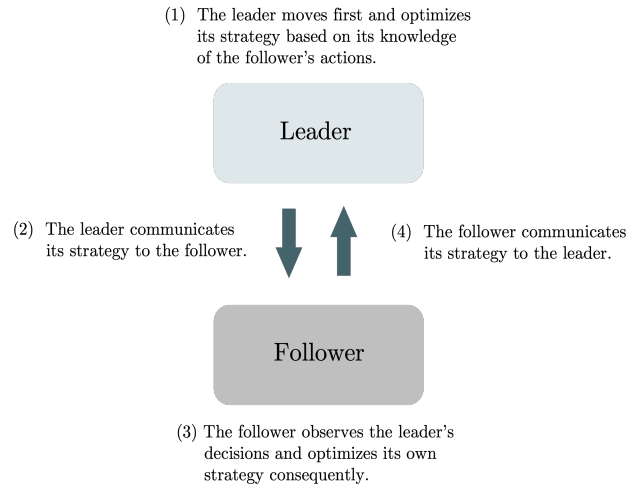


Figure 2.6. Interactions between the leader and the follower in a Stackelberg game

where \mathbf{x} is the vector of upper-level variables, \mathbf{y} is the vector of lower-level variables, F is the upper-level objective function, f is the lower-level objective function, G_i are the upper-level constraints and g_i are the lower-level constraints.

The bilevel problem can be interpreted as a hierarchical Stackelberg game between two decision-makers: the leader and the follower. In this context, the leader and the follower corresponds to the upper-level and lower-level problems, repectively. As can be shown in FIGURE 2.6, the leader is the first actor to decide, it tries to find the action that minimizes its objective function F , having full knowledge of the follower's problem. The follower, on its side, observes the leader's actions and optimizes its own objective function f consequently. In PROBLEM 2.8, the follower corresponds to the following minimization problem:

$$H(\mathbf{x}) = \mathbf{y} \in \operatorname{argmin}_{\mathbf{y} \in Y} \{f(\mathbf{x}, \mathbf{y}) \mid g_j(\mathbf{x}, \mathbf{y}) \leq 0, \quad j = 1, 2, \dots, m\} \quad (2.9)$$

where $H(\mathbf{x})$ represents the set of optimal solutions of the lower-level problem.

In scenarios where the lower-level problem has multiple solutions, there can be several optimal strategies to choose from. In such cases, two assumptions can be made: either the follower selects the most favorable solution in alignment with the leader's strategy, known as the *optimistic approach*, or it chooses the solution opposing the leader's strategy, called the *pessimistic approach*. For the purpose of this study, the optimistic approach is employed, as demonstrated in a previous work [43] to generally present an easier problem to solve compared to the pessimistic bilevel problem. To elaborate further, most techniques for addressing the optimistic scenario simplify the complex bilevel optimization problem into a single-level problem. However, it is worth noting that the optimistic assumption is frequently not verified in practice, particularly when considering grid users as the followers and the Distribution Network Operator (DNO) as the leader. Indeed, grid users do not always select strategies that also benefit the DNO. In [44], the authors underscore the distinction between these two variations when the lower-level problems correspond to electricity consumers and the leader corresponds to their electricity retailer.

Furthermore, bilevel programming exhibits several significant properties [33], [34]:

- There is no guarantee to find a solution to a bilevel problem, even when the functions F , G , f and g are restricted to be continuous and bounded.
- The order in which the decisions are made is crucial : there is non-interchangeability of leader and follower roles.
- Bilevel programming is proven to be NP-hard, even in their linear formulation.

Due to these properties, programs of this class often become intractable. Consequently, it is essential to exercise caution and strive to maintain a simple formulation of the problem, especially concerning the lower-level formulation.

2.5.2 Solving Bilevel Programming Problems

To tackle a bilevel program, a common and straightforward approach is to transform it into a single-level problem. When dealing with optimistic bilevel problems featuring a convex lower level, there exist two main methods to carry out the single-level reformulation:

- **Replacing the lower-level by its KKT conditions or,**
- **Applying the strong duality reformulation.**

In the first case, the lower-level problem is replaced with its KKT conditions. This is only feasible for convex programs since the KKT conditions need to be necessary and sufficient for this reformulation to be effective. This transformation gives rise to a problem known as mathematical problem with equilibrium constraints (MPEC) [45]. Solving MPECs becomes challenging due to their nonlinearity caused by the introduction of complementary slackness conditions. To address this difficulty, the most common approach found in the literature involves utilizing MILP techniques to linearize the KKT complementarity conditions. On the other hand, the strong duality reformulation leverages the insight that at optimality, the objective function values of the primal and the dual are equal. Consequently, the principle is to introduce constraints that enforce strong duality between the primal and the dual.

The nature of the solution algorithms that are used to solve the reformulation heavily relies on the methods employed to address the complementarity conditions. For instance, when MILP technique are employed to reformulate these conditions, famous MILP solvers provided by Gurobi [39] or CPLEX [40] can be used. However, alternative reformulations, such as special ordered sets, also come with their own dedicated resolution algorithms [46].

2.5.3 Comparison Between Multi-Objective Optimization and Bilevel Optimization

The objective of this section is to compare the theories of multi-objective optimization and bilevel optimization. To illustrate their distinctions, a simplified "toy" bilevel program is presented and compared with its multi-objective optimization counterpart. The intention is to demonstrate to readers why employing bilevel programming seems like a good choice when modeling the interactions between the DNO and its network users. This section draws significant inspiration from Chapter 3.4 in the book [31] and from the slides [34].

In various real-world applications, we frequently encounter problems involving multiple objective functions that need to be optimized. For instance, when selecting a smartphone, we might strive to find one that excels in photo quality while also being available at an optimal price. In Mathematical programming, it is the *Multi-Objective optimization (MO)* field that specifically deals with this kind of problems. In MO programs, the objective functions are considered simultaneously, and the goal is to identify the best trade-off among all the objectives. To assess the quality of a feasible solution of a MO program, the notion of domination is introduced. From [34], we get the following definition.

Domination in Multi-Objective Optimization

A feasible solution A is said to *dominate* a feasible solution B if:

- B is at least as good as A with respect to every objective,
- B strictly better than A with respect to at least one objective.

The set of all non-dominated solutions is called the *Pareto Front*. It is one's role to select the point in the Pareto front that represents the best trade-off with respect to the application. One solution to find a Pareto optimal point is to combine the multiple objective functions into a weighted sum. The main difficulty of this approach is the selection of the weights. To readers who want to know more about MO optimization, we recommend this reference [47].

The key difference between bilevel optimization and multi-objective optimization lies in how they treat the objectives: while bilevel optimization considers the objectives sequentially, multi-objective optimization treat them simultaneously. On one hand, multi-objective optimization offers several optimal solutions along a trade-off curve known as the Pareto front. All points on this curve satisfy the same set of constraints, which remains independent of the values of the objectives. On the other hand, the objective in a bilevel program is to optimize a function $F(\mathbf{x}, \mathbf{y})$ over a set defined, in part, by the lower-level optimization problem $H(\mathbf{x})$, parametrized by the upper-level variables \mathbf{x} . Unlike multi-objective optimization, there is no trade-off involved in a bilevel program. The lower-level optimization merely restricts the feasible region from which the upper-level can select its unique optimal solution.

According to [31], a solution from the Pareto front in multi-objective optimization is generally not feasible for the bilevel programming problem. Conversely, the optimal solution of a bilevel program is not necessarily a Pareto optimal solution. Now, let's illustrate these key differences using a small toy example:

Definition of the toy example

$$\begin{aligned}
 \min_x \quad & F(x, y) = 2y + \frac{1}{3}x \\
 \text{s.t.} \quad & 1 \leq x \leq 5 \\
 & x \in \mathbb{R}_+ \\
 \min_y \quad & f(x, y) = -y \\
 & y + \frac{1}{2}x \leq 7 \\
 & 4y - x \geq 5 \\
 & 2y - x \leq 10 \\
 & y \in \mathbb{R}_+
 \end{aligned} \tag{2.10}$$

$$\begin{aligned}
 \min_{x,y} \quad & F(x, y) = 2y + \frac{1}{3}x \quad (w_1) \\
 \min_{x,y} \quad & f(x, y) = -y \quad (w_2) \\
 \text{s.t.} \quad & 1 \leq x \leq 5 \\
 & y + \frac{1}{2}x \leq 7 \\
 & 4y - x \geq 5 \\
 & 2y - x \leq 10 \\
 & x \in \mathbb{R}_+, \quad y \in \mathbb{R}_+
 \end{aligned} \tag{2.11}$$

where PROBLEM 2.10 is a linear bilevel problem, PROBLEM 2.11 is a multi-objective program adapted from PROBLEM 2.10, w_1 and w_2 are the weights of the two objective functions when the weighted-sum method is used to find a solution of the multi-objective PROBLEM 2.11.

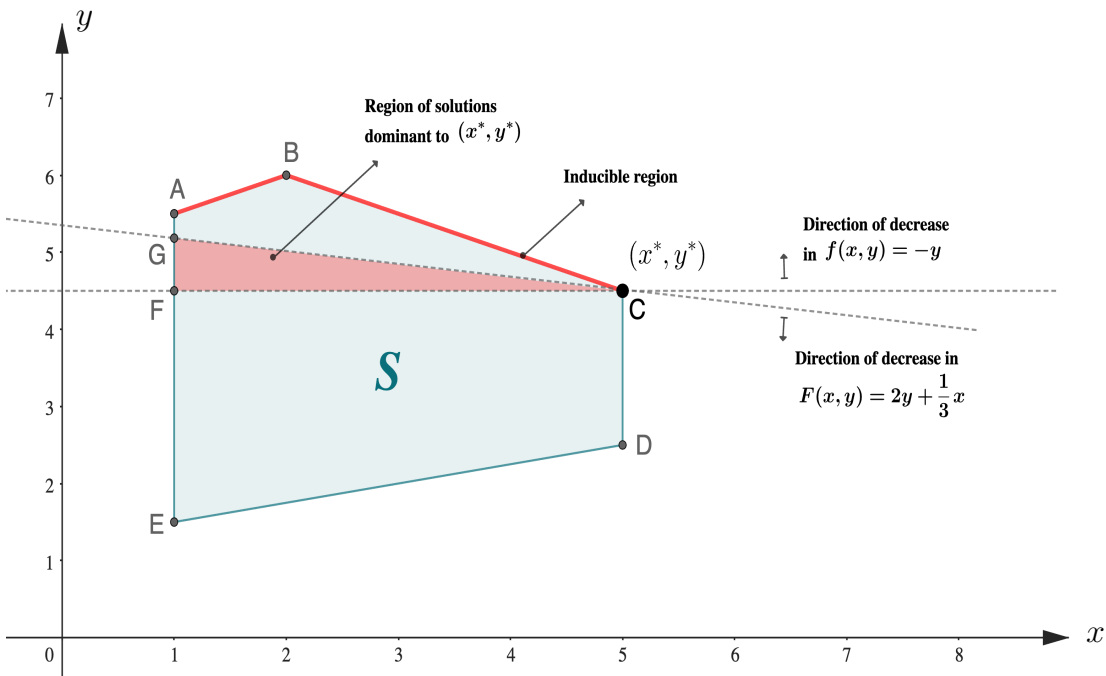


Figure 2.7. Representation of the set S of shared constraints between the upper and lower levels of PROBLEM 2.10. In this figure, the bilevel optimal solution is denoted (x^*, y^*) and it belongs to the bilevel feasible set, also called inducible region. The area colored in red corresponds to a region of S where points are dominant to the optimal bilevel solution in terms of multi-objective optimization.

FIGURE 2.7 represents the shared constraint set S , which is the polyhedron resulting from the upper-level and lower-level constraints of PROBLEM 2.10. Due to the constraints imposed by the lower-level problem, the optimal solution (x^*, y^*) of PROBLEM 2.10 must belong to the bilevel feasible set, or *inducible region*. This region is the region that minimizes $f(x, y) = -y$ for a given x . The area colored in red corresponds to a region of S where points are dominant to the solution (x^*, y^*) in terms of multi-objective optimization. This indicates that the solution obtained from the bilevel program does not strike a favorable trade-off when simultaneously considering the lower-level and upper-level objective functions. Furthermore, FIGURE 2.8 shows the Pareto Front of PROBLEM 2.11. It demonstrates that the optimal solution of the bilevel program is not on the Pareto front. Furthermore, this figure demonstrates that solving PROBLEM 2.11 using the weighted-sum method with two sets of weights results in significantly distinct solutions compared to solving a bilevel program. However, it should be noted that in certain instances, the bilevel solution might coincide with a Pareto optimal solution, but this is more of an exceptional case that arises under very specific conditions.

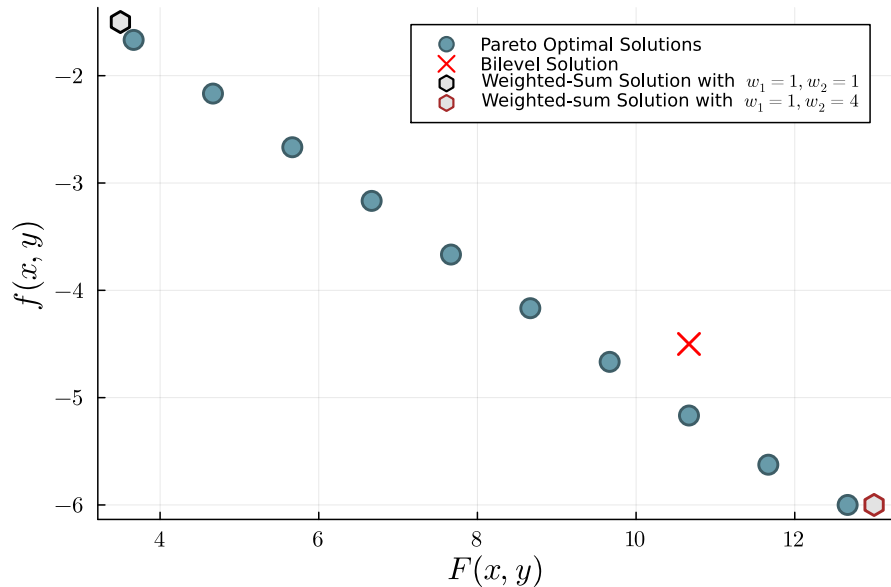


Figure 2.8. Pareto front of the multi-objective program of PROBLEM 2.11 represented in the objective space. Additionally, this figure shows the bilevel optimal solution of PROBLEM 2.10 and two Pareto optimal solutions obtained with a weighted-sum method to solve the multi-objective problem

Chapter 3

A STORY OF DATA

This chapter aims to introduce to the input data required for the implementation of our bilevel DNDP model.

3.1 Load Profiles

In order to devise strategies for the reinforcement of distribution networks, it is of paramount importance to develop a means of generating long-term electricity load forecasts across the planning horizon, typically ranging from 10 to 30 years. This task can be very challenging due to the complex nature of electricity load time series. These time series contain daily, weekly, and seasonal fluctuations, along with stochastic components linked, for instance, to grid users' electricity consumption patterns, the time of the year, the LCTs used, etc.

Within the context of the DNDP problem, numerous approaches exist for considering the electricity load forecasts on which the network reinforcement decisions will be based. One potential approach involves taking into account a single power injection profile, e.g. the worst-case moment of the year. This method is adopted in the DNEP formulations presented in [12] and [23]. This solution might lack accuracy as it is difficult to select the worst-case moment of the year, especially with the massive integration of RES and LCT. An alternative strategy involves selecting a set of representative daily load profiles that aim to capture diverse situations throughout a year. These profiles could correspond to typical weekdays, weekend days, winter days, summer days, and more. They are generally generated through the use of machine learning techniques. For instance, a method based on the K-means algorithm to generate representative days for expansion decisions in power systems is proposed in [48]. Although this approach accounts for a broader number of scenarios and thus enhances long-term load forecasting accuracy, the task of finding a large number of representative days over a long planning horizon remains complex.

For this reason, this master thesis considers only **two representative days**: one occurring in the summer and the other in winter. We are aware that this choice is limiting as those days won't be able to capture the weekly fluctuations of the electricity consumption as well as the consumption habits during autumn and spring. In the future, it will therefore be necessary to expand the number of representative days to achieve more accurate results with our DNDP model. In this work, the electricity load data is drawn from reference [8], which provides a dataset of load profiles for each of the two representative days. Every dataset is stored in an Excel file, containing 100 columns that correspond to distinct residential daily load profiles, and spanning 288 rows to account for the number of 5-minute time steps in a day. It is also essential to add that the loads are assumed to have an inductive power factor equals to 0.95. These profiles are derived from a computational model developed by CREST (Centre for Renewable Energy Systems Technology) at Loughborough University [49], which builds profiles based on variables such as the number of occupants in a household, the type of day, the month, and the uses of the appliances [8]. Moreover, the profiles within each dataset are chosen in a way that reflects the UK statistics on household composition. This means maintaining in the dataset the same proportions of profiles from single-person households (29%), two-person households (35%), three-person households (16%), and households with four or more occupants (20%) as found in the UK population.

FIGURE 3.1 illustrates the daily load profiles that are contained in the dataset focused on the summer scenario. Specifically, FIGURE 3.1a presents three examples of profiles from the dataset collection. This figure highlights the variability in peak consumption times across the day, along with disparities in peak consumption magnitudes among the diverse load profiles. Besides, FIGURE 3.1b displays the collective trend that emerges from aggregating all load profiles, indicating a common trend of high consumption during both the morning hours (i.e. approximately between 6 AM and 8 AM) and the evening hours (i.e. approximately between 8 PM and 10 PM).

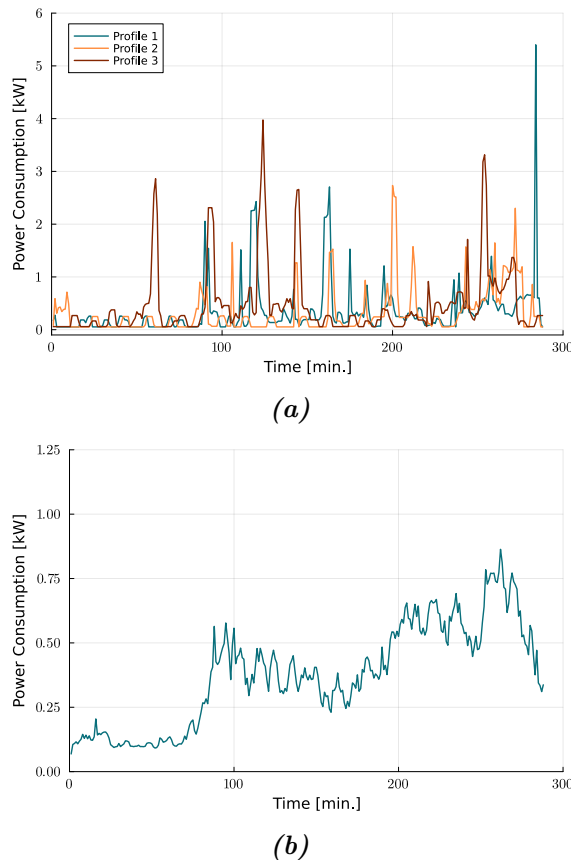


Figure 3.1. Daily load profiles in summer: (a) three individual profiles from the dataset, (b) the mean aggregated profile of the dataset (from [8]).

On the other hand, FIGURE 3.2 depicts the daily load profiles contained in the dataset centered around the winter scenario. Similar conclusions to those drawn during the summer period can be made while examining FIGURE 3.2, with the exception that the peak value of the aggregated profile seen in FIGURE 3.2b is roughly 15% higher compared to the summer case. Furthermore, the time at which the evening peak consumption begins shifts earlier (i.e. around 5 PM) in contrast to the summer scenario (i.e. around 8 PM).

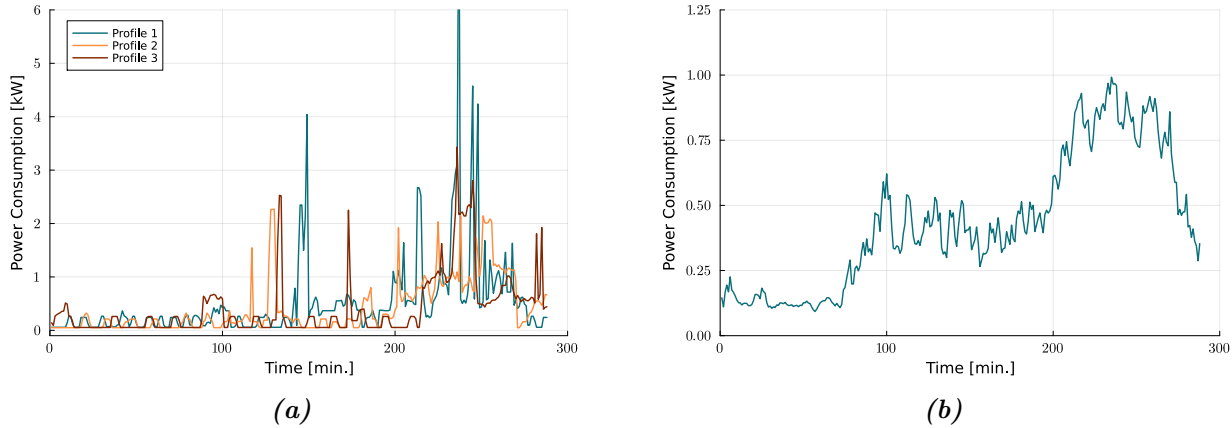


Figure 3.2. Daily load profiles in winter: (a) three individual profiles from the dataset, (b) the mean aggregated profile of the dataset (from [8]).

3.2 Low Carbon Technologies Profiles

To investigate the impact of LCTs on distribution network planning, acquiring profiles for these technologies is essential. In this work, we have opted to integrate the option of incorporating two categories of LCT profiles into users' daily consumption profiles: electric vehicles (EVs) and electric heat pumps (EHPs) profiles. These profiles are available in the EHP and EV profile datasets sourced from the same reference as the load profiles datasets [8]. Those datasets share the same shape as the load profiles datasets described in SECTION 3.1. Besides, a unit power factor is assumed for both datasets. A single dataset is available for each LCT technology, as these profiles are only defined for the winter day. To account for the use of these profiles during the summer day, this thesis introduces a summer/winter scaling factor, denoted $\sigma_{s/w}^x \in [0, 1]$, where x represents a profile to scale. This factor allows to define the summer profile of a LCT as being a scaled version of its worst-case winter profile. In this study, $\sigma_{s/w}^{EHP}$ is set to zero for EHP profiles, meaning they are only used for heating during the winter period. Additionally, for EV, $\sigma_{s/w}^{EV}$ is set to 1, implying that grid users possessing an EV maintain the same usage pattern for their vehicle in both winter and summer seasons.

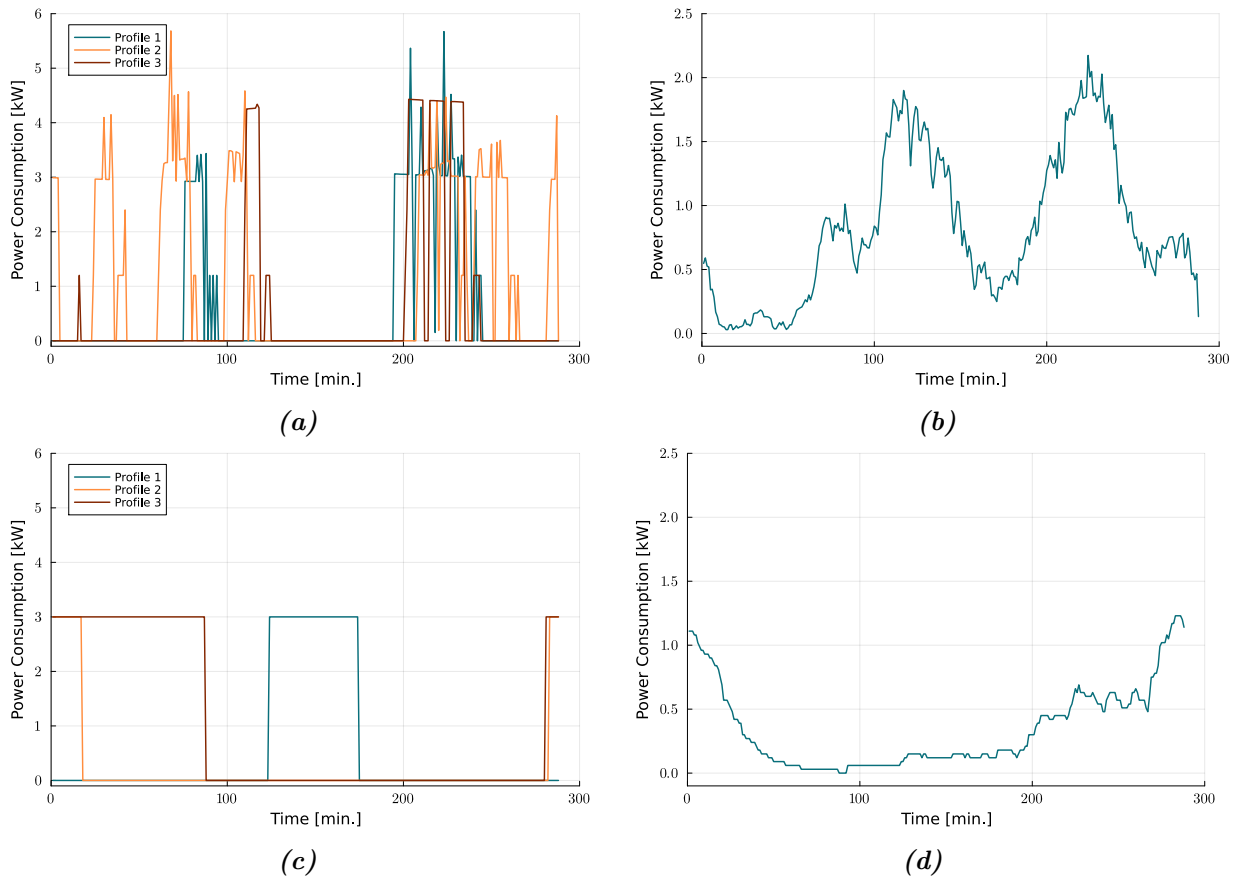


Figure 3.3. Daily LCTs profiles in winter: (a) three individual profiles from the EHPs dataset, (b) the mean aggregated profile of the EHPs dataset (from [8]), (c) three individual profiles from the EVs dataset (d) the mean aggregated profile of the EVs dataset (from [8]).

FIGURE 3.3 illustrates individual and aggregated LCTs profiles contained in the two datasets from [8]. Specifically, FIGURES 3.3a and 3.3b present the power consumption profile of three distinct EHP units and the aggregated mean profile of the dataset 100 EHP units, respectively. This aggregated EHP profile, as depicted in Figure 3.3b, exhibits an average peak demand of approximately 2 kW. Concerning EV profiles, Figures 3.3c and 3.3d demonstrate the charging power profiles of three individual EV units and the mean profile of the dataset 100 EV units, respectively. Notably, Figure 3.3c reveals a charging capacity of 3 kW. Additionally, Figure 3.3d indicates that high charging powers predominantly occur during the nighttime hours, with a peak charging power value of around 1.2 kW occurring at approximately 11 PM.

3.3 PV Profiles

In this work, we limit our analysis to residential PV installations for evaluating the effects of RES on distribution networks. While various RES options, such as wind power generation or larger PV installations, can impact distribution networks, our primary focus remains on RES installations feasible within households. Profiles representing PV power production during a representative summer day are available in a dataset provided by [8].

This dataset shares the same number of profiles and time granularity as the datasets described in SECTIONS 3.1 and 3.2. All 100 daily PV production profiles from the dataset are based on the same solar irradiance data but exhibit variations proportional to the PV installation capacity. This is a consequence of the fact that in distribution networks, the users are often located within a same restricted geographical area.

Only one dataset for PV production profiles is accessible, containing profiles for optimal summer conditions. In this thesis, we derive winter PV production profiles from the best-case summer profiles by employing a scaling factor $\sigma_{w/s}^{PV} \in [0, 1]$. We set this factor to 0.1, translating a 90% reduction in winter PV production compared to summer PV production.

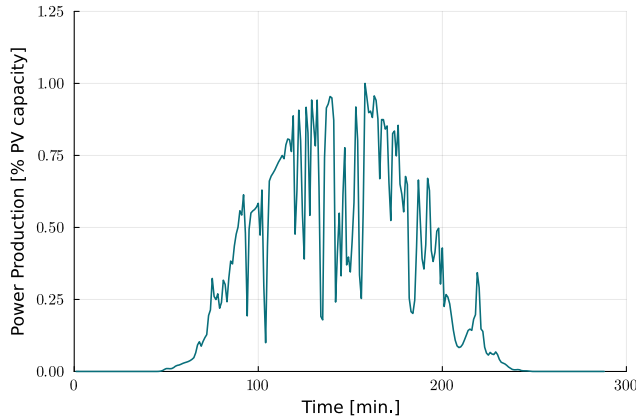


Figure 3.4. Normalized daily PV production profile expressed as a percentage of the maximum power capacity of the PV installation (from [8]).

3.4 Profiles Summary

The purpose of this section is to provide a summary table of the power demand and production time-series described in SECTIONS 3.1 to 3.3. This summary table corresponds to TABLE 3.1. In this table, #profiles denotes the count of distinct profiles within a dataset, Δt is the dataset time granularity, $\cos(\phi)$ represents the considered power factor, and σ represents the scaling factor between summer and winter profiles when only one dataset is available for either of these seasons.

Dataset	#profiles [-]	Δt [min.]	$\cos(\phi)$ [-]	σ [-]
Summer Loads	100	5	0.95 (inductive)	—
Winter Loads	100	5	0.95 (inductive)	—
Winter EHPs	100	5	1.0	$\sigma_{s/w}^{EHP} = 0$
Winter EVs	100	5	1.0	$\sigma_{s/w}^{EV} = 1$
Summer PV	100	5	—	$\sigma_{w/s}^{PV} = 0.1$

Table 3.1. Characteristics of the load profiles, LCTs profiles and PV profiles datasets.

3.5 Test Network

When building DNDP models, it is crucial to verify our formulation with test networks before applying it to real-world network instances. In this master thesis, the 23-node test network of [50] is employed for this purpose. This network is a balanced 34.5kV medium voltage network that contains 23 buses and 34 possible line routes, as illustrated in FIGURE 3.5. Among the buses, there are two possible substations and 21 nodes with loads that we consider independent users of the network. For each line routes, four types of conductors can be used when it is built. The characteristics of these conductors are listed in TABLE 3.2. The load data of TABLE VI in [50] is used for testing the DNEP models proposed in [12] and [23]. For the simulations presented in this master thesis, the load and generation profiles at buses of the network are the ones described in section 3.1 to 3.3. The load profiles are however scaled so that the peak of the total consumption is equal to 7 MVA on a five-minute time scale, as in TABLE VI in [50]. This results in a total energy consumed in the network of 16440 MWh/year.

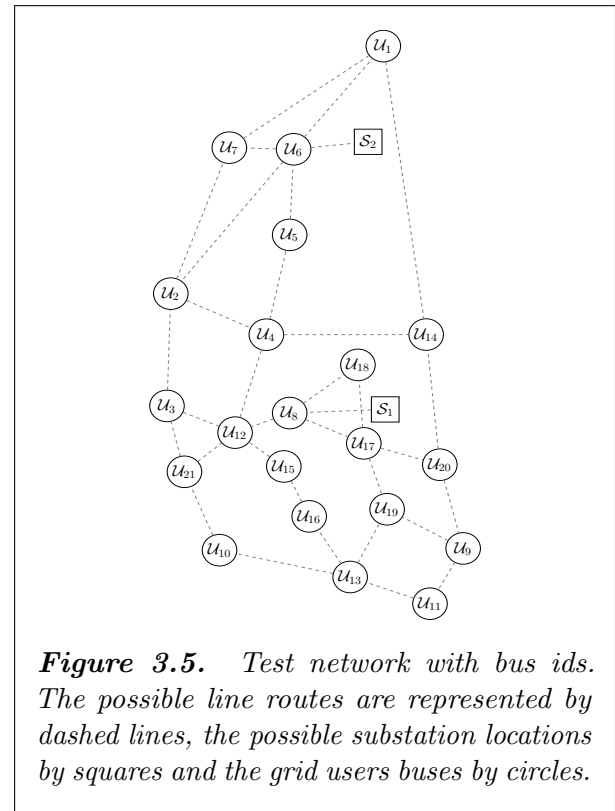


Figure 3.5. Test network with bus ids. The possible line routes are represented by dashed lines, the possible substation locations by squares and the grid users buses by circles.

Code word	q [mm^2]	r [Ω/km]	x_l [Ω/km]	i_{\max} [kA]	cost [$\text{k€}/\text{km}$]
Poppy	53.50	0.5502	0.429	0.23	10
Oxlip	107.3	0.2747	0.402	0.34	12
Daisy	135.3	0.2180	0.394	0.46	15
Tulip	170.6	0.1732	0.381	0.53	20

Table 3.2. All Aluminum Conductors (data from [51]).

Chapter 4

MICROGRID OPTIMIZATION

4.1 Description of the problem

The lower-level problem of our bilevel approach is obtained by combining the optimization programs solved by the users of a distribution grid. Specifically, each user's optimization program is an instance of the widely studied *microgrid optimization* problem, aimed at finding the optimal investment decisions in generating (and storage) units as well as the optimal energy usage decisions over a defined planning horizon. This problem is assumed to be *single-stage* as the investment decisions related to generating (and storage) units are taken at the beginning of the planning horizon and have, thereby, influence on this entire horizon.

As we want to optimize simultaneously the strategies of several grid users, the lower-level can be classified as a multi-objective (MO) optimization program, with distinct objective functions corresponding to each user's optimization objectives. Since this study excludes local energy communities, grid users are independent of each other as there is no energy exchange opportunity. As a result, the problem can be presented either individually for each user or collectively as a unified problem. This unified problem can be achieved through the aggregation of user-specific objective functions using a weighted-sum methodology. In our formulation of the lower-level problem, we employ the latter methodology to shape the objective function.

Moreover, our intention is for the upper-level formulation to be based on two assumptions that simplify the representation of our model:

- *Users are modeled as perfectly rational agents*, capable of optimizing their investment decisions and energy consumption considering factors like equipment costs and grid connection capacity. This rationality extends to them having complete knowledge of the future.
- *User demand is fixed*. This assumption excludes the possibility of demand-side flexibility in the distribution network.

4.2 The Lower-Level Optimization Program

This section describes the optimization program designed for addressing the MO microgrid optimization problem described in the previous section. In this section, the sets, indices, parameters, and variables that compose our formulation are precisely defined. Subsequently, the MO microgrid optimization problem is formalized as a LP program. As explained in SECTION 2.5, we seek to achieve a LP formulation for the lower-level problem because it allows the single-level reformulation of the BP program through the utilization of the KKT conditions and, therefore, reduces the computational burden of our BP model.

Notations

Sets and indices

t	index of a time period
T	number of time periods
\mathcal{T}	set of time periods, with $\mathcal{T} = \{1, 2, \dots, T\}$
i	index of a grid user
n_u	number of grid users
\mathcal{B}_U	set of grid users, with $\mathcal{B}_U = \{1, 2, \dots, n_u\}$

Parameters

$p_{i,t}^D$	active power demand of user i at time period t , in kW
$q_{i,t}^D$	reactive power demand of user i at time period t , in kVar
$P_{i,t}^{PV}$	shape of the forecast power generation profile of the PV installation of user i at time period t , in $[0, 1]$
Δt	duration of a time period, in hours
γ^{PVC}	amortization period of a power converter, in years
γ^{PV}	amortization period of a PV installation, in years
α	scaling factor of the simulation, such that $\alpha = d^{year}/d^{rep}$
d^{rep}	number of representative days
d^{year}	number of days in a year
π^{PVC}	unitary cost for converter capacity, in €/kW
π^{PV}	unitary cost for installed PV peak power capacity in €/kWp
π^{GC}	unitary cost for grid connection capacity, in €/kW
π^{EI}	unit price of energy imported from the grid at time period t , in €/kWh
π^{EE}	unit price of energy exported to the grid at time period t , in €/kWh
Π^{EI}	grid tariff imposed by the DNO on the energy imported from the grid at time period t , in €/kWh
Π^{EE}	grid tariff imposed by the DNO on the energy exported to the grid at time period t , in €/kWh

Variables

c_i^{PV}	total PV investment costs of user i , in €
c_i^{grid}	total grid capacity costs of user i , in €
$c_{i,t}^{grid}$	grid tariff costs of user i at time period t , in €
$c_{i,t}^{imp}$	total cost of user i for the energy imported from the grid at time t , in €
$c_{i,t}^{exp}$	total revenue of user i for the energy exported to the grid at time period t , in €
\bar{s}_i^{PVC}	maximum power capacity of the PV converter of user i , in kW
\bar{p}_i^{PV}	peak power capacity of the PV installation of user i , in kW
\bar{s}_i^{grid}	grid connection capacity of user i , in kVA
$p_{i,t}^{imp}$	active power imported from the grid for user i at time period t , in kW
$q_{i,t}^{imp}$	reactive power imported from the grid for user i at time period t , in kVar
$p_{i,t}^{exp}$	active power exported to the grid by user i at time period t , in kW
$q_{i,t}^{exp}$	reactive power exported to the grid by user i at time period t , in kVar
$p_{i,t}^{PV}$	active power produced by the PV installation of user i at time period t , in kW
$q_{i,t}^{PV}$	reactive power produced by the PV installation of user i at time period t , in kW
$\mathcal{P}_{i,t}^{PV}$	polyhedron defining the PV installation PQ diagram of user i at time period t

Formulation

The LP optimization program proposed as the lower-level problem of our bilevel approach is the following:

Lower-Level Formulation

$$\min \sum_{i \in \mathcal{B}_u} (c_i^{PV} + c_i^{grid}) + \sum_{i \in \mathcal{B}_u} \alpha \sum_{t \in \mathcal{T}} (c_{i,t}^{imp} - c_{i,t}^{exp} + c_{i,t}^{grid}) \quad (4.1a)$$

$$\text{s.t.: } c_i^{PV} = 1/\gamma^{PVC} \cdot (\bar{s}_i^{PVC} \cdot \pi^{PVC}) + 1/\gamma^{PV} \cdot (\bar{p}_i^{PV} \cdot \pi^{PV}) \quad \forall i \in \mathcal{B}_U \quad (4.1b)$$

$$c_i^{grid} = \bar{s}_i^{grid} \cdot \pi^{GC} \quad \forall i \in \mathcal{B}_U \quad (4.1c)$$

$$c_{i,t}^{grid} = (p_{i,t}^{imp} \cdot \Pi^{EI} + p_{i,t}^{exp} \cdot \Pi^{EE}) \cdot \Delta t \quad \forall i \in \mathcal{B}_U, \forall t \in \mathcal{T} \quad (4.1d)$$

$$c_{i,t}^{imp} = p_{i,t}^{imp} \cdot \pi^{EI} \cdot \Delta t \quad \forall i \in \mathcal{B}_U, \forall t \in \mathcal{T} \quad (4.1e)$$

$$c_{i,t}^{exp} = p_{i,t}^{exp} \cdot \pi^{EE} \cdot \Delta t \quad \forall i \in \mathcal{B}_U, \forall t \in \mathcal{T} \quad (4.1f)$$

$$p_{i,t}^{imp} - p_{i,t}^{exp} = p_{i,t}^D - p_{i,t}^{PV} \quad \forall i \in \mathcal{B}_U, \forall t \in \mathcal{T} \quad (4.1g)$$

$$q_{i,t}^{imp} - q_{i,t}^{exp} = q_{i,t}^D - q_{i,t}^{PV} \quad \forall i \in \mathcal{B}_U, \forall t \in \mathcal{T} \quad (4.1h)$$

$$p_{i,t}^{imp} \leq \bar{s}_i^{grid} \quad \forall i \in \mathcal{B}_U, \forall t \in \mathcal{T} \quad (4.1i)$$

$$q_{i,t}^{imp} \leq \bar{s}_i^{grid} \quad \forall i \in \mathcal{B}_U, \forall t \in \mathcal{T} \quad (4.1j)$$

$$p_{i,t}^{exp} \leq \bar{s}_i^{grid} \quad \forall i \in \mathcal{B}_U, \forall t \in \mathcal{T} \quad (4.1k)$$

$$q_{i,t}^{exp} \leq \bar{s}_i^{grid} \quad \forall i \in \mathcal{B}_U, \forall t \in \mathcal{T} \quad (4.1l)$$

$$p_{i,t}^{PV} \leq \bar{s}_i^{PVC} \quad \forall i \in \mathcal{B}_U, \forall t \in \mathcal{T} \quad (4.1m)$$

$$p_{i,t}^{exp} \leq p_{i,t}^{PV} \quad \forall i \in \mathcal{B}_U, \forall t \in \mathcal{T} \quad (4.1n)$$

$$(p_{i,t}^{PV}, q_{i,t}^{PV}) \in \mathcal{P}_{i,t}^{PV} \quad \forall i \in \mathcal{B}_U, \forall t \in \mathcal{T} \quad (4.1o)$$

$$(\text{+ storage constraints}_t) \quad \forall t \in \mathcal{T} \quad (4.1p)$$

In this formulation, the objective function is built by aggregating the investment costs and energy usage costs of all users of the distribution grid. Specifically, the objective function in EQUATION (4.1a) sums the total expenditures on local generation investments, i.e. $\sum_{i \in \mathcal{B}_u} c_i^{PV}$, the grid connection capacity expenses, i.e. $\sum_{i \in \mathcal{B}_u} c_i^{grid}$, the electricity import costs, i.e. $\sum_{i \in \mathcal{B}_u} \alpha \sum_{t \in \mathcal{T}} c_{i,t}^{imp}$ and the energy grid tariffs imposed by the DNO to users that use its network, i.e. $\sum_{i \in \mathcal{B}_u} \alpha \sum_{t \in \mathcal{T}} c_{i,t}^{grid}$. This sum is then diminished by the revenues derived from electricity injected into the grid, i.e. $\sum_{i \in \mathcal{B}_u} \alpha \sum_{t \in \mathcal{T}} c_{i,t}^{exp}$. The definition of the costs constituting the objective function are available in CONSTRAINTS (4.1b) to (4.1f). Moreover, the factor α in the objective function expression represents the scaling factor that allows to recover the yearly values of the costs from a simulation with a number d^{rep} of representative days.

The primary decision variables of this model consist of the grid connection capacity (\bar{s}_i^{grid}), the PV installation size (\bar{p}_i^{PV}), and the active and reactive power exchanges ($p_{i,t}^{imp}$, $q_{i,t}^{imp}$, $p_{i,t}^{exp}$, $q_{i,t}^{exp}$) with the grid at each time step.

Regarding constraints, CONSTRAINTS (4.1g) and (4.1h) correspond to the bus active and reactive power balances for all time steps, respectively. CONSTRAINTS (4.1i) and (4.1j) bound the apparent power imported from the grid at each time step, whereas CONSTRAINTS (4.1k) and (4.1l) bound the apparent power injected to the grid at each time step. Together, CONSTRAINTS (4.1i) to (4.1m) therefore define the grid connection capacity. Furthermore, CONSTRAINT (4.1m) restricts the active power generated by the PV plant at each time step and CONSTRAINT (4.1n) imposes that the power exported by a grid user must be lower than its PV plant production at each time step. Finally, CONSTRAINT (4.1o) specifies that the active and reactive power operating points of a PV plant must fall within its PQ diagram at every time step. We want the PQ diagram to be defined by linear relationships which implies that it needs to be a polyhedron. In this thesis, we do not include the PQ diagram in our formulation, as the decision was made to disregard the reactive power associated with a PV plant, i.e. $q_{i,t}^{PV}$. At present, this assumption seems to be valid in practice due to the absence of configuration in PV converters for managing reactive power to regulate voltage at an electric bus. Indeed, when bus voltage exceeds the acceptable operational limits, PV converters are promptly deactivated, resulting in the complete loss of PV power generation. Given these considerations, CONSTRAINT (4.1o) is simplified to:

$$p_{i,t}^{PV} \leq \bar{p}_i^{PV} \cdot P_{i,t}^{PV} \quad \forall i \in \mathcal{B}_U, \forall t \in \mathcal{T} \quad (4.2)$$

EQUATION (4.2) thus constrains the PV power generation of user i 's PV installation to be bounded at each time step t by the PV generation forecast at that same time step t .

4.3 Adding Storage

The microgrid optimization problem can be enhanced by introducing the possibility for grid users to use storage devices. This is highlighted in PROBLEM 4.1 with CONSTRAINT (4.1p). In order to introduce storage in this optimization program, the active power balance written in EQUATION (4.1g) must be adapted to integrate the charging power $p_{i,t}^{stc}$ and the discharging power $p_{i,t}^{sts}$ of the storage unit of user i at time period t . Both variables are expressed in kW. This results in the following power balance:

$$p_{i,t}^{imp} - p_{i,t}^{exp} = p_{i,t}^D - p_{i,t}^{PV} + p_{i,t}^{stc} - p_{i,t}^{std} \quad \forall t \in \mathcal{T}, \forall i \in \mathcal{B}_U \quad (4.3)$$

Furthermore, it is necessary to augment the problem formulation with equations that characterize the battery's charging and discharging dynamics. To achieve this, it is imperative to integrate an equation that updates the state of charge, i.e. $SOC_{i,t}$, based on its previous state and the charging and discharging powers of user i 's storage unit at time period t . Such equation requires to know two additional parameters: the charging efficiency, i.e. ϵ^{stc} , and the discharging efficiency, i.e. ϵ^{std} . These efficiencies are considered as constant regardless of the storage unit's state of charge and take values within the $[0, 1]$ interval. Besides, it is essential to note that our optimization program time frame, i.e. T , integrates multiple representative days. To decorrelate the distinct representative days, we suggest a boundary condition wherein storage units initial state of charge are established at the beginning of each representative day. Additionally, we introduce a constraint that ensures storage units state of charge remain below their storage capacity. Let \mathcal{T}^1 and \mathcal{T}^{end} denote the set of initial time periods and final time periods across all representative days, respectively. The storage dynamics is subsequently represented by the following linear constraints:

$$SOC_{i,t} = e_i^{st,init} \cdot \bar{e}_i^{st} \quad \forall i \in \mathcal{B}_U, \forall t \in \mathcal{T}^1 \quad (4.4a)$$

$$SOC_{i,t} = SOC_{i,t-1} + (\epsilon^{stc} \cdot p_{i,t}^{stc} - 1/\epsilon^{std} \cdot p_{i,t}^{std}) \cdot \Delta t \quad \forall i \in \mathcal{B}_U, \forall t \in \mathcal{T} \setminus (\mathcal{T}^1 \cup \mathcal{T}^{end}) \quad (4.4b)$$

$$SOC_{i,t} \leq \bar{e}_i^{st} \quad \forall i \in \mathcal{B}_U, \forall t \in \mathcal{T} \quad (4.4c)$$

where \bar{e}_i^{st} represents the energy storage capacity of a storage unit, expressed in kWh, $e_i^{st,init} \in [0, 1]$ is a parameter that sets the initial state of a storage unit as being a proportion of its energy capacity.

To conclude, adding storage to the lower-level model described in SECTION (4.2) introduces four additional variables, i.e. \bar{e}^{st} , SOC , p^{stc} and p^{std} , and three additional parameters, i.e. ϵ^{stc} , ϵ^{std} and $e_i^{st,init}$, to the model in SECTION (4.2). It also requires the addition of CONSTRAINTS (4.4a) to (4.4c). Furthermore, adding storage maintains the LP property of the optimization program.

Chapter 5

DISTRIBUTION NETWORK EXPANSION PLANNING

This chapter begins by recalling the objectives of the DNDP bilevel optimization program that we aim to establish in this master thesis. Subsequently, it explains the modular implementation in Julia [52] used for evaluating various configurations of the bilevel formulation. Finally, two sensitivity analyses are carried out. The first analysis is performed without making changes to the model formulation, whereas the second analysis utilizes the modular implementation to explore additional configurations.

5.1 Description of the Problem

As explained in SECTION 1.3, we want to derive the upper-level problem, or leader, of our bilevel model from the well-known distribution network expansion planning (DNEP) problem. The instance of the DNEP problem that we want to solve in our upper-level problem corresponds to the optimization problem that is solved by the distribution network operator (DNO) that seeks the following objectives:

1. The DNO aims to identify the optimal investment decisions for conductors and substations within a specified planning horizon, typically spanning from 10 to 30 years. Optimal decisions correspond to strategies that reduce both the initial capital expenditure (CAPEX) associated with investments in conductors and substations, as well as the continuous operational costs (OPEX), represented by the cost of losses in the network.
2. The distribution network topology resulting from these choices should ensure the connection of all grid users to a substation. Mathematically, this requirement translates to seeking a distribution network graph that is *radial*.
3. The distribution network must have the capacity to accommodate the predicted electricity demand from users throughout the entire planning period.

4. The distribution network needs to have a high *reliability*, which implies satisfying the operational constraints on bus voltages and line currents.
5. The money invested by the DNO, plus a margin to remunerate its activities has to be recovered through the network tariffs applied to the grid users. This is the so-called *budget-balance* constraint.

Moreover, a series of assumptions are introduced to simplify the formulation of our upper-level model:

- We approach our problem as if we are creating an entirely new distribution network. However, our model can be easily adapted to model an already existing network.
- As for the lower-level problem described in CHAPTER 4, the upper-level problem is *single-stage*. This implies that the DNO makes investment decisions only once, at the beginning of the planning period.
- A single-phase equivalent network is considered, assuming a balanced three phase regime. Nevertheless, especially in the context of distribution networks, an unbalanced three-phase representation is often more suitable. Investigating this aspect should be a focus of future research.

5.2 The AC Power Flow Equations

To be able to satisfy the third and fourth objectives described in SECTION 5.1, the DNO must be able to forecast the state of its network throughout the whole planning horizon. This is done by introducing in the DNEP problem the well-known *AC power flow equations*. These equations allow to determine the active and reactive power flows through the network from input data such as the topology of the network as well as the power injections and voltage at nodes of the network. For a more detailed explanation of the AC power flow equations, we recommend the following reference [53]. These equations form the key constraints in the DNEP problem as much of the complexity of the optimization program resulting from this problem depends on the formulation of the AC power flow equations that is used. In their exact formulation, this set of constraints introduce nonlinear relationships between the voltage phasors and the power injection at buses of a power system. When the exact formulation is used, the DNEP problem therefore results in a mixed-integer nonlinear program (MINLP), which, as described in SUBSECTION 2.4.4 of CHAPTER 2, is both NP-hard to solve and incomputable. In other words, there is no guarantee that an efficient solution method exists for addressing such problems, and moreover, no existing method is capable of solving every type of MINLP problem.

This results in the need to simplify the DNEP formulation to have an optimization program that becomes more tractable to solve. In the literature, there exist approximation and convex relaxation methods that are aimed to simplify the AC power flow equations formulation. The two concepts are illustrated in FIGURE 5.1 found in the book by Daniel K. Molzahn and Ian A. Hiskens [54].

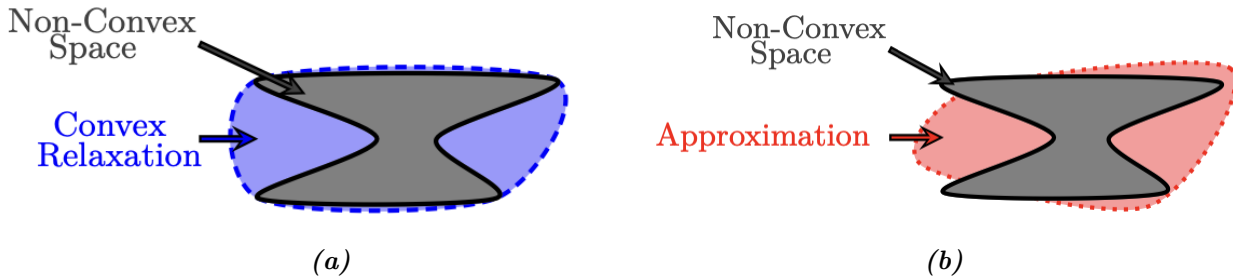


Figure 5.1. Conceptual illustrations showing a convex relaxation (blue region on SUBFIGURE (a)) and an approximation (red region on SUBFIGURE (b)) for the gray non-convex space (figure taken from [54]).

This master thesis focuses on employing convex relaxations of AC power flow equations to incorporate into our upper-level problem, as they can allow, if some sufficient conditions are satisfied, to provide the global optimal solution for certain classes of optimization programs. We provide a concise overview of the theory behind these relaxations in this section, drawing information from the reference book [54].

5.2.1 Power Flow Convex Relaxations

Jabr's relaxation

Jabr's relaxation provides a second-order cone programming (SOCP) relaxation for the AC power flow equations in the context of a radial balanced, single-phase equivalent network representation. This relaxation technique was introduced by Jabr in his paper titled “Radial distribution load flow using conic programming” [55]. It is based on the bus-injection model (BIM) of the power flow equations, which is a representation of the power flow equations that relate the electrical quantities at each bus. We refer the readers to the SUBSECTION 2.1.1 in CHAPTER 2 of [54] for a detailed presentation of the mathematical formulations of power flow equations in the context of BIM representations. Based on this power flow equations representation, Jabr's relaxation then transforms an equality into inequality to establish a rotated SOCP constraint. In [54], it is stated that Jabr's relaxation accurately captures radial networks, but does not inherently ensure consistent angles around cycles in mesh networks.

The Branch-Flow Relaxation

The Branch-Flow relaxation provides also a second-order conic programming (SOCP) relaxation for the AC power flow equations in the context of a radial balanced, single-phase equivalent network representation. The primary differentiation from Jabr's approach lies in the representation of the AC power flow equations on which the relaxation is constructed. Indeed, as its name indicates, the Branch-Flow relaxation is based on the Branch-Flow Model (BFM) representation of the power flow equations in a radial network, also called the DistFlow Equations [56]. In contrast to the BIM representation which formulates power flow equations in relation to quantities at individual buses, the DistFlow equations focus on the quantities flowing through the lines of the network. We refer the readers to the SUBSECTION 2.1.2 in CHAPTER 2 of [54] for a detailed presentation of the mathematical formulations of power flow equations in the context of BFM representations. According to [54], this relaxation has the same tightness as Jabr's relaxation and also neglects the voltage phase angles.

In [54], it is stated that the BFM relaxation is stronger than the Jabr's relaxation in terms of numerical convergence characteristics because it avoids the existence of variables that share the same values. In particular, the authors of the book state that the numerical superiority of the BFM is further enhanced when considering three-phase power flow models and large-scale single-phase systems.

5.3 The Radiality Constraints

The second objective of the DNO that is stated in SECTION 5.1 amounts to finding a topology of the distribution network that is such that the graph $\mathcal{G} = \{\mathcal{B}, \mathcal{E}\}$ describing the distribution network is *radial*. In this graph, the nodes \mathcal{B} correspond to electrical buses and edges \mathcal{E} are routes between buses where conductors can be placed to develop the distribution network. Some electrical buses are candidate substations where the distribution network under consideration can connect to a higher-voltage network, which is assumed already developed, and withdraw or inject power. Buses are indexed as $1, 2, \dots, n$ and the candidate substations buses \mathcal{B}_s are the first $n_s < n$ indices. Users can connect to the distribution network at buses that are not candidate substations, that is, buses $\mathcal{B}_u = \mathcal{B} \setminus \mathcal{B}_s$. The radial topology that we are looking consists in finding one or several distribution networks out of \mathcal{G} such that all users are connected to a substation. Each distribution network must contain only one substation and have a radial structure to be coherent with the usual distribution network operation rules. Mathematically, we want the optimal topology $\mathcal{G}^* = \bigcup \mathcal{G}_i(\mathcal{B}_i, \mathcal{E}_i)$, $\mathcal{B} = \bigcup \mathcal{B}_i$, $\bigcap \mathcal{B}_i = \emptyset$, $\bigcup \mathcal{E}_i \subseteq \mathcal{E}$, where \mathcal{E}_i contains selected routes that form a spanning tree of \mathcal{B}_i , $\forall i$, $\bigcap \mathcal{E}_i = \emptyset$, and each \mathcal{B}_i contains one substation node.

The network graph \mathcal{G} must therefore be defined by one or several spanning trees. Such graph is called a *spanning forest* or a κ -tree where κ represents the number of substations nodes [57]. Examples of spanning tree and spanning forest are depicted in FIGURE 5.2 taken from [57].

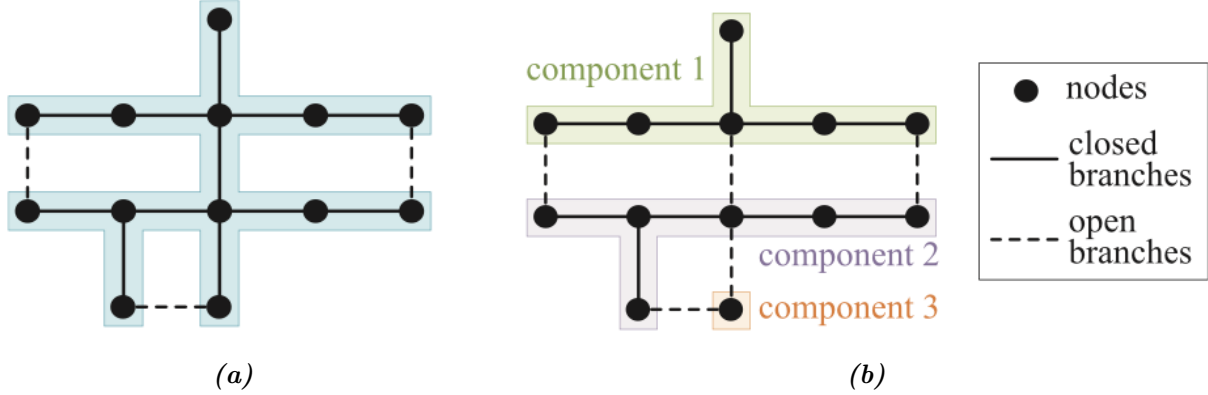


Figure 5.2. (a) A spanning tree, (a) A spanning forest. In this figure, open branches indicate potential locations for line routes in the distribution network where lines are not built, while closed branches correspond to locations where lines are built (figure taken from [57]).

To achieve this purpose, the DNEP models in [12] and [23] propose a simple radiality constraint formulation that amounts to say that the number of lines built in the network should be equal to the number of load buses n_u . This constraint is however not sufficient when we integrate distributed generation (DG) units in the distribution network, which is the case in our bilevel optimization program. For this reason, it is required to introduce loop elimination constraints in our upper-level formulation. We decided to test the three loop elimination proposed in [12]:

- **single-commodity flow constraints,**
- **multi-commodity flow constraints** and,
- **spanning tree constraints.**

5.4 Examples of DNEP Models from the Literature

Before deriving the formulation for the upper-level of our bilevel model, two versions of the DNEP problem available in the literature were studied. The first DNEP model, proposed in [12], consists in a MISOCP optimization program based on Jabr's SOCP relaxation of the power flow equations. On the other hand, [23] proposes a MISOCP model based on a BFM convex relaxation. The two models possess nearly identical objective functions and share a substantial number of constraints. Consequently, their differentiation lies primarily in the type of convex relaxation employed for the power flow equations.

The implementation of MISOCP formulations was carried out to facilitate a comparison between Jabr's convex relaxation and the BFM relaxation when integrated into a DNEP model. For our testing, we utilized the 23-node test network described in SECTION 3.5 of CHAPTER 3. The load data utilized corresponds to the dataset provided in TABLE VI in [50], which yields a total peak demand of 7.04 MVA. We allowed the selection from four conductor types for constructing line routes. The physical characteristics of these four conductors are provided in TABLE 3.2 from CHAPTER 3. Additionally, we assumed a substation construction cost of 1000 k€/MVA, a substation operation cost of 0.0001 k€/kVA², a power factor $\cos(\phi)$ of 0.95, a time step length Δt of one hour, a line loss factor of 0.35, an interest rate of 0.1 for both substations and circuits, and a loss cost of 0.05 €/kWh. We considered maximum and minimum voltage limits of respectively 0.95 per unit and 1.05 per unit, respectively. Substations that are built are assigned a voltage magnitude of 1 per unit.

We limited the planning horizon to one year, specifically for the purpose of comparing the two models. Both models were implemented in the Julia programming language [52], utilizing the JuMP library [58], and solved with the Gurobi [39] MIP solver. The results of our experiment are presented in TABLE 5.1 and the resulting networks in FIGURE 5.3.

Model	Objective [k€/year]	Gap [%]	Solve Time [sec.]	# binary	# continuous	# constraints	# quad. constraints
Jabr	1286.0	0	131.1	172	4716	2944	138
BFM	1285.0	0	0.4977	206	738	1809	36

Table 5.1. Results of the implementation of the MISCOP programs proposed in [12] and [23]

where “Gap” denotes the MIP gap in the solution provided by the Gurobi solver “Objective” denotes the objective function value at optimality, “# binary” indicates the count of binary variables in the model, “# continuous” indicates the count of continuous variables in the model, “# constraints” represents the total quantity of constraints, and finally, “# quad. constraints” represents the number of quadratic constraints.

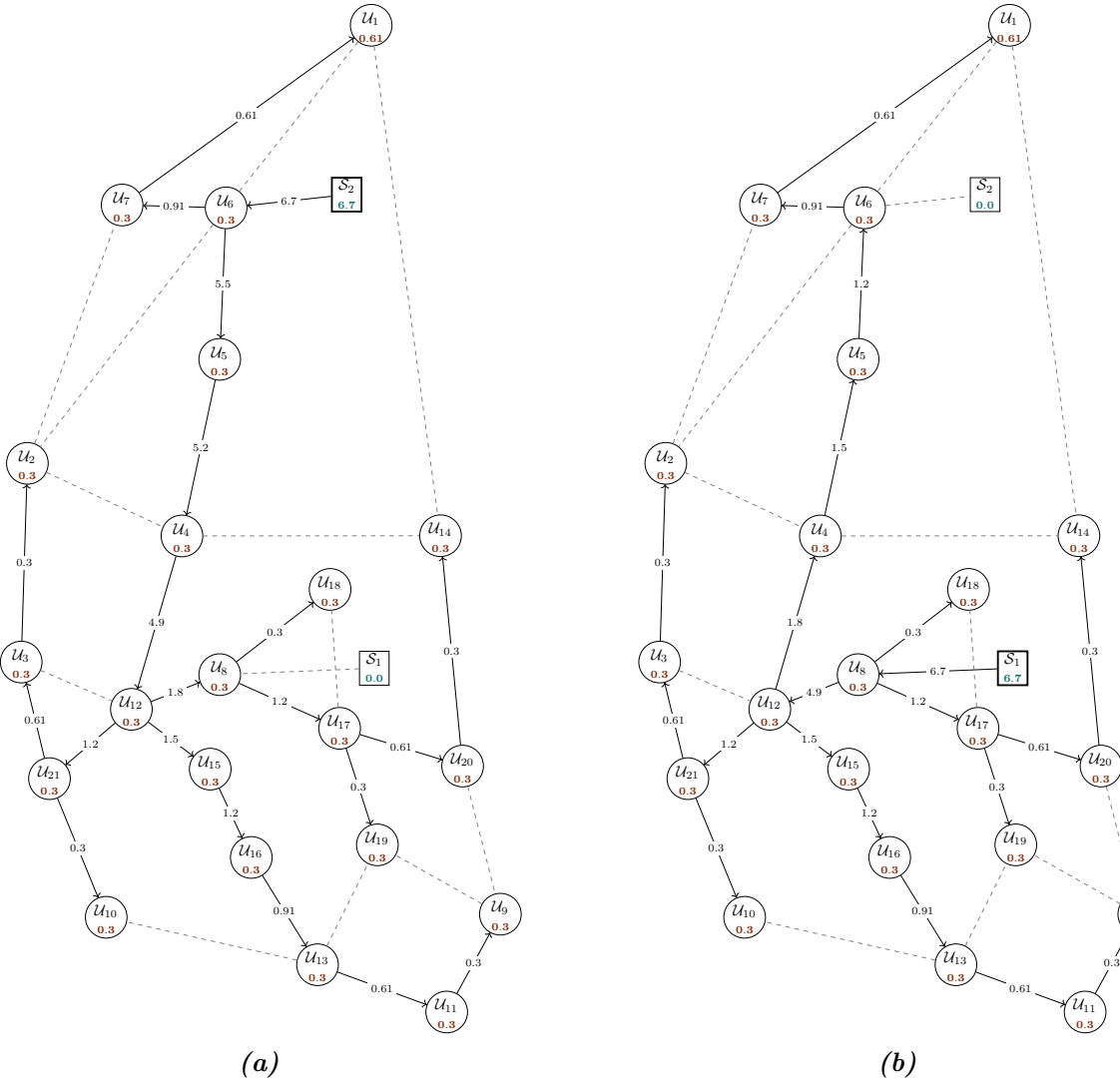


Figure 5.3. Resulting networks from the implementation of (a) the DNEP model in [12] and (b) the DNEP model in [23].

As anticipated in accordance with the theoretical findings elucidated in SUBSECTION 5.2.1, the DNEP model based on the BFM relaxation introduces a smaller number of variables and constraints, leading to more efficient problem-solving. Specifically, it is solved in 0.4977 seconds, in contrast to the 131.1 seconds required by Jabr's model.

An additional observation emerges from the relaxation based on Jabr's approach, as it fails to accurately model the square magnitude of currents flowing through line routes. We observed that these currents turn negative when no constraint is imposed to ensure their positivity, and become zero when such constraints are applied. Since our aim is to model the square magnitude of currents in order to directly constrain this value within the model, it appears rational that for modeling branch quantities, a relaxation based on a BFM (Branch Flow Model) would be more suitable. The absence of knowledge regarding the current

value within the model necessitates the establishment of operational limits on power flows rather than currents. This approach is less in line with the current practices of power system management, where both line overloading and voltage levels are managed independently.

Furthermore, we observed situations in which both formulations yielded inaccurate outcomes regarding the apparent power supplied by the substations. In certain cases, this quantity fell below the aggregate sum of all load demands. To rectify this issue, a *load oversatisfaction* constraint was introduced. This constraint guarantees that the power supplied within the network always maintains a value greater or equal than the power consumed.

To conclude, considering both resolution efficiency and the inability of Jabr's model to model the square magnitude of currents correctly, we have opted to adopt the BFM relaxation to represent the power flow equations in our upper-level problem.

5.5 The Upper-Level Optimization Program

In this section, we present the MISOCP upper-level optimization program we derived by following the objectives stated in SECTION 5.1. Taking into account the discussions in previous sections, our decision has been to adopt an upper-level problem formulation rooted in the BFM SOCP relaxation of power flow equations. This formulation incorporates loop elimination constraints, guaranteeing the radial nature of the distribution network graph when distributed generation (DG) units are integrated into the network. Our resulting formulation is written as PROBLEM 5.1.

The optimization problem spans a number of time steps over a planning horizon T , which is discretized in a finite number of equal steps of size Δt . In PROBLEM (5.1), the objective function (5.1a) represents the goal of the DNO to minimize the sum of (5.1b), i.e. the costs of new conductors C^{cond} , and (5.1c), i.e. the cost of substations C^{sub} . Added to this are the yearly values of (5.1d), i.e. $\alpha \sum_{t \in \mathcal{T}} C_t^{loss}$, and yearly values of (5.1e), capturing the penalty for violations of current constraints as $\alpha \sum_{t \in \mathcal{T}} \omega^I \cdot \Phi_t^I$. Moreover, investment costs, i.e. $C^{cond} + C^{sub}$, are scaled by the amortization period Γ in order for the objective function to be expressed in a yearly basis.

CONSTRAINT (5.1f) represents the so-called *budget-balance* discussed in SECTION (5.1). CONSTRAINTS (5.1g) to (5.1i) simply define branch physical quantities. CONSTRAINTS (5.1j) and (5.1l) represent active and reactive power balances at substation nodes of the network, whereas CONSTRAINTS (5.1m) and (5.1n) consider the lower-level variables p^{imp} and p^{exp} to write the active and reactive power balances at grid users' nodes. Regarding power flow constraints, the BFM relaxation of power flow constraints is adapted in CONSTRAINTS (5.1o) to (5.1q) to take into account conductor choices. Specifically, CONSTRAINT (5.1q) is the rotated SOCP constraint which provides a guarantee for optimality when it is tight.

CONSTRAINTS (5.1r) to (5.1t) model the decision of building a substation by introducing the binary variables β_i . In these constraints, \bar{S}_i^{sub} represents the allocated substation capacity. Reference voltages are set to 1 pu at substation nodes through the introduction of CONSTRAINTS (5.1u) and (5.1v). CONSTRAINTS (5.1w) to (5.1y) impose a null active and reactive power flow when conductor k is not selected for the line ij . This is done by considering the binary variable $\lambda_{ij,k}$ that is equal to one when conductor k is selected for line ij , and 0 otherwise. The relaxation of the current limit is expressed by introducing in CONSTRAINT (5.1z) the slack variable $h_{ij,k,t}$. CONSTRAINTS (5.1aa) introduces the binary variable $I_{ij,k,t}^{lim}$ equal to one when the current limit constraint is violated. The binary variable Λ_{ij} is introduced in CONSTRAINT (5.1bb). Finally, the radiality constraints comprise the simple radiality constraint (5.1cc) and the loop elimination constraints (5.1dd).

Notations

Sets and indices

t	index of a time period
T	number of time periods
\mathcal{T}	set of time periods, with $\mathcal{T} = \{1, 2, \dots, T\}$
i/j	index of an electrical bus
n	number of electrical buses
n_s	number of substation buses
n_u	number of grid users' buses
\mathcal{B}	set of electrical buses
\mathcal{B}_s	set of substation buses, with $\mathcal{B}_s = \{1, \dots, n_s\}$
\mathcal{B}_u	set of grid users' buses, with $\mathcal{B}_u = \{n_s + 1, \dots, n\}$
ij	index of a line route connecting the sending bus i to the receiving bus j
l	index of a line route
L	number of possible line routes
\mathcal{L}	set of possible line routes, with $ \mathcal{L} = L$
K	number of conductor choices
\mathcal{K}	set of possible conductor choices, with $\mathcal{K} = \{1, \dots, K\}$

Upper-Level Parameters

τ	interest rate of the DNO, in $[0, 1]$
Δt	duration of a time period, in hours
Γ	amortization period of investments for new line routes and substations, in years
α	scaling factor of the simulation, such that $\alpha = d^{year}/d^{rep}$
d^{rep}	number of representative days
d^{year}	number of days in a year
ω^I	unit cost for violating a current operational constraint, in k€
$\Pi_{ij, k}^{cond}$	unit cost for building the new line route ij with conductor k , in k€
Π^{sub}	unit cost for a new substation, in k€/MVA
Π^{loss}	unit cost of losses, in k€/MWh
$R_{ij, k}$	resistance of the line route ij when built with conductor k , in Ω
$X_{ij, k}$	reactance of the line route ij when built with conductor k , in Ω
M	big M constant used in CONSTRAINTS 5.1m and 5.1n
$\bar{S}_i^{sub, max}$	maximum allowed substation capacity at node i , with $i \in \mathcal{B}_s$, in MVA
\bar{V}_i	maximum voltage magnitude allowed at bus i , with $i \in \mathcal{B}$, in kV

\underline{V}_i minimum voltage magnitude allowed at bus i , with $i \in \mathcal{B}$, in kV

$\bar{I}_{ij, k}$ maximum current magnitude allowed in line ij with conductor k , in kA

Upper-Level Variables

C^{cond}	total DNO conductor investement costs of, in k€
C^{sub}	total DNO substation investement costs of, in k€
C_t^{loss}	total DNO loss costs at time period t , in k€
Φ_t^I	amount of overloaded lines at time t
$\lambda_{ij, k}$	binary variable equal to 1 when the conductor k is selected for line ij , and 0 otherwise
Λ_{ij}	binary variable equal to 1 when the line route ij is built, and 0 otherwise
\bar{S}_i^{sub}	substation power capacity at bus i , with $i \in \mathcal{B}_s$, in MVA
S_i^{sub}	apparent power supplied by the substation at bus i , with $i \in \mathcal{B}_s$, in MVA
$P_{i, t}^{sub}$	active power supplied by substation i at time t , with $i \in \mathcal{B}_s$, in MW
$Q_{i, t}^{sub}$	reactive power supplied by substation i at time t , with $i \in \mathcal{B}_s$, in MVar
β_i	binary variable equal to 1 if the substation at bus i is built, and 0 otherwise, with $i \in \mathcal{B}_s$
$I_{ij, k, t}^2$	square magnitude of the current in line ij at time period t when the conductor k is selected, in $(kA)^2$
$I_{ij, t}^2$	square magnitude of the current in line ij at time period t , in $(kA)^2$
$I_{ij, k, t}^{lim}$	binary variable equal to 1 when the current in line ij at time period t when the conductor k is selected violates the current operational limits, and 0 otherwise.
$h_{ij, k, t}$	slack variable of current CONSTRAINT 5.1aa
$P_{ij, k, t}$	active power flow at sending bus i in line ij at time period t when conductor k is selected, in MW
$P_{ij, t}$	active power flow at sending bus i in line ij at time period t , in MW
$Q_{ij, k, t}$	reactive power flow at sending bus i in line ij at time period t when conductor k is selected, in MVar
$Q_{ij, t}$	reactive power flow at sending bus i in line ij at time period t , in MVar
$V_{i, t}^2$	square magnitude of the voltage at bus i , at time period t , with $i \in \mathcal{B}$, in $(kV)^2$

Notations (cont'd)

Lower-Level Variables

c_i^{grid}	total grid capacity costs of user i , in €
$c_{i,t}^{grid}$	grid tariff costs of user i at time period t , in k€
$p_{i,t}^{imp}$	active power imported from the grid for user i at time period t , in MW
$q_{i,t}^{imp}$	reactive power imported from the grid for user i at time period t , in MVar
$p_{i,t}^{exp}$	active power exported to the grid by user i at time period t , in MW
$q_{i,t}^{exp}$	reactive power exported to the grid by user i at time period t , in MW

The Formulation

Upper-Level Formulation

$$\min \quad \frac{1}{\Gamma} \cdot \left(C^{cond} + C^{sub} \right) + \alpha \sum_{t \in \mathcal{T}} \left(C_t^{loss} + \omega^I \Phi_t^I \right) \quad (5.1a)$$

$$\text{s.t.: } C^{cond} = \sum_{ij \in \mathcal{L}} \sum_{k \in K} \lambda_{ij,k} \cdot \Pi_{ij,k}^{cond} \quad (5.1b)$$

$$C^{sub} = \sum_{i \in \mathcal{B}_s} \bar{S}^{sub} \cdot \Pi^{sub} \quad (5.1c)$$

$$C_t^{loss} = \sum_{ij \in \mathcal{L}} \sum_{k \in K} (R_{ij,k} \cdot I_{ij,k}^2) \cdot \Delta t \cdot \Pi^{loss} \quad \forall t \in \mathcal{T} \quad (5.1d)$$

$$\Phi_t^I = \sum_{ij \in \mathcal{L}} \sum_{k \in K} I_{ij,k,t}^{lim} \quad \forall t \in \mathcal{T} \quad (5.1e)$$

$$(1+\tau)^{\Gamma} \cdot \left(C^{sub} + C^{cond} \right) + \Gamma \cdot \alpha \sum_{t \in \mathcal{T}} C_t^{loss} \leq \Gamma \sum_{i \in \mathcal{B}_u} \left(c_i^{grid} + \alpha \sum_{t \in \mathcal{T}} c_i^{grid} \right) \quad (5.1f)$$

$$P_{ij,t} = \sum_{k \in K} P_{ij,k,t} \quad \forall ij \in \mathcal{L}, \forall t \in \mathcal{T} \quad (5.1g)$$

$$Q_{ij,t} = \sum_{k \in K} Q_{ij,k,t} \quad \forall ij \in \mathcal{L}, \forall t \in \mathcal{T} \quad (5.1h)$$

$$I_{ij,t}^2 = \sum_{k \in K} I_{ij,k,t}^2 \quad \forall ij \in \mathcal{L}, \forall t \in \mathcal{T} \quad (5.1i)$$

$$-P_{i,t}^{sub} = \sum_{k \in K} P_{mi,k,t} - R_{mi,k} \cdot I_{mi,k,t}^2 - \sum_{k \in K} P_{ij,k,t} \quad \forall i \in \mathcal{B}_s, \forall t \in \mathcal{T} \quad (5.1j)$$

$$-Q_{i,t}^{sub} = \sum_{k \in K} Q_{mi,k,t} - X_{mi,k} \cdot I_{mi,k,t}^2 - \sum_{k \in K} Q_{ij,k,t} \quad \forall i \in \mathcal{B}_s, \forall t \in \mathcal{T} \quad (5.1k)$$

$$p_{i,t}^{imp} - p_{i,t}^{exp} = \sum_{k \in K} P_{mi,k,t} - R_{mi,k} \cdot I_{mi,k,t}^2 - \sum_{k \in K} P_{ij,k,t} \quad \forall i \in \mathcal{B}_u, \forall t \in \mathcal{T} \quad (5.1l)$$

$$q_{i,t}^{imp} - q_{i,t}^{exp} = \sum_{k \in K} Q_{mi,k,t} - X_{mi,k} \cdot I_{mi,k,t}^2 - \sum_{k \in K} Q_{ij,k,t} \quad \forall i \in \mathcal{B}_u, \forall t \in \mathcal{T} \quad (5.1m)$$

$$\begin{aligned} V_{j,t}^2 - V_{i,t}^2 &\leq \sum_{k \in K} (-2 \cdot (R_{ij,k} \cdot P_{ij,k,t} + X_{ij,k} \cdot Q_{ij,k,t}) \\ &\quad + (R_{ij,k}^2 + X_{ij,k}^2) \cdot I_{ij,k,t}^2) + M \cdot (1 - \Lambda_{ij}) \end{aligned} \quad \forall ij \in \mathcal{L}, \forall t \in \mathcal{T} \quad (5.1n)$$

$$\begin{aligned} V_{j,t}^2 - V_{i,t}^2 &\geq \sum_{k \in K} (-2 \cdot (R_{ij,k} \cdot P_{ij,k,t} + X_{ij,k} \cdot Q_{ij,k,t}) \\ &\quad + (R_{ij,k}^2 + X_{ij,k}^2) \cdot I_{ij,k,t}^2) - M \cdot (1 - \Lambda_{ij}) \end{aligned} \quad \forall ij \in \mathcal{L}, \forall t \in \mathcal{T} \quad (5.1o)$$

$$V_{i,t}^2 \cdot I_{ij,t}^2 \geq P_{ij,t}^2 + Q_{ij,t}^2 \quad \forall ij \in \mathcal{L}, \forall t \in \mathcal{T} \quad (5.1p)$$

$$(S_{i,t}^{sub})^2 \geq (P_{i,t}^{sub})^2 + (Q_{i,t}^{sub})^2 \quad \forall i \in \mathcal{B}_s, \forall t \in \mathcal{T} \quad (5.1q)$$

$$\begin{aligned}
S_{i,t}^{sub} &\leq \bar{S}_i^{sub} & \forall i \in \mathcal{B}_s, \forall t \in \mathcal{T} & (5.1r) \\
\bar{S}_i^{sub} &\leq \beta_i \cdot \bar{S}_i^{sub,max} & \forall i \in \mathcal{B}_s & (5.1s) \\
V_{i,t}^2 - 1 &\leq (\bar{V}^2 - 1) \cdot (1 - \beta_i) & \forall i \in \mathcal{B}_s & (5.1t) \\
V_{i,t}^2 - 1 &\geq (\underline{V}^2 - 1) \cdot (1 - \beta_i) & \forall i \in \mathcal{B}_s & (5.1u) \\
P_{ij,k,t} &\leq \lambda_{ij,k} \cdot \bar{I}_{ij,k} \cdot \bar{V} & \forall ij \in \mathcal{L}, \forall k \in \mathcal{K}, \forall t \in \mathcal{T} & (5.1v) \\
P_{ij,k,t} &\geq -\lambda_{ij,k} \cdot \bar{I}_{ij,k} \cdot \bar{V} & \forall ij \in \mathcal{L}, \forall k \in \mathcal{K}, \forall t \in \mathcal{T} & (5.1w) \\
Q_{ij,k,t} &\leq \lambda_{ij,k} \cdot \bar{I}_{ij,k} \cdot \bar{V} & \forall ij \in \mathcal{L}, \forall k \in \mathcal{K}, \forall t \in \mathcal{T} & (5.1x) \\
Q_{ij,k,t} &\geq -\lambda_{ij,k} \cdot \bar{I}_{ij,k} \cdot \bar{V} & \forall ij \in \mathcal{L}, \forall k \in \mathcal{K}, \forall t \in \mathcal{T} & (5.1y) \\
h_{ij,k,t} &\leq (\bar{I}_{ij,k})^2 \cdot I_{ij,k,t}^{lim} & \forall ij \in \mathcal{L}, \forall k \in \mathcal{K}, \forall t \in \mathcal{T} & (5.1z) \\
I_{ij,k,t}^2 - h_{ij,k,t} &\leq (\bar{I}_{ij,k})^2 \cdot \lambda_{ij,k} & \forall ij \in \mathcal{L}, \forall k \in \mathcal{K}, \forall t \in \mathcal{T} & (5.1aa) \\
\sum_{k \in \mathcal{K}} \lambda_{ij,k} &= \Lambda_{ij} & \forall ij \in \mathcal{L} & (5.1bb) \\
\sum_{ij \in \mathcal{L}} \Lambda_{ij} &= n_u & \forall t \in \mathcal{T} & (5.1cc) \\
+ \text{radiality constraints} & & & (5.1dd)
\end{aligned}$$

Chapter 6

THE LEADER-FOLLOWER PROBLEM

6.1 Description of the Problem

As a recall of SECTION 1.3, the objective of this master thesis consisted in developing a first bilevel programming (BP) approach for developing distribution network development plans. This bilevel problem introduces two players:

- The *upper-level*, also referred to as the *leader*, is the optimization program solved by the distribution network operator (DNO). Its objective is to discover an ideal configuration of the distribution network that minimizes both CAPEX and OPEX costs, all while effectively addressing the needs of grid users. This topology should also simultaneously ensure a sufficiently high reliability, imposed as operational constraints on grid voltages and line currents in the problem. Additionally, the DNO intends to fulfill a *budget balance* constraint. This constraint reflects the DNO's ability to recoup its investment, alongside an allocated margin, through the grid tariffs imposed on users of the network. This actor considers a sufficiently large planning horizon to cover representative system conditions. A more comprehensive description of this problem is available in CHAPTER 5.
- The *lower-level*, also called the *follower*, embodies the optimization efforts of all grid users within the leader's network. Each individual user can choose between several options to satisfy their energy requirements. They can buy from the DNO some capacity to withdraw or inject into the distribution network. They can also decide to invest in generation and storage. The total cost of a user is minimizing is the addition of these investments and operational costs, such as the electricity purchased from the public grid. A more detailed version of the description of this problem is provided in CHAPTER 4.

Our aim is to assess the influence of the alternatives of the users and the DNO on the equilibrium state of the overall system. In other words, we seek to understand the extent of necessary investments by both the DNO in its network and users in their personal generation and storage resources.

6.2 The Optimization Program

The bilevel programming (BP) optimization program we derived is built by introducing the lower-level problem defined in PROBLEM 4.1 in the constraints of the upper-level problem defined in PROBLEM 5.1. Insights into the methodologies employed to derive these two optimization programs can be found in CHAPTERS 4 and 5. This leads to an *optimistic* BP program, where the upper-level is formulated as a MISOCP program, while the lower-level adopts a linear programming (LP) structure. As elaborated upon in SECTION 2.5, solving this program is NP-hard. Nevertheless, the optimistic approach, coupled with the simplicity of the lower-level problem, allows its transformation into a single-level formulation through the application of KKT conditions. Therefore, we can write the general form our bilevel optimization program as in PROBLEM 6.1:

The Bilevel Optimization Program

$$\min \quad \text{Upper-Level Objective Function 5.1a} \quad (6.1a)$$

$$\text{s.t. : } \text{Upper-Level Constraints 5.1b to 5.1dd} \quad (6.1b)$$

$$(p^{imp}, p^{exp}, q^{imp}, q^{exp}, c^{grid}) \in \operatorname{argmin} \{4.1a \mid \text{s.t.: 4.1b to 4.1o}\} \quad (6.1c)$$

In this formulation, the objective function (6.1a) and CONSTRAINT (6.1b) define the upper-level optimization program. On the other hand, CONSTRAINT (6.1c) corresponds to the lower-level optimization program. The lower-level variables $p^{imp}, p^{exp}, q^{imp}, q^{exp}, c^{grid}$ are shared with the upper-level. These variables are constrained to align with the optimal solutions of the lower-level problem, consequently delimiting the range of feasible options accessible for the upper-level problem to explore in its pursuit of a solution.

6.3 Sensitivity Analysis Performed for the ISGT Conference Paper

An initial sensitivity analysis was conducted on key parameters to acquire a deeper understanding of how equilibrium evolves within our bilevel model. This analysis was explained in the paper called “A one-leader multi-follower approach to distribution network development planning”, co-authored by Pr. Bertrand Cornélusse, Dr. Mevludin Glavčić, Geoffrey Bailly, and myself, which was has been accepted to present during the IEEE PES ISGT EUROPE 2023 conference [24]. The purpose of this section is to explain the analysis presented in the aforementioned paper.

Methodology

To capture the impact of key parameters on the outcomes of some bilevel model simulations, we conducted this analysis by establishing a base case scenario, whose characteristics are highlighted in grey in TABLE 6.1. Subsequently, except for the worst-case scenario, the key parameters were altered one by one, relative to this base case scenario. As a result, each simulation involved a single change in parameter value. Although we recognize the limitations inherent in this approach, considering the bilevel model high complexity, we sought to enhance our understanding before delving further into a more complete analysis that consider, for instance, the correlation between the different parameters. The six resulting test cases we chose to present are described TAB 6.1.

EV: add electric vehicles' consumption, HP: add heat pumps' consumption, MPV: Maximum PV capacity per bus (MVA), EIP: energy import price (k€/MWh), GT: grid tariff (k€/MWh), EEP: energy export price (k€/MWh), GCC: grid connection cost (k€/MVA/y). False (F), true (T).

Case	EV	HP	MPV	EIP	GT	EEP	GCC
Base	F	F	0.4	0.3	0.1	0.1	80
Worst	T	T	0	0.3	0.1	0.1	80
Best	F	F	0.8	0.3	0.1	0.1	80
EIP inc.	F	F	0.4	0.6	0.1	0.1	80
GT inc.	F	F	0.4	0.3	0.2	0.1	80
EEP inc.	F	F	0.4	0.3	0.1	0.2	80
GCC inc.	F	F	0.4	0.3	0.1	0.1	120

Table 6.1. Description of test cases used for the ISGT sensitivity analysis.

Input data

The input data for load and PV generation profiles as well as the test network used in our simulations are described in CHAPTER 3. In the base case, the aggregated demand profile is scaled so that the peak load is 7 MVA on a five-minute time scale, pro-rata of the load data in TABLE VI of [50]. As for the available conductors, they are listed in TABLE 3.2. The amortization periods are 50 years for the DNO investment, 30 years for the PV panels, and ten years for the PV inverters. The other relevant parameters are summarized in Table 6.3, where the grey row in the base case.

KPIs results

We decide to assess the results of our different scenarios based on several key performance indicators (KPIs). Each test case is then compared to the *Base* case based on the KPIs values. These results are available in TABLE 6.2.

#LC i : Number of lines built with conductor i , ISC: Installed substation capacity (MVA), CAPEX: DSO annual amortized cost of investments (M€/y), OPEX: DSO cost of losses (M€/y), UPVC: Users' PV annual amortized cost of investments (M€/y), UGCC: Users' annual grid connection cost (M€/y), UNEEC: Users' net annual electricity exchange cost (M€/y), USS: Users' average self-sufficiency (%), USC: Users' average self-consumption (%).

Case	Network topology					KPIs						
	#LC1	#LC2	#LC3	#LC4	ISC	CAPEX	OPEX	UPVC	UGCC	UNEEC	USS	USC
Base	21	0	0	0	5.66	0.116	0.138	0.240	2.14	3.44	42.7	72.3
Worst	13	1	5	2	19.18	0.388	1.575	0	7.38	15.91	0	0
Best	18	1	0	2	5.64	0.117	0.125	0.405	2.16	2.96	49.4	69.2
EIP inc.	17	3	1	0	5.68	0.117	0.343	0.240	2.17	7.09	42.7	72.3
GT inc.	21	0	0	0	5.65	0.116	0.081	0.240	3.13	3.68	42.7	72.3
EEP inc.	21	0	0	0	5.88	0.121	0.134	0.302	2.73	2.06	42.7	72.3
GCC inc.	21	0	0	0	5.66	0.116	0.128	0.240	2.29	3.64	42.7	72.3

Table 6.2. Results obtained with the bilevel model for the ISGT sensitivity analysis.

In the most extreme scenario, i.e. the *Worst* case, the demand is very high because of heat pumps and electric vehicles, and we assumed no PV can be installed. While this scenario lacks practical realism since grid users typically don't adopt heat pumps and EVs without PV panels, it serves as a kind of "apocalyptic" case that offers insights into the worst possible impacts on the system. The main consequence of this case is, as expected, a great increase in the DSO CAPEX and OPEX expenses. Approximately half of the lines necessitate upgrades, and both substations require significant reinforcement. Meanwhile, users experience an almost fivefold rise in costs, even though the energy demand has merely tripled. Specifically, the peak load has reached 18.85 MVA, with an annual total energy consumption of 53,110 MWh.

In the *Best* case, users can double their PV installation, resulting in reduced user costs and increased self-sufficiency by nearly 50%. DNO costs do not see a significant increase in this scenario. In the *EIP inc.* case, where energy import prices double, user costs rise, similar to the *GT inc.* scenario where grid tariffs are increased. This is expected since the base case's budget balance is already satisfied. Consequently, an elevation in the network tariff corresponds, in essence, to an augmentation in the commodity price from the user's standpoint, thereby eliminating the requirement for further DNO investments. In the *EEP inc.* case, users install more PV capacity, exporting excess generation to the grid. This leads to slight impacts on DSO costs and generates user revenues, causing a decrease in the net electricity expenses (UNEEC). Finally, in the *GCC inc.* case, where grid connection costs increase, the results remain largely unaffected.

6.4 Implementation of the Model

The BP optimization program from PROBLEM 6.1 was implemented using the Julia programming language [52] with the JuMP package [58]. More specifically, we used an extension of the JuMP package, known as BilevelJuMP [46], that offers an interface to write BP programs in Julia. Besides providing an interface, it also offers methods to reformulate BP programs as single-level problems, such as replacing the lower-level by its KKT conditions or applying the strong duality reformulation. In this master thesis, we used the strong duality method for the reformulation of our bilevel problem. Additionally, Gurobi [39] was employed as the MIP solver to tackle the single-level reformulation of the BP program, featuring the following parameters:

- The MIP gap is equal to 0.01%. According to the Gurobi website [39], it is computed with the following formula:

$$\frac{|\text{ObjBound} - \text{ObjVal}|}{|\text{ObjVal}|}$$

- The time limit for solving the model is set to 1200 seconds.
- The MIP focus parameter is set to 1, a choice that prioritizes swiftly obtaining a feasible solution.

Moreover, since the main focus of this master thesis revolved around devising a bilevel formulation, it was essential to explore diverse configurations of the bilevel formulation. This exploration aimed to identify the configuration that best aligns with our expectations regarding tractability. This led to the implementation of a modular code, called `Bilevel.jl`. The structure of the `Bilevel.jl` module, which was implemented to enable the creation of various bilevel model formulations, is depicted in FIGURE 6.1. The figure also displays the array of alternative formulations available within this module, situated in the *Formulation* section. These options include, among others, the experimentation with two convex relaxation formulations for power flow equations, the relaxation of current and voltage constraints, the introduction of network reconfiguration possibilities over the temporal horizon, and the exploration of multiple loop elimination constraints.

This module marks an initial attempt to furnish a tool for DNOs to devise distribution network development plans that are fit to their specific requirements. Its modular nature sets the stage for easy extensions to incorporate additional formulation alternatives. In addition to offering the `Bilevel.jl` module, this code was also crafted with an implementation organized into data structures. This organizational structure is depicted in FIGURE 6.2.

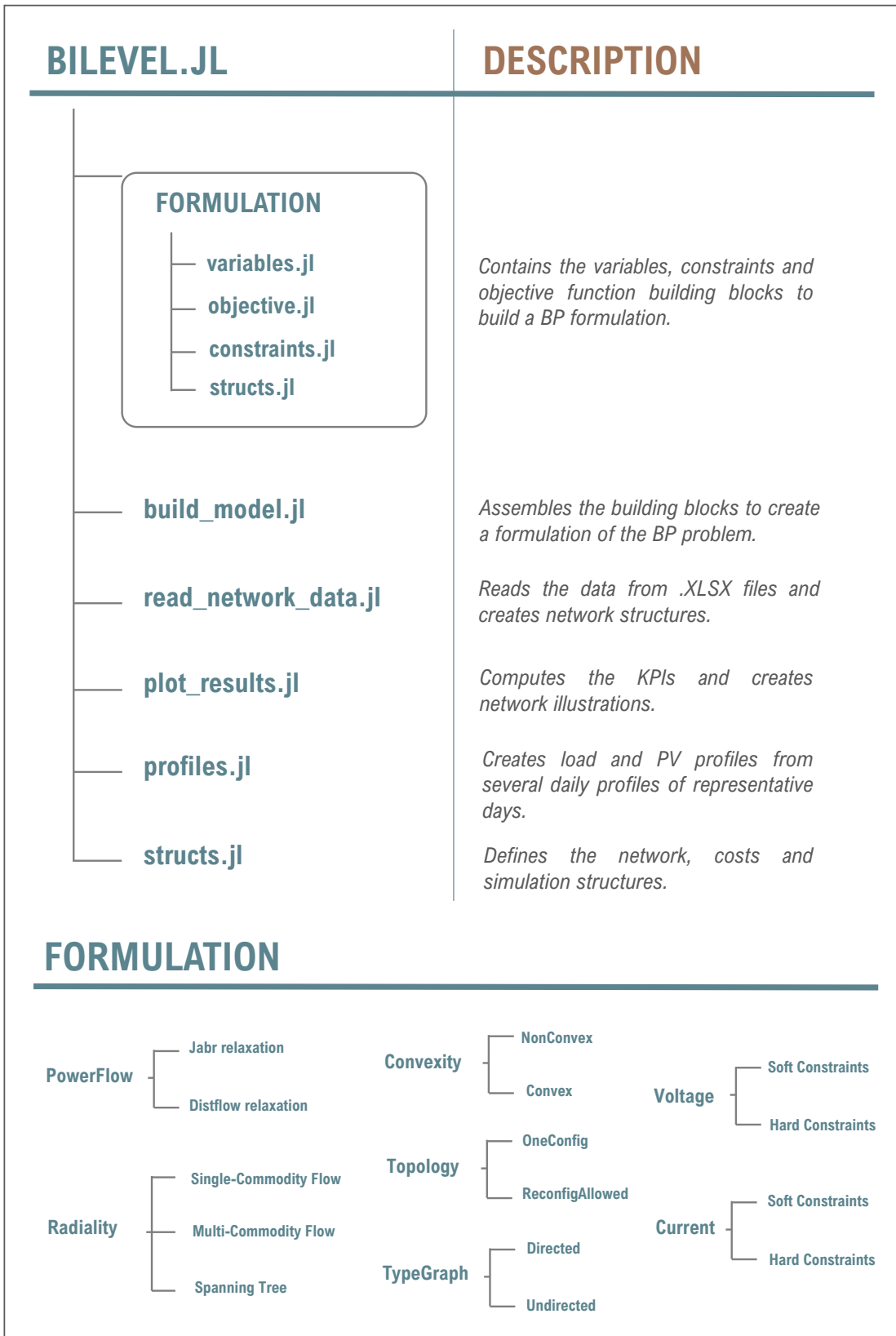


Figure 6.1. The `Bilevel.jl` module implemented for the purpose of this master thesis. It allows to build different formulations of our bilevel framework for the DNDP problem.

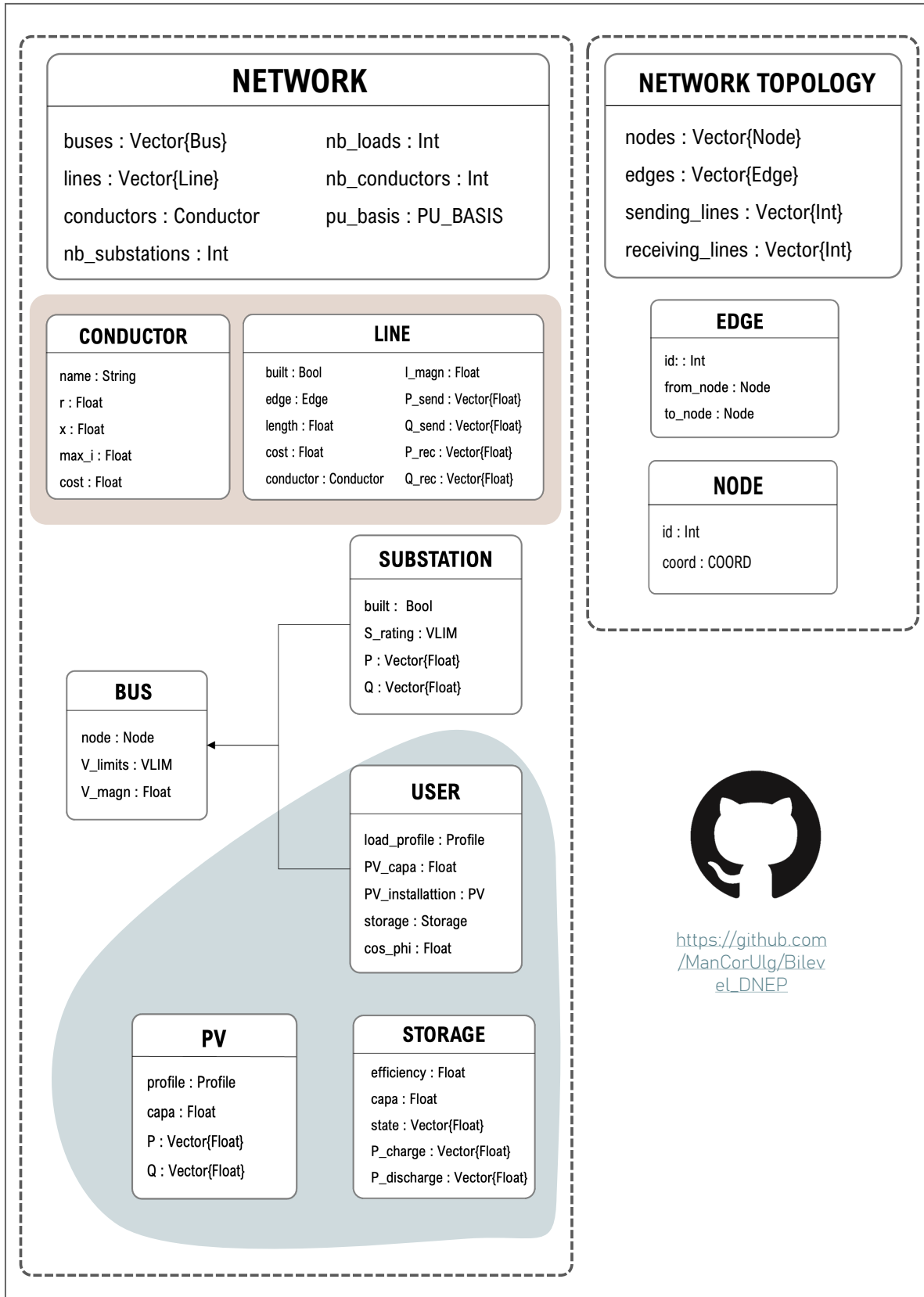


Figure 6.2. Data types in the Julia implementation of the Bilevel.jl module

6.5 Sensitivity Analysis performed with the Bilevel.jl module

A second sensitivity analysis was conducted to elucidate the dynamics of equilibrium within our bilevel model. This secondary analysis had two main objectives. Firstly, it aimed to reproduce certain findings from SECTION 6.3 by utilizing the newly-developed Bilevel.jl module, thereby validating its reliability. Secondly, it sought to extend beyond the previous analysis by incorporating storage units in the lower-level problem. Additionally, it also added the bilevel model against its reformulation as a multi-objective optimization program and also evaluated the impact of allowing the network to operate radially. This means that while the topology need not be radial at all times, the lines utilized during each time step of a simulation should compose a radial topology. Finally, we also sought in this part of the work to compare the three loop elimination constraints formulations described in 5.3.

SID: Simulation ID, **EV:** add electric vehicles' consumption, **EHP:** add heat pumps' consumption, **ST:** add storage devices, **STC:** storage cost (k€/MWh), **NR:** allow network reconfiguration, **BLV:** Bilevel formulation, **MPV:** Maximum PV capacity per bus (MVA), **PVC:** PV cost (k€/MWp), **GT:** grid tariff (k€/MWh), **EIP:** energy import price (k€/MWh), **EEP:** energy export price (k€/MWh), **GCC:** grid connection cost (k€/MVA/y), **WI:** weight of the current constraint violation in the objective. **F:** False, **T:** True.

SID	EV	EHP	ST	STC	NR	BLV	MPV	PVC	EIP	EEP	GT	GCC	WI
	[–]	[–]	[–]	[k€/MWh]	[–]	[–]	[MVA]	[k€/MWp]	[k€/MWh]	[k€/MWh]	[k€/MWh]	[k€/MVA/y]	[k€]
0	F	F	F	–	F	T	0.4	500	0.3	0.1	0.1	80	0.01
1	T	F	F	–	F	T	0.4	500	0.3	0.1	0.1	80	0.01
2	F	T	F	–	F	T	0.4	500	0.3	0.1	0.1	80	0.01
3	F	F	T	500	F	T	0.4	500	0.3	0.1	0.1	80	0.01
4	F	F	T	300	F	T	0.4	500	0.3	0.1	0.1	80	0.01
5	F	F	T	600	F	T	0.4	500	0.3	0.1	0.1	80	0.01
6	F	F	F	–	T	T	0.4	500	0.3	0.1	0.1	80	0.01
7	F	F	F	–	F	F	0.4	500	0.3	0.1	0.1	80	0.01
8	F	F	F	–	F	T	0.0	500	0.3	0.1	0.1	80	0.01
9	F	F	F	–	F	T	0.8	500	0.3	0.1	0.1	80	0.01
10	F	F	F	–	F	T	1.6	500	0.3	0.1	0.1	80	0.01
11	F	F	F	–	F	T	0.4	300	0.3	0.1	0.1	80	0.01
12	F	F	F	–	F	T	0.4	600	0.3	0.1	0.1	80	0.01
13	F	F	F	–	F	T	0.4	500	0.6	0.1	0.1	80	0.01
14	F	F	F	–	F	T	0.4	500	0.9	0.1	0.1	80	0.01
15	F	F	F	–	F	T	0.4	500	0.3	0.2	0.1	80	0.01
16	F	F	F	–	F	T	0.4	500	0.3	0.3	0.1	80	0.01
17	F	F	F	–	F	T	0.4	500	0.3	0.1	0.2	80	0.01
18	F	F	F	–	F	T	0.4	500	0.3	0.1	0.3	80	0.01
19	F	F	F	–	F	T	0.4	500	0.3	0.1	0.1	120	0.01
20	F	F	F	–	F	T	0.4	500	0.3	0.1	0.1	160	0.01
21	F	F	F	–	F	T	0.4	500	0.3	0.1	0.1	80	0.001
22	F	F	F	–	F	T	0.4	500	0.3	0.1	0.1	80	0.1

Table 6.3. Description of test cases used in the sensitivity analysis. In this table, the row colored in grey highlights the base case scenario

Methodology

The simulations were conducted using the `Bilevel.jl` module. To capture the impact of key parameters on the outcomes of the bilevel model simulations, we used the same methodology as in SECTION 6.3. The description of the 23 cases tested in our sensitivity analysis are presented in TABLE 6.3, in which the base case scenario (highlighted in grey in the table) is the same as in SECTION 6.3. Moreover, the 23 test cases were tested each with the three types of loop elimination constraints. This resulted in 69 simulations.

Input data

The same input data as for the ISGT conference analysis from SECTION 6.3 was used for this analysis.

Results of the simulations

The results of the 69 test case simulations are described in this section.

Solve Time and MIP Gap

This part discusses the results of the 23 test cases, tested each on the three types of loop elimination constraints. The aim is to determine which constraint formulation yields the most favorable computational results. The different loop elimination constraints are compared based on their MIP gap at optimality and solution time, as presented in TABLE 6.4.

The data in TABLE 6.4 indicates that nearly every simulation was prematurely terminated due to the imposed time limit of 1200 seconds. This observation underscores the potential need to extend this time limit or simplify the complexity of the bilevel model. Additionally, the spanning tree constraints deliver the most favorable results in terms of MIP gap across a majority of test cases.

One of the main conclusion that can be drawn from this table is that none of the simulations that introduced storage in the bilevel formulation resulted in a feasible solution. This highlights a potential issue in the formulation or a too high complexity for the resulting bilevel model to be solved. Another interesting result is the fact that network reconfiguration, i.e. the 6th case, and reformulating the problem under the form of a multi-objective (MO) program, i.e. the 7th case, gave the best results in terms of convergence. While this outcome was anticipated for the MO program due to its simpler formulation, it is particularly interesting for the 7th case, which still involves a bilevel structure. This implies that granting the DNO greater flexibility in selecting network topologies renders the bilevel problem more computationally tractable. In subsequent sections, our focus narrows down to the results of simulations conducted using the loop elimination constraints that exhibited the most favorable MIP gap. These simulations are highlighted in blue in TABLE 6.4.

SID	Single-Commodity Flow		Multi-Commodity Flow		Spanning Tree	
	MIP Gap	Solve Time	MIP Gap	Solve Time	MIP Gap	Solve Time
	[%]	[sec.]	[%]	[sec.]	[%]	[sec.]
0	3.592	1200	3.759	1200	5.236	1200
1	97.79	1200	17.93	1200	-	-
2	-	-	-	-	-	-
3	-	-	-	-	-	-
4	-	-	-	-	-	-
5	-	-	-	-	-	-
6	0.7676	705.9	1.213	1200	0.7723	418.6
7	0.1266	919.7	0.1386	128.8	0.1119	58.25
8	2.821	1200	2.716	1200	2.657	1200
9	3.344	1200	4.836	1200	78.45	1200
10	2.243	1200	2.38	1200	3.964	1200
11	2.528	1200	98.87	1200	2.6	1200
12	4.727	1200	-	-	2.29	1200
13	-	-	-	-	5.479	1200
14	92.73	1200	-	-	5.472	1200
15	98.87	1200	3.352	1200	3.293	1200
16	98.67	1200	97.3	1200	2.835	1200
17	5.927	1200	3.59	1200	2.29	1200
18	99.04	1200	99.05	1200	2.285	1200
19	3.244	1200	2.605	1200	2.086	1200
20	3.921	1200	2.396	1200	2.451	1200
21	5.012	1200	3.65	1200	2.73	1200
22	99.88	1200	3.553	1200	2.303	1200

Table 6.4. Solve Time and MIP Gap of the BP program for every radiality constraint formulation across all 23 simulation configurations. A dash in the table denotes simulations that were unable to find a feasible solution within the allocated time.

Resulting Network

The results regarding the DNO's network topology for simulations with the best MIP gap are presented in TABLE 6.5. The DNO allocates the substation capacity across the two substations solely in the 6th scenario, which enables network reconfiguration. In this very scenario, it is shown that allowing reconfiguration maintains the same line count, but a reduction in the quantity of larger conductors. Considering that TABLE 6.4 indicates a lower MIP gap when network reconfiguration is allowed, this option brings us closer to the optimal solution compared to the base case. This probably explains the lower number of large conductors in the optimal network topology. Besides, the 7th case, which tests a multi-objective optimization program based on the bilevel optimization, converges towards a different solution in terms of network topology.

As expected, the 9th and 10th scenario result in a high allocated PV capacity as the PV capacity limit is increased at each network node in both cases. Besides, FIGURES 6.3 and 6.4 illustrates two examples of resulting network configurations at specific time periods of the base case simulation. FIGURE 6.3 shows that, during a summer day with the best condition for PV productions, grid users inject the surplus PV generation in the grid network that reinject power also at the level of its substation. During a winter day at night, FIGURE 6.4 outlines the situation with very high electricity demand.

SID	ISC1 [MVA]	ISC2 [MVA]	#LC1 [-]	#LC2 [-]	#LC3 [-]	#LC4 [-]	PVCA [MVA]
0	0	5.711	15	0	2	4	8.4
1	0	11.57	19	2	0	0	8.4
2	-	-	-	-	-	-	-
3	-	-	-	-	-	-	-
4	-	-	-	-	-	-	-
5	-	-	-	-	-	-	-
6	4.174	1.524	18	0	1	2	8.4
7	0	5.72	20	1	0	0	8.4
8	0	5.731	15	0	0	6	0.0
9	0	5.689	16	1	2	2	16.02
10	0	5.647	15	0	2	4	28.27
11	0	5.707	16	0	1	4	8.4
12	0	5.706	10	7	0	4	8.354
13	0	5.709	14	0	0	7	8.4
14	0	5.706	13	2	1	5	8.4
15	0	5.884	14	1	2	4	8.4
16	0	7.045	14	1	1	5	8.4
17	0	5.706	15	1	2	3	8.4
18	0	5.706	15	0	2	4	8.4
19	0	5.706	16	1	1	3	8.4
20	0	5.706	14	2	0	5	8.4
21	0	5.708	16	1	3	1	8.4
22	0	5.707	16	0	3	2	8.4

Table 6.5. Characteristics of the resulting network in the 23 test cases. A dash in the table denotes simulations that were unable to find a feasible solution within the allocated time.

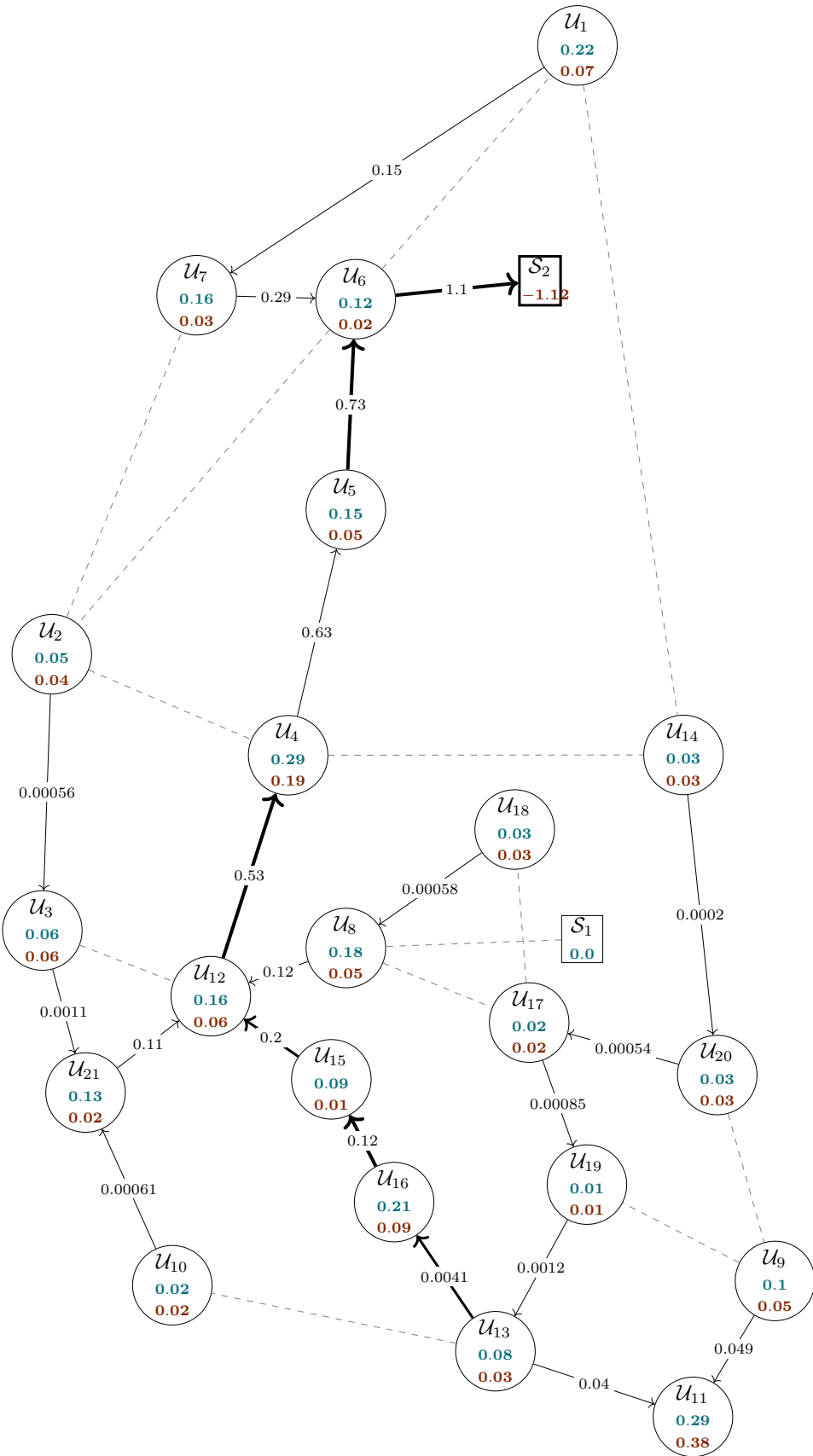


Figure 6.3. Resulting network from a simulation of our bilevel model at noon during the summer day with the base case configuration for the input parameters.

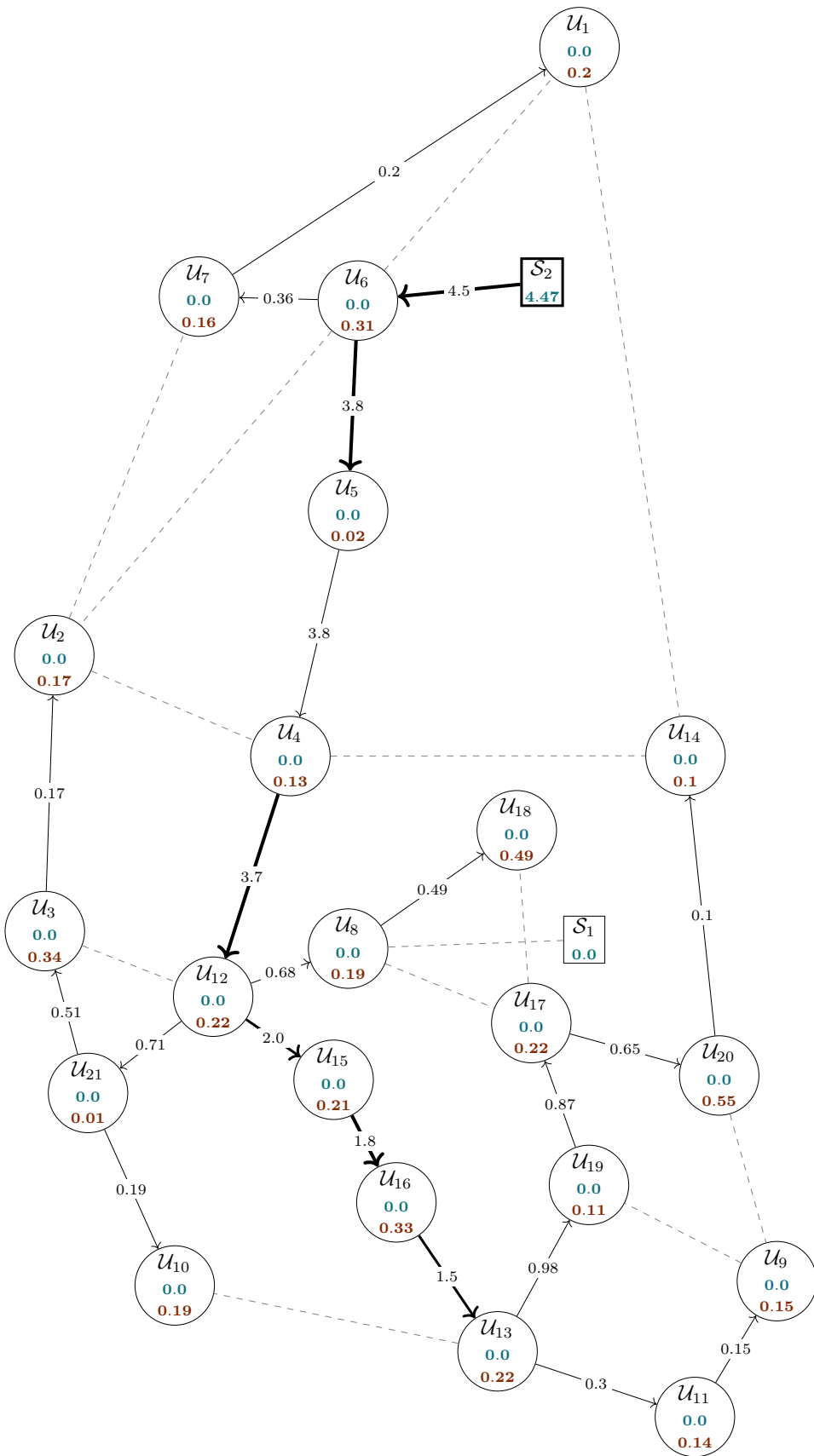


Figure 6.4. Resulting network from a simulation of our bilevel model at night during the winter day with the base case configuration for the input parameters.

Resulting KPIs In evaluating the strategies of both players in our bilevel programming approach, we opted to compute various key performance indicators (KPIs) based on the outcomes of our simulations. These results are illustrated in FIGURE 6.5.

Among the primary insights gained from these results is the observation that incorporating EVs profiles alongside the base consumption profiles nearly doubles the DNO's investments in terms of Capital Expenditure (CAPEX) compared to the base case. Additionally, this trend exhibits a marginal inclination to encourage users to enhance their PV investments for charging their EVs. This inclination is depicted by a higher User PV capacity (UPVC) KPI in the second simulation compared to the base case. Correspondingly, the User Grid Connection Costs (UGCC) also double to accommodate the heightened electricity demand. The user energy exchange costs (EEC) rise because they have a limited PV capacity that constrain them to consume electricity from the network. In this situation, it could be interesting to enhance the PV capacity at each node. The average self-sufficiency of users, which represents the percentage of their electricity demand met by their PV systems, diminishes in comparison to the base case. This decline is attributed to the increase in electricity consumption, while PV production remains nearly constant, mirroring the conditions of the base case.

Enabling network reconfiguration in the 6th test case results in the lowest lost costs among all scenarios, as indicated by the OPEX KPI. This results in an approximate 75% reduction compared to the base case scenario. In the context of the multi-objective program scenario, specifically the 7th simulation, the OPEX costs for the DNO experience an almost twofold increase. Nevertheless, the outcomes align with those obtained from the bilevel approach concerning the strategies adopted by grid users. This observation potentially underscores a situation where the weight assigned to grid users' objectives within the multi-objective function surpasses the weight allocated to the DNO's objective. Consequently, this leads to a Pareto optimal solution that tends to favor the preferences of grid users.

The other dynamics are very similar to the ones explained in SECTION 6.3.

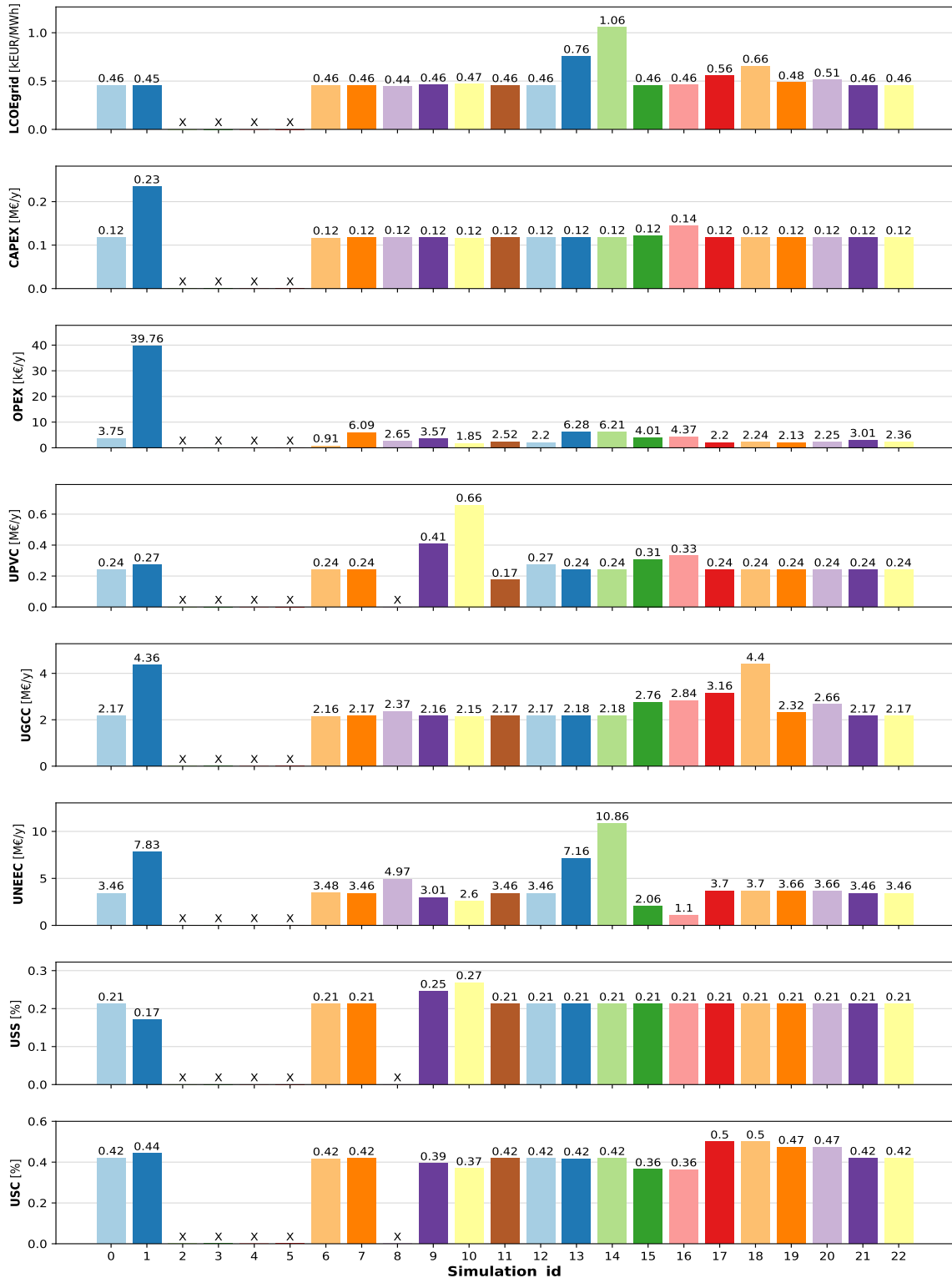


Figure 6.5. Simulation results acquired from a sensitivity analysis of the bilevel model. The analysis comprehensively assesses all 23 configurations specified in TABLE ??, employing a formulation that takes into account the **radiality constraints formulation that have the smallest MIP gap**. The results are presented through 8 KPIs: the LCOE grid ($k\text{€}/\text{MWh}$), CAPEX ($M\text{€}/\text{year}$), OPEX ($k\text{€}/\text{year}$), UPVC ($M\text{€}/\text{year}$), UGCC ($M\text{€}/\text{year}$), UNEEC ($M\text{€}/\text{year}$), USS (%), and USC (%).

Chapter 7

CONCLUSION AND PERSPECTIVES

7.1 Summary of Results

The objective of this master thesis consisted in devising a bilevel programming (BP) model for developing distribution network development plans (DNDP). The primary aim of this co-optimization approach was to capture the interplay between two key actors: the distribution network operator (DNO), considered as the leader, who aims to minimize its investment and operational costs and the grid users, considered as the followers, aiming to make optimal investment decisions concerning photovoltaic (PV) installations and storage solutions. This approach is innovative from prior DNDP frameworks as it allows to consider the grid users' perspective. This consideration becomes indeed crucial, given the rising involvement of grid users in the energy transition.

This master thesis was a first step in the development of a broader project whose objective would be to eventually develop decision-making tools for DNOs that seek to optimize in an smart manner their investments in their network. Indeed, we managed to provide a first formulation of the bilevel programming approach with a MISOCP upper-level program and a LP lower-level program. We were able to test several configurations of this formulation using the `Bilevel.jl` module. This module was implemented with the aim to be extended and to facilitate the integration of new formulation alternatives. In its actual form, the module is able to integrate, among others, storage in the BP program, several AC power flow equations relaxations and network reconfiguration, which states that the network should be radial in operation.

Two sensitivity analysis were provided at the end of this work in order to gain insights in the equilibrium that is reached by our bilevel program. The first analysis was jointly conducted with the research team involved in this study, aiming to contribute to the ISGT paper. It underscored, among various observations, that raising the energy import price or the grid tariffs resulted in similar outcomes and that the key performance indicators (KPIs) are almost unaltered when grid connection capacity price increases.

In the second sensitivity analysis, 69 test cases were simulated. This analysis initially emphasized that none of the test cases managed to find a feasible solution when storage was incorporated into the bilevel model. This could be attributed to either an inadequately formulated approach or the introduction of excessive complexity due to the inclusion of additional grid users' choices. Furthermore, it highlighted that among the radiality constraints, the spanning tree constraints exhibited superior overall convergence. Lastly, some of the most interesting findings emerged during the examination of a formulation for the bilevel model allowing the DNO to identify a network configuration that operates radially without requiring radial topology for every time step. This particular bilevel formulation yielded the most favorable convergence outcomes.

The conclusions derived from these two analyses, however, were not particularly insightful, as the approach of systematically altering a single key parameter at a time didn't significantly challenge the equilibrium and yielded largely comparable KPIs across nearly all scenarios. Nevertheless, this method was essential to begin with as the high complexity of the bilevel model makes it challenging to comprehend the outcomes when multiple parameters are simultaneously modified.

This has outlined the necessity to perform more in-depth analyses of the correlations between several input parameters. Furthermore, it has been shown that the 1200-second limit fixed for finding a solution of the bilevel program was too low as the model never reaches optimality within this timeframe. This limit must therefore be increased. Another solution would be to find a more computationally-efficient formulation of our bilevel program. For instance, we could replace the AC power flow equations convex relaxation with a linear relaxation.

To conclude, my personal contribution lies in having participated, with Geoffrey Bailly, in the formulation of the bilevel optimization program. Specifically, I made the formulation for the upper-level problem based on two papers from the literature [12] and [23]. I also came up with a modular implementation of our bilevel framework that allows to test several configurations of the formulation. This code could set the path to a more comprehensive decision-making tool that would be able to simulate various configurations of the co-optimization distribution network development planning problem.

7.2 Discussion and Future Work

As previously explained, this master thesis is part of a broader research project aimed at creating an entirely novel bilevel framework, designed to empower DNOs in enhancing their distribution network development strategies. The formulation represents an initial attempt at a bilevel program that addresses the research project. However, there remains considerable potential for enhancing the model formulation. The following list outlines a few possibilities:

- Regarding input data, we could incorporate a broader range of representative days into the simulations of the bilevel program. This approach would enable the inclusion of a wider spectrum of scenarios that occur throughout the year, resulting in more accurate and realistic insights.
- The `Bilevel.jl` module could integrate linear relaxations of the power flow equations. This enhancement would enable the exploration of more computationally-tractable formulations within our bilevel framework.
- Furthermore, there is a need for deeper exploration of storage solutions. It's acknowledged that due to time constraints, we couldn't thoroughly examine the formulation of the storage dynamics within our model. This limitation could potentially account for the unfavorable results observed in our analysis when storage was incorporated.
- In this thesis, we introduced certain robust assumptions for the sake of simplicity. For instance, we assumed users to exhibit perfectly rational behavior. Additionally, when users encounter multiple optimal solutions, they select the one that suits the most the DNO's objective function. This comes from the *optimistic* approach in bilevel programming. However, it's essential to recognize that both these assumptions deviate from reality. To be more realistic, we could investigate the concept of *bounded rationality* for the grid users' optimization programs.
- Another suggested consideration from the paper is to investigate the influence of climate change on the distribution network. This could involve implementing a constraint that places limits on the greenhouse gas emissions related to equipment construction and operation.

This list is by no means exhaustive, given that the problem is inherently complex, intertwining physical, economic, and behavioral constraints.

APPENDIX

Appendix A: KPIs results

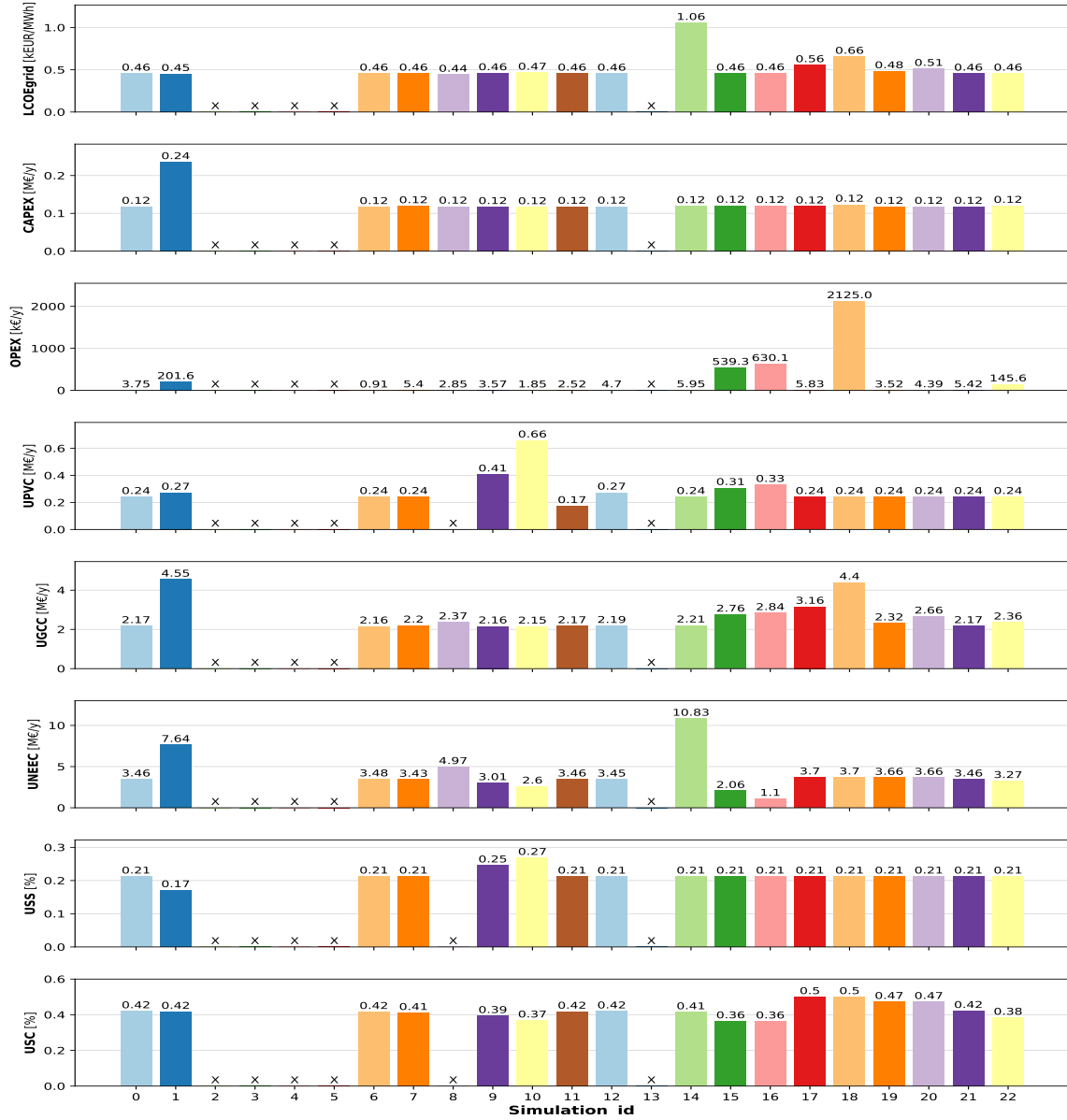


Figure 7.1. Simulation results acquired from a sensitivity analysis of the bilevel model. The analysis comprehensively assesses all 23 configurations specified in TABLE ??, employing a formulation that takes into account **single commodity radiality constraints**. The results are presented through of 8 KPIs: the LCOE grid (k€/MWh), CAPEX (M€/year), OPEX (k€/year), UPVC (M€/year), UGCC (M€/year), UNEEC (M€/year), USS (%) and USC (%).

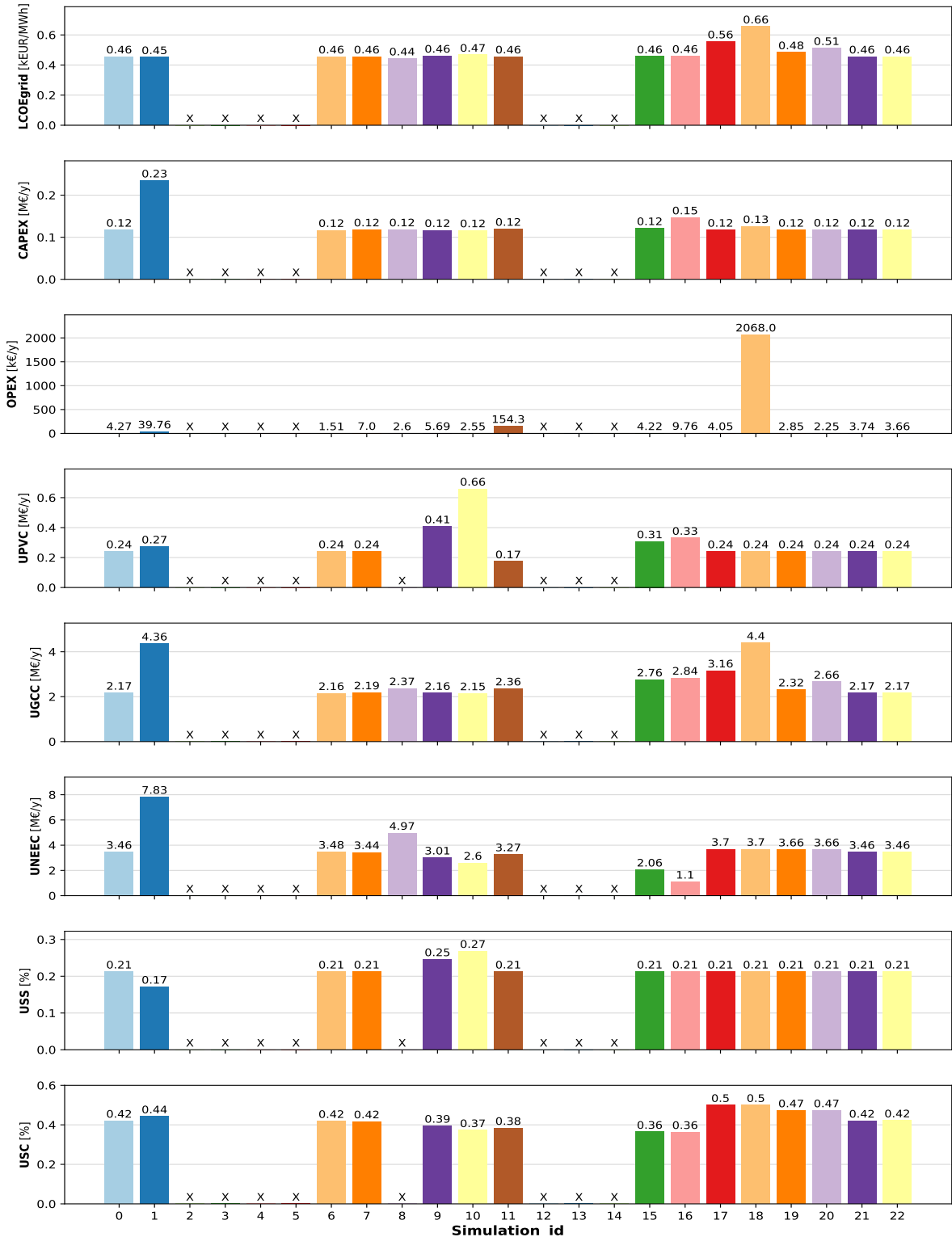


Figure 7.2. Simulation results acquired from a sensitivity analysis of the bilevel model. The analysis comprehensively assesses all 23 configurations specified in TABLE ??, employing a formulation that takes into account **multi commodity radiality constraints**. The results are presented through 8 KPIs: the LCOE grid (k€/MWh), CAPEX (M€/year), OPEX (k€/year), UPVC (M€/year), UGCC (M€/year), UNEEC (M€/year), USS (%) and USC (%).

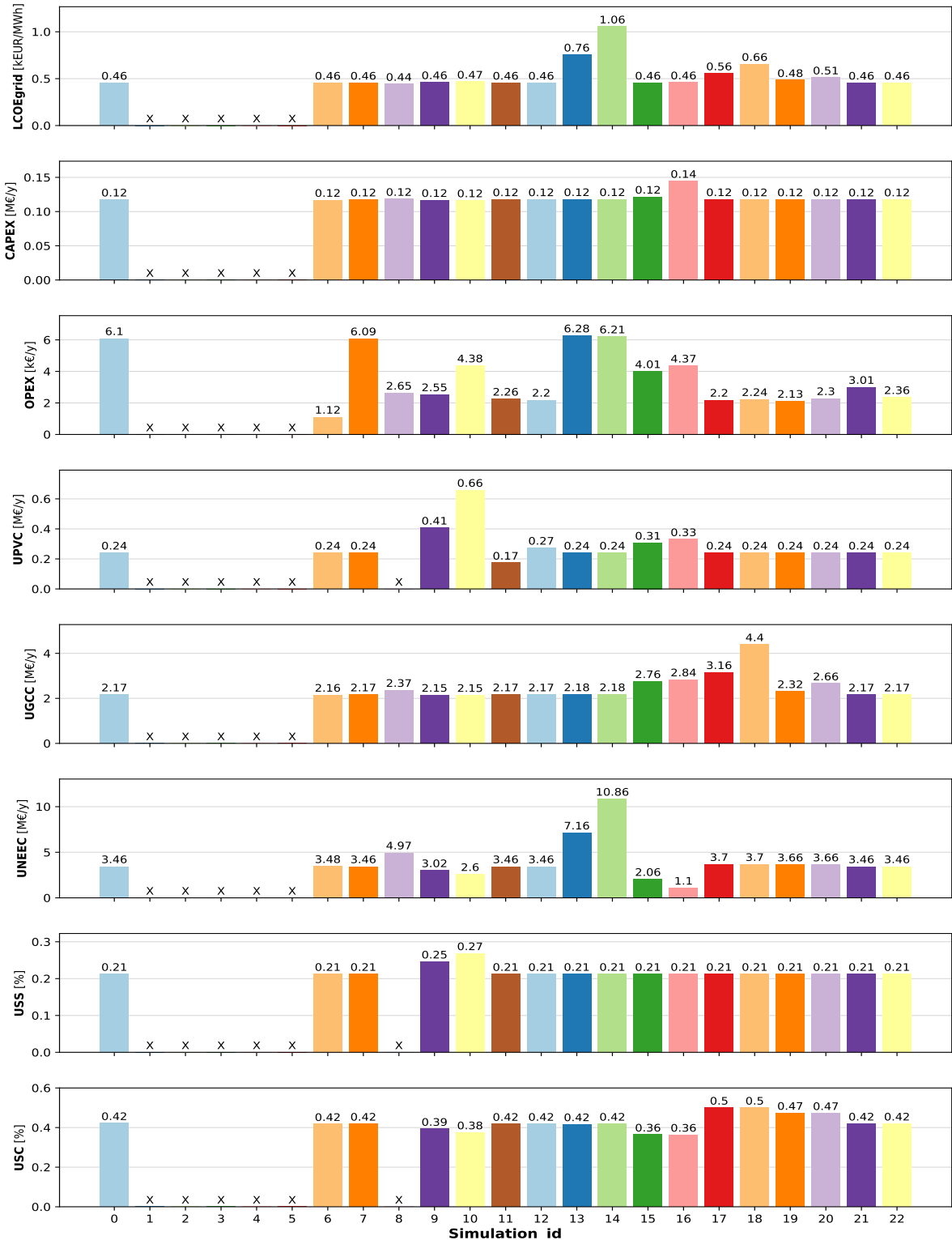


Figure 7.3. Simulation results acquired from a sensitivity analysis of the bilevel model. The analysis comprehensively assesses all 23 configurations specified in TABLE ??, employing a formulation that takes into account **spanning tree radiality constraints**. The results are presented through 8 KPIs: the LCOE grid (k€/MWh), CAPEX (M€/year), OPEX (k€/year), UPVC (M€/year), UGCC (M€/year), UNEEC (M€/year), USS (%) and USC (%).

Bibliography

- [1] C. Fetting, “The european green deal,” *ESDN report*, vol. 53, 2020.
- [2] Commission to the european parliament, the Council, the European Economic and Social Committee and the Committee of the Regions, “Stepping up europe’s 2030 climate ambition: Investing in a climate-neutral future for the benefit of our people,” European Commission, Tech. Rep., Sep. 2020.
- [3] Elia, “Belgian electricity scenario: Final report,” Elia, Tech. Rep., Nov. 2021. [Online]. Available: https://www.elia.be/-/media/project/elia/elia-site/public-consultations/2022/20211115_20220124_final-scenario-report.pdf.
- [4] W. E. Forum. “Artificial intelligence is critical enabler of the energy transition, study finds.” (2021), [Online]. Available: <https://www.weforum.org/press/2021/09/artificial-intelligence-energy-transition> (visited on 08/01/2023).
- [5] CEER Distribution Systems Working Group, “Ceer views on electricity distribution network development plans,” CEER, Tech. Rep., Nov. 2021. [Online]. Available: <https://www.ceer.eu/documents/104400/-/-/2da60a45-6262-c6bc-080a-4f24b4c542cd>.
- [6] C. Masters, “Voltage rise: The big issue when connecting embedded generation to long 11 kv overhead lines,” *Power Engineering Journal*, vol. 16, no. 1, pp. 5–12, 2002. DOI: [10.1049/pe:20020101](https://doi.org/10.1049/pe:20020101).
- [7] A. N. Espinosa and L. Ochoa, “Low voltage networks models and low carbon technology profiles,” *ENWL LV Network Solutions Dissemination Document*, 2015.
- [8] A. N. Espinosa, *Dissemination document “low voltage networks models and low carbon technology profiles”*, 2015.
- [9] M. Resener, S. Haffner, L. A. Pereira, and P. M. Pardalos, “Optimization techniques applied to planning of electric power distribution systems: A bibliographic survey,” *Energy Systems*, vol. 9, pp. 473–509, Jan. 2018. DOI: [10.1007/s12667-018-0276-x](https://doi.org/10.1007/s12667-018-0276-x).
- [10] P. Georgilakis and N. Hatziargyriou, “A review of power distribution planning in the modern power systems era: Models, methods and future research,” *Electric Power Systems Research*, vol. 121, Apr. 2015. DOI: [10.1016/j.epsr.2014.12.010](https://doi.org/10.1016/j.epsr.2014.12.010).
- [11] H. Xing, H. Cheng, Y. Zhang, and P. Zeng, “Active distribution network expansion planning integrating dispersed energy storage systems,” *IET Generation, Transmission & Distribution*, vol. 10, no. 3, pp. 638–644, 2016. DOI: [10.1049/iet-gtd.2015.0411](https://doi.org/10.1049/iet-gtd.2015.0411).

- [12] R. A. Jabr, "Polyhedral formulations and loop elimination constraints for distribution network expansion planning," *IEEE Transactions on Power Systems*, vol. 28, no. 2, pp. 1888–1897, 2013. DOI: [10.1109/TPWRS.2012.2230652](https://doi.org/10.1109/TPWRS.2012.2230652).
- [13] Q. Gemine, D. Ernst, and B. Cornélusse, "Active network management for electrical distribution systems: Problem formulation, benchmark, and approximate solution," English, *Optimization and Engineering*, vol. 18, no. 3, 2016. DOI: [10.1007/s11081-016-9339-9](https://doi.org/10.1007/s11081-016-9339-9).
- [14] D. T.-C. Wang, L. F. Ochoa, and G. P. Harrison, "Dg impact on investment deferral: Network planning and security of supply," *IEEE Transactions on Power Systems*, vol. 25, no. 2, pp. 1134–1141, 2010. DOI: [10.1109/TPWRS.2009.2036361](https://doi.org/10.1109/TPWRS.2009.2036361).
- [15] R. Hemmati, R.-A. Hooshmand, and N. Taheri, "Distribution network expansion planning and dg placement in the presence of uncertainties," *International Journal of Electrical Power and Energy Systems*, vol. 73, pp. 665–673, Dec. 2015. DOI: [10.1016/j.ijepes.2015.05.024](https://doi.org/10.1016/j.ijepes.2015.05.024).
- [16] A. Bagheri, H. Monsef, and H. Lesani, "Integrated distribution network expansion planning incorporating distributed generation considering uncertainties, reliability, and operational conditions," *International Journal of Electrical Power and Energy Systems*, vol. 73, pp. 56–70, 2015. DOI: <https://doi.org/10.1016/j.ijepes.2015.03.010>.
- [17] X. Shen, M. Shahidehpour, Y. Han, S. Zhu, and J. Zheng, "Expansion planning of active distribution networks with centralized and distributed energy storage systems," *IEEE Transactions on Sustainable Energy*, vol. 8, pp. 1–1, Jan. 2016. DOI: [10.1109/TSTE.2016.2586027](https://doi.org/10.1109/TSTE.2016.2586027).
- [18] S. Dakir and B. Cornélusse, "Combined thermal and electrical optimization for the sizing of residential microgrids," in *2022 IEEE International Conference on Environment and Electrical Engineering and 2022 IEEE Industrial and Commercial Power Systems Europe (EEEIC / I&CPS Europe)*, 2022, pp. 1–6. DOI: [10.1109/EEEIC/ICPSEurope54979.2022.9854541](https://doi.org/10.1109/EEEIC/ICPSEurope54979.2022.9854541).
- [19] B. Cornélusse, I. Savelli, S. Paoletti, A. Giannitrapani, and A. Vicino, "A community microgrid architecture with an internal local market," *Applied Energy*, vol. 242, pp. 547–560, 2019. DOI: <https://doi.org/10.1016/j.apenergy.2019.03.109>.
- [20] J. Lu, C. Shi, and G. Zhang, "On bilevel multi-follower decision making: General framework and solutions," *Information Sciences*, vol. 176, no. 11, pp. 1607–1627, Jun. 2006.

- [21] M. Asensio, G. Munoz-Delgado, and J. Contreras, "Bi-level approach to distribution network and renewable energy expansion planning considering demand response," *IEEE Trans. Power Syst.*, vol. 32, no. 6, pp. 4298–4309, Nov. 2017.
- [22] M. Kabirifar, M. Fotuhi-Firuzabad, M. Moeini-Aghetaie, N. Pourghaderi, and P. Dehghanian, "A bi-level framework for expansion planning in active power distribution networks," *IEEE Trans. Power Syst.*, vol. 34, no. 7, pp. 2639–2654, Jul. 2022.
- [23] J. F. Franco, M. J. Rider, and R. Romero, "A mixed-integer quadratically-constrained programming model for the distribution system expansion planning," *International Journal of Electrical Power & Energy Systems*, vol. 62, pp. 265–272, Nov. 2014. DOI: [10.1016/j.ijepes.2014.04.048](https://doi.org/10.1016/j.ijepes.2014.04.048).
- [24] *IEEE PES ISGT EUROPE 2023*, Grenoble, France, 2023.
- [25] S. P. Boyd and L. Vandenberghe, *Convex optimization*. Cambridge university press, 2004.
- [26] Q. Louveaux, "Numerical optimization," 2022.
- [27] J. A. Snyman, D. N. Wilke, *et al.*, *Practical mathematical optimization*. Springer, 2005.
- [28] T. F. Edgar, D. M. Himmelblau, and L. S. Lasdon, *Optimization of chemical processes*. McGraw-Hill College, 2001.
- [29] Q. Louveaux, "Discrete optimization," 2022.
- [30] J. Lee and S. Leyffer, *Mixed integer nonlinear programming*. Springer Science & Business Media, 2011.
- [31] S. Dempe, *Foundations of bilevel programming*. Springer Science & Business Media, 2002.
- [32] S. Dempe, V. Kalashnykov, G. Perez-Valdez, and N. Kalashnykova, *Bilevel Programming Problems: Theory, Algorithms and Applications to Energy Networks*. Heidelberg, Germany: Springer, 2015.
- [33] M. Cerulli, "Bilevel optimization and applications," Theses, Institut Polytechnique de Paris, Dec. 2021. [Online]. Available: <https://theses.hal.science/tel-03587548>.
- [34] C. Fricke, "An introduction to bilevel programming," 2003.
- [35] G. Dantzig, *Maximization of a linear function of variables subject to linear inequality. 1947. published in koopmans tc (ed.): Activity analysis of production and allocation*, 1951.

- [36] N. Karmarkar, “A new polynomial-time algorithm for linear programming,” in *Proceedings of the sixteenth annual ACM symposium on Theory of computing*, 1984, pp. 302–311.
- [37] D. A. Spielman and S.-H. Teng, “Smoothed analysis of algorithms: Why the simplex algorithm usually takes polynomial time,” *Journal of the ACM (JACM)*, vol. 51, no. 3, pp. 385–463, 2004.
- [38] F. Geth, R. D’hulst, and D. Van Hertem, “Convex power flow models for scalable electricity market modelling,” *CIRED-Open Access Proceedings Journal*, vol. 1, pp. 989–993, 2017.
- [39] L. Gurobi Optimization, *Gurobi optimizer reference manual*, 2023. [Online]. Available: <https://www.gurobi.com>.
- [40] I. I. Cplex, *User’s manual for cplex*, 2023. [Online]. Available: https://www.ibm.com/products/ilog-cplex-optimization-studio?mhsrc=ibmsearch_a&mhq=cplex.
- [41] J. Bracken and J. T. McGill, “Mathematical programs with optimization problems in the constraints,” *Operations research*, vol. 21, no. 1, pp. 37–44, 1973.
- [42] H. Von Stackelberg, *Marktform und gleichgewicht*, 1934.
- [43] B. Zeng, “A practical scheme to compute the pessimistic bilevel optimization problem,” *INFORMS Journal on Computing*, vol. 32, no. 4, pp. 1128–1142, 2020. DOI: [10.1287/ijoc.2019.0927](https://doi.org/10.1287/ijoc.2019.0927).
- [44] T. Kis, A. Kovács, and C. Mészáros, “On optimistic and pessimistic bilevel optimization models for demand response management,” *Energies*, vol. 14, no. 8, 2021. DOI: [10.3390/en14082095](https://doi.org/10.3390/en14082095).
- [45] Z.-Q. Luo, J.-S. Pang, and D. Ralph, *Mathematical programs with equilibrium constraints*. Cambridge University Press, 1996.
- [46] J. D. Garcia and G. Bodin and A, Street, “Bileveljump.jl: Modeling and solving bilevel optimization in julia,” arXiv, Tech. Rep., Jun. 2022. [Online]. Available: <https://arxiv.org/abs/2205.02307>.
- [47] M. T. Emmerich and A. H. Deutz, “A tutorial on multiobjective optimization: Fundamentals and evolutionary methods,” *Natural computing*, vol. 17, pp. 585–609, 2018.
- [48] Á. García-Cerezo, L. Baringo, and R. García-Bertrand, “Representative days for expansion decisions in power systems,” *Energies*, vol. 13, no. 2, 2020. DOI: [10.3390/en13020335](https://doi.org/10.3390/en13020335).
- [49] E. McKenna, M. Thomson, and J. Barton, “CREST Demand Model,” May 2020. DOI: [10.17028/rd.lboro.2001129.v8](https://doi.org/10.17028/rd.lboro.2001129.v8). [Online]. Available: https://repository.lboro.ac.uk/articles/dataset/CREST_Demand_Model_v2_0/2001129.

- [50] J. M. Nahman and D. M. Peric, “Optimal planning of radial distribution networks by simulated annealing technique,” *IEEE Transactions on Power systems*, vol. 23, no. 2, pp. 790–795, 2008. DOI: [10.1109/TPWRS.2008.920047](https://doi.org/10.1109/TPWRS.2008.920047).
- [51] L. L. Grigsby, *The electric power engineering handbook-five volume set*. CRC press, 2018.
- [52] J. Bezanson, A. Edelman, S. Karpinski, and V. B. Shah, “Julia: A fresh approach to numerical computing,” *SIAM Review*, vol. 59, no. 1, pp. 65–98, 2017. DOI: [10.1137/141000671](https://doi.org/10.1137/141000671). [Online]. Available: <https://epubs.siam.org/doi/10.1137/141000671>.
- [53] D. P. Kothari and I. Nagrath, *Power system engineering*. Tata McGraw-Hill New Delhi, India, 2008.
- [54] D. K. Molzahn, I. A. Hiskens, *et al.*, “A survey of relaxations and approximations of the power flow equations,” *Foundations and Trends in Electric Energy Systems*, vol. 4, no. 1-2, pp. 1–221, 2019.
- [55] R. A. Jabr, “Radial distribution load flow using conic programming,” *IEEE transactions on power systems*, vol. 21, no. 3, pp. 1458–1459, 2006. DOI: [10.1109/TPWRS.2006.879234](https://doi.org/10.1109/TPWRS.2006.879234).
- [56] M. Baran and F. Wu, “Optimal capacitor placement on radial distribution systems,” *IEEE Transactions on Power Delivery*, vol. 4, no. 1, pp. 725–734, 1989. DOI: [10.1109/61.19265](https://doi.org/10.1109/61.19265).
- [57] S. Lei, C. Chen, Y. Song, and Y. Hou, “Radiality constraints for resilient reconfiguration of distribution systems: Formulation and application to microgrid formation,” *IEEE Transactions on Smart Grid*, vol. 11, no. 5, pp. 3944–3956, 2020. DOI: [10.1109/TSG.2020.2985087](https://doi.org/10.1109/TSG.2020.2985087).
- [58] M. Lubin, O. Dowson, J. Dias Garcia, J. Huchette, B. Legat, and J. P. Vielma, “JuMP 1.0: Recent improvements to a modeling language for mathematical optimization,” *Mathematical Programming Computation*, 2023. DOI: [10.1007/s12532-023-00239-3](https://doi.org/10.1007/s12532-023-00239-3).